

Rotating MHD fluids in planetary interiors: convection, dynamos, and waves

Kumiko Hori

National Institute for Fusion Science



MAX PLANCK INSTITUTE
FOR SOLAR SYSTEM RESEARCH



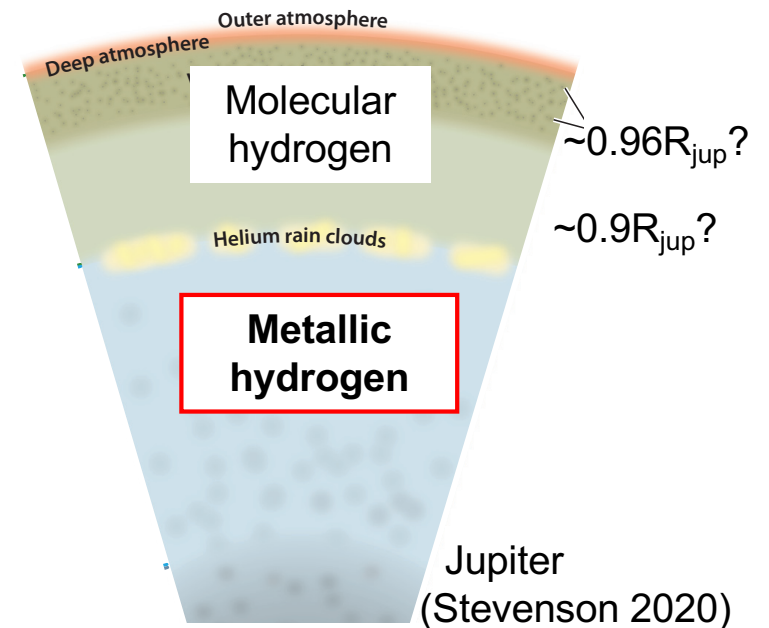
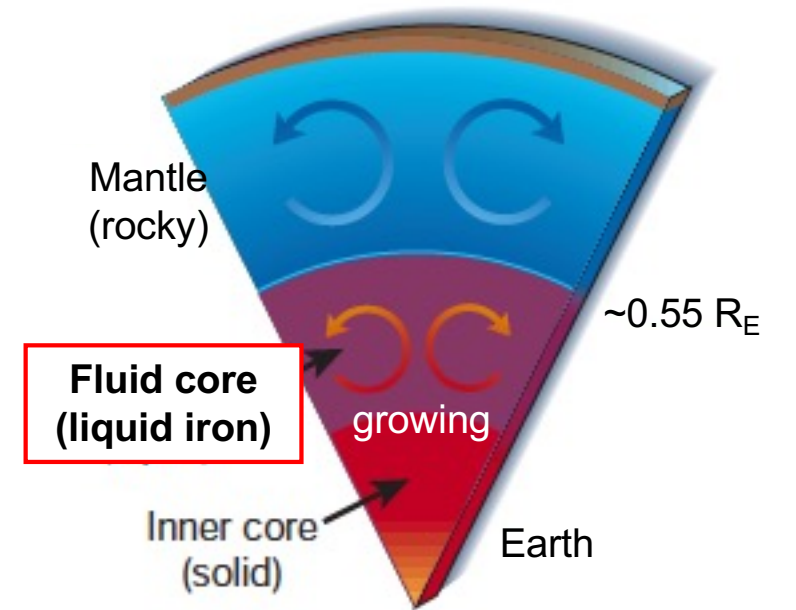
gfd seminars 1
Hokkaido, 15-16 March 2025



JAPAN SOCIETY FOR THE PROMOTION OF SCIENCE
日本学術振興会

地球惑星内部の回転(磁気)流体

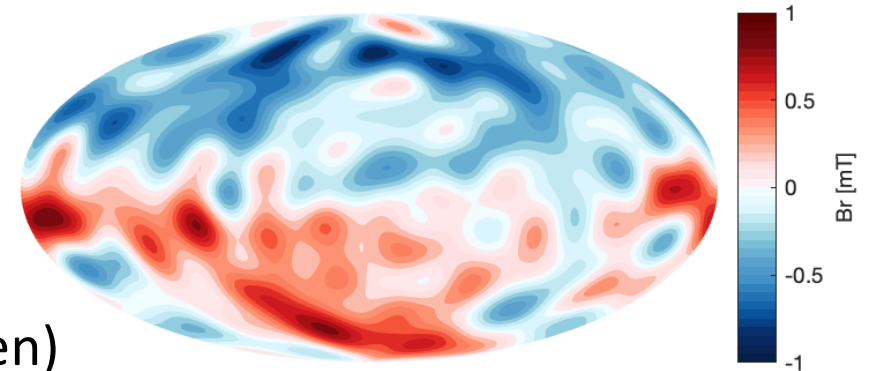
- Fluid cores (liquid iron outer cores) in rocky planets
 - cf. viscous/rocky mantles
 - e.g. our Earth
- Outer envelopes (ionised/metallic hydrogen) in gaseous planets
 - e.g. Jupiter
- Hosting their large-scale magnetic fields
- MHD of rotating fluids
 - as a blend in the classic subfield
 - G "A" FD if you like..



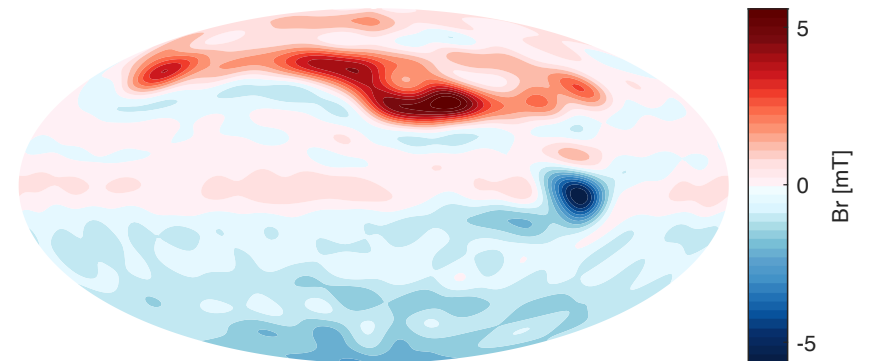
地球惑星内部の回転(磁気)流体

- Fluid cores (liquid iron outer cores) in rocky planets
 - cf. viscous/rocky mantles
 - e.g. our Earth
- Outer envelopes (ionised/metallic hydrogen) in gaseous planets
 - e.g. Jupiter
- Hosting their large-scale magnetic fields
- MHD of rotating fluids
 - as a blend in the classic subfield
 - G "A" FD if you like...

chaos7: core field $n \leq 13$, B_r at $\sim 0.54699R_E$ in 01-Apr-2020



JRM33: $n \leq 18$, B_r at $\sim 0.85R_J$



基礎方程式

- MHD of rotating fluids in spherical shells (or plane layers)
 - in the Boussinesq + MHD approximation (for constant diffusivities)

$$\begin{aligned}\left(\frac{\partial}{\partial t} + \mathbf{u} \cdot \nabla\right) \mathbf{u} + 2\boldsymbol{\Omega} \times \mathbf{u} &= -\nabla \frac{p'}{\rho_0} + \alpha g T' \hat{\mathbf{r}} + \frac{1}{\rho_0} \mathbf{j} \times \mathbf{B} + \nu \nabla^2 \mathbf{u} & \nabla \cdot \mathbf{u} &= 0 \\ \left(\frac{\partial}{\partial t} + \mathbf{u} \cdot \nabla\right) T' &= -\frac{dT_0}{dr} u_r + \kappa \nabla^2 T' \\ \left(\frac{\partial}{\partial t} + \mathbf{u} \cdot \nabla\right) \mathbf{B} &= \mathbf{B} \cdot \nabla \mathbf{u} + \eta \nabla^2 \mathbf{B} & \nabla \cdot \mathbf{B} &= 0, & \mu_0 \mathbf{j} &= \nabla \times \mathbf{B}\end{aligned}$$

- (必要最低限の) 方程式系から何がでてくるか、とその応用
 - できるだけ(流体の)基礎方程式そのままに --> “DNS” の世界
 - 古典本 e.g. Greenspan (1968), Chandrasekhar (1961), Roberts (1967)
 - 文化/歴史の違いをご理解ください
- 主なこと: 対流、磁場形成、振動・波動、(乱流、etc)

問題設定

$$\left(\frac{\partial}{\partial t} + \mathbf{u} \cdot \nabla\right) \mathbf{u} + 2\boldsymbol{\Omega} \times \mathbf{u} = -\nabla \frac{p'}{\rho_0} + \alpha g T' \hat{\mathbf{r}} + \frac{1}{\rho_0} \mathbf{j} \times \mathbf{B} + \nu \nabla^2 \mathbf{u} \quad \nabla \cdot \mathbf{u} = 0$$

- Of interest:

- 粘性項 $Ek = Ta^{-1/2} \sim 10^{-15} - 10^{-9} \ll 1$

- 慣性/移流項 $Ro = Re Ek \sim 10^{-5} \ll 1$

- leading to a geo-strophic balance

- 空間スケール比 $\delta = D/L \sim O(1)$ (cf. atmosphere, ocean)

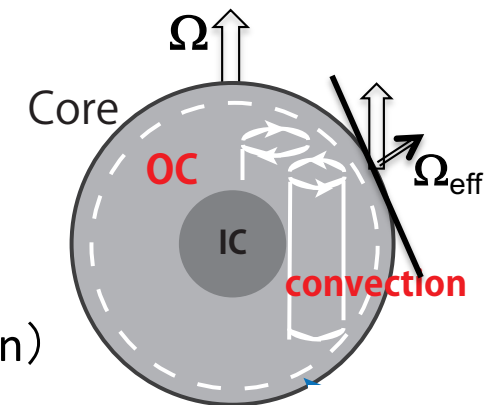
- 磁気流体性(?) Elsasser 数 $\Lambda = B^2/\mu\rho\eta\Omega = Q Ek = O(1)$

- leading to a **magneto-strophic** balance (Acheson & Hide 1973)

- Earth/planet-like と信じられる (cf. sun/solar)

- 流体/物理的にいろいろ特有なことが起こる(だろう)

- 対流、磁場形成、振動・波動 で実際に見てみたい



Convection

- Nicely introduces the subject
 - more details in FDEPS lectures by Jones (2017), Christensen (2006)
- Rotating magneto-**convection**

(e.g. Chandrasekhar 1952-54; in lab, Nakagawa 1957-59)

 - where a background magnetic field \mathbf{B}_0 is externally imposed
 - cf. dynamos, where magnetic field \mathbf{B} is self-excited
 - in plane layers where $\boldsymbol{\Omega} \parallel \mathbf{B}_0 \parallel \mathbf{g}$



(no $\boldsymbol{\Omega}$ no \mathbf{B}_0 ; Ishiwatari et al. 1994)

V

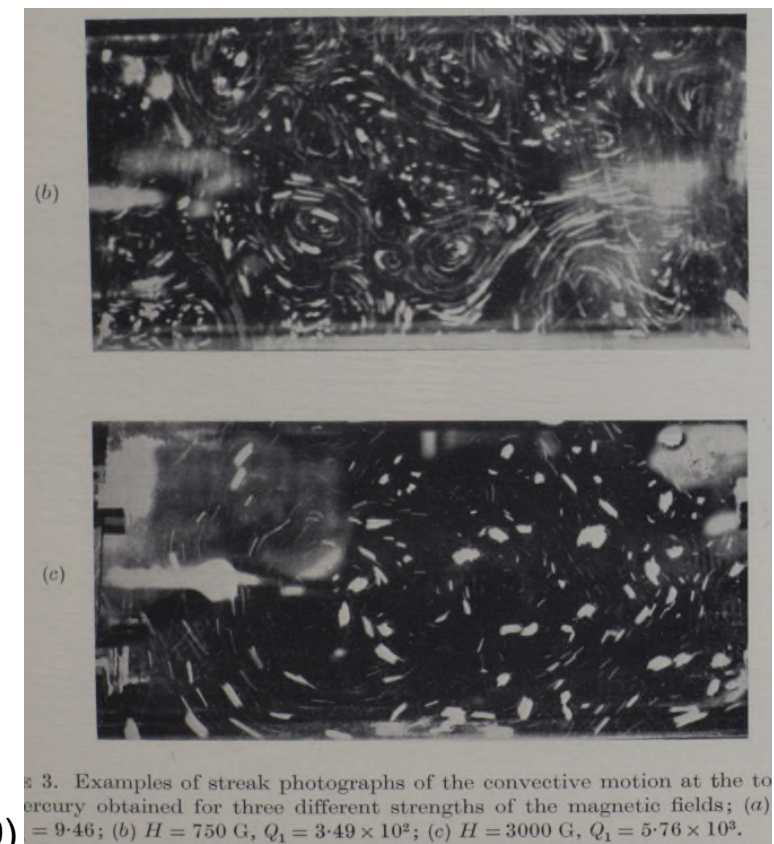
THE THERMAL INSTABILITY OF A LAYER OF
FLUID HEATED FROM BELOW

4. THE EFFECT OF ROTATION AND MAGNETIC FIELD

49. The like and the contrary effects of rotation and magnetic field on fluid behaviour

In the last two chapters we have studied the effect of rotation and magnetic field, acting separately, on the onset of thermal instability in layers of fluid heated from below. In some respects the effects are remarkably alike: they both inhibit the onset of instability; and they

(Chap. 5; Chandrasekhar 1961)



(Nakagawa 1959)

Fig. 3. Examples of streak photographs of the convective motion at the top surface of mercury obtained for three different strengths of the magnetic fields; (a) $H = 9.46$; (b) $H = 750$ G, $Q_1 = 3.49 \times 10^2$; (c) $H = 3000$ G, $Q_1 = 5.76 \times 10^3$.

Convection (cont'd)

- Linear stability analyses

- the linearised, governing equations: e.g.

$$\frac{\partial \tilde{\mathbf{u}}}{\partial \tilde{t}} + \frac{2}{E} \hat{\mathbf{e}}_z \times \tilde{\mathbf{u}} = -\tilde{\nabla} \tilde{P} + \frac{Ra}{Pr} \tilde{\theta} \hat{\mathbf{e}}_z - \frac{Q}{Pm} \hat{\mathbf{e}}_z \times \tilde{\mathbf{j}} + \tilde{\nabla}^2 \tilde{\mathbf{u}}$$

$$\frac{\partial \tilde{\theta}}{\partial \tilde{t}} = \hat{\mathbf{e}}_z \cdot \tilde{\mathbf{u}} + \frac{1}{Pr} \tilde{\nabla}^2 \tilde{\theta}$$

$$\frac{\partial \tilde{\mathbf{b}}}{\partial \tilde{t}} = \hat{\mathbf{e}}_z \cdot \nabla \tilde{\mathbf{u}} + \frac{1}{Pm} \tilde{\nabla}^2 \tilde{\mathbf{b}}$$

- with a reduced numbers of parameters

$$Ra = \frac{\alpha g \beta_0 d^4}{\nu \kappa}, \quad Pr = \frac{\nu}{\kappa}, \quad E = \frac{\nu}{\Omega d^2}, \quad Q = \frac{B_0^2 d^2}{\rho \mu_0 \nu \eta}, \quad Pm = \frac{\nu}{\eta}$$

- To yield the Ra needed for the instability

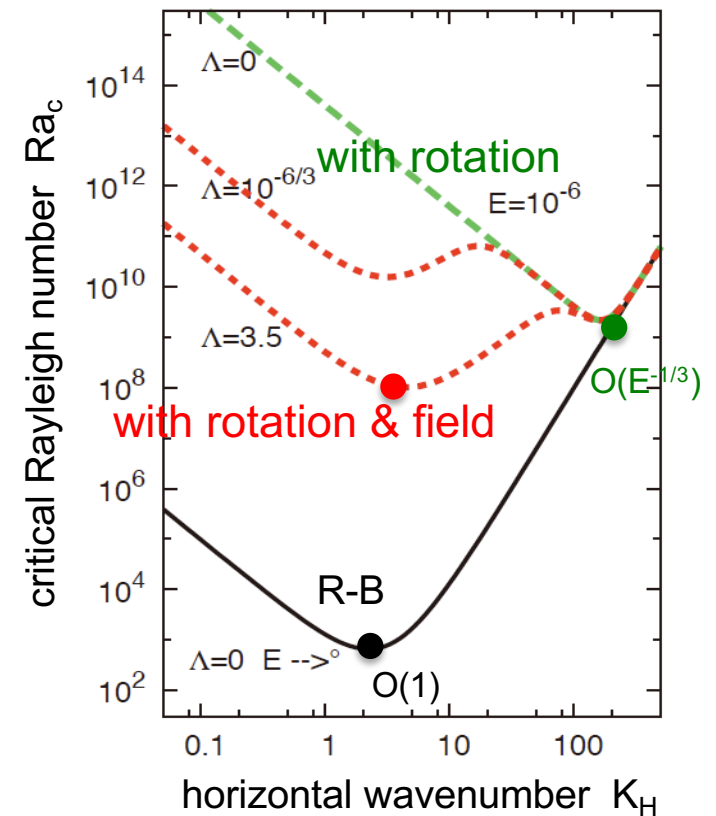
- e.g. for the stationary mode:

$$Ra_c = \frac{K_H^2 + \pi^2}{K_H^2} \left[(K_H^2 + \pi^2)^2 + \pi Q + \frac{4\pi^2}{E^2} \frac{K_H^2 + \pi^2}{(K_H^2 + \pi^2)^2 + Q\pi^2} \right]$$

- increases when either rotation (Q = 0) or magnetic field (E → ∞) alone is at play
- **decreases in the presence of both** as Q E = Λ → O(1)
 - to get back to ~nonrot. nonmag. behaviours (!)



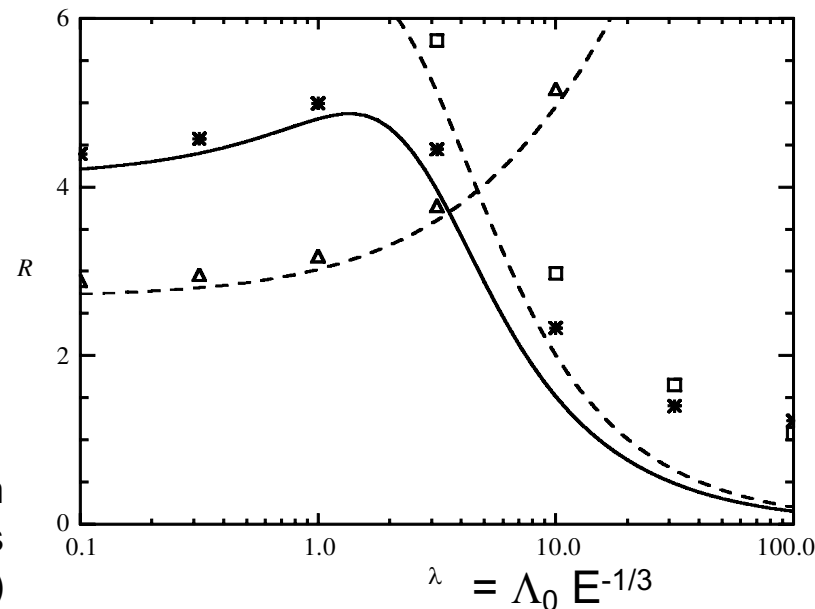
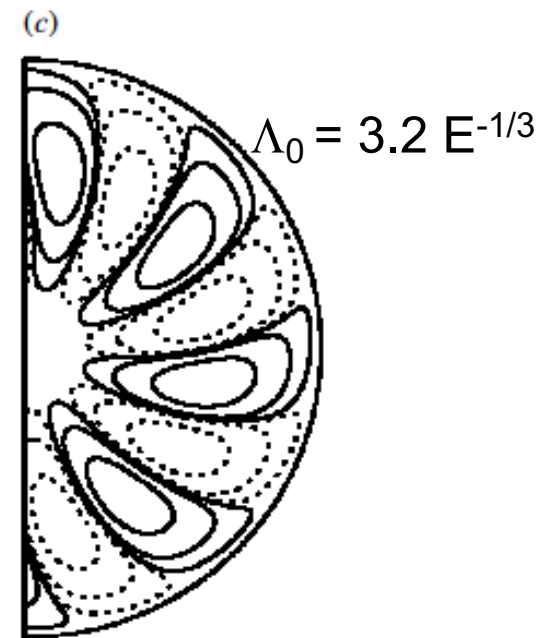
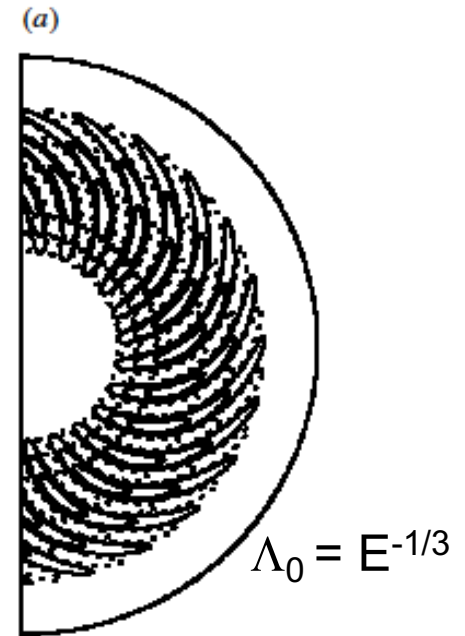
(adopted from Ishiwatari et al. 1994)



(after Chandrasekhar 1961)

Spherical convection

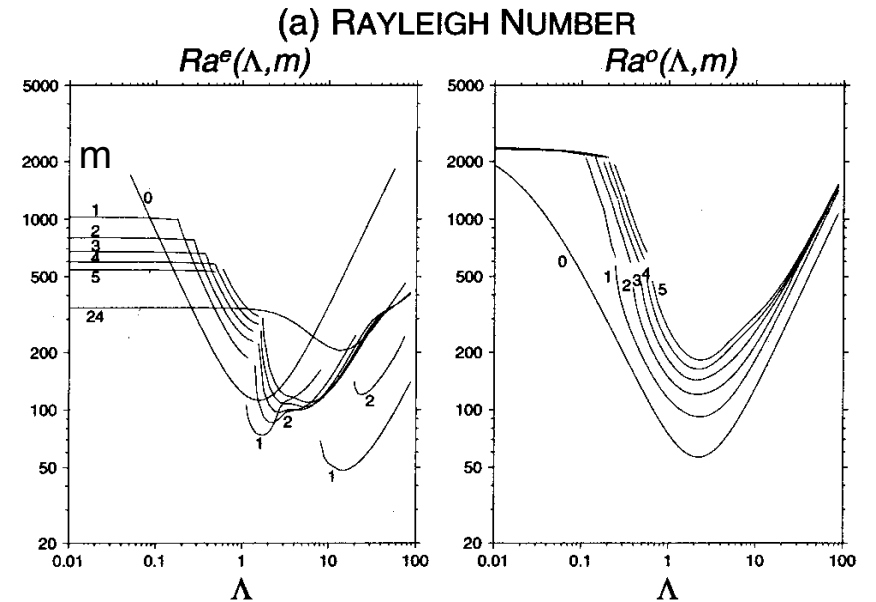
- Linear stability in spheres/spherical shells
 - e.g. Fearn 1979; Jones+ 2003; Sakuraba 2002; also a review by Zhang & Schubert 2000
- Given a proper condition, as $\Lambda_0 \rightarrow O(1)$
 - thermal instability, $Ra_{\text{crit}} = O(E^{-4/3}) \rightarrow O(E^{-1})$
 - wavenumber, $k_{\text{crit}} = O(E^{-1/3}) \rightarrow O(1)$
 - nonaxisymmetric modes preferred
 - frequency, $\omega_{\text{crit}} = O(E^{-2/3}) \rightarrow O(1)$



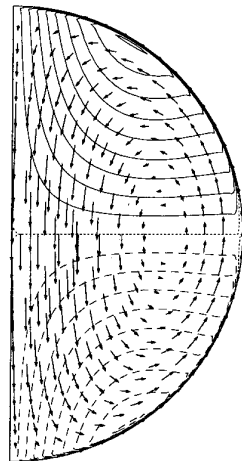
Rotating magnetoconvection
 applied by Malkus field $B_\phi = B_0 s$
 (Jones et al. 2003)

Spherical convection

- Linear stability in spheres/spherical shells
 - e.g. Fearn 1979; Jones+ 2003; Sakuraba 2002; also a review by Zhang & Schubert 2000
- Given a proper condition, as $\Lambda_0 \rightarrow O(1)$
 - thermal instability, $Ra_{crit} = O(E^{-4/3}) \rightarrow O(E^{-1})$
 - wavenumber, $k_{crit} = O(E^{-1/3}) \rightarrow O(1)$
 - nonaxisymmetric modes preferred
 - frequency, $\omega_{crit} = O(E^{-2/3}) \rightarrow O(1)$

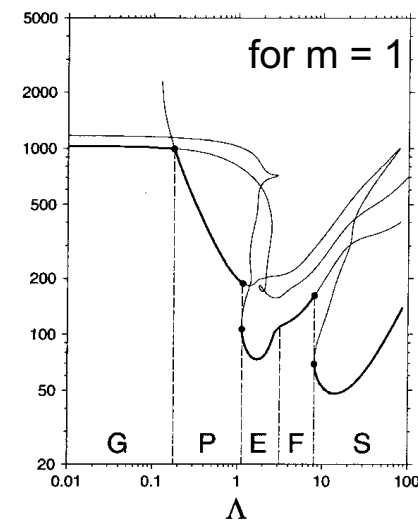


velocity
(cont.int.= 5, max.= 48.11)

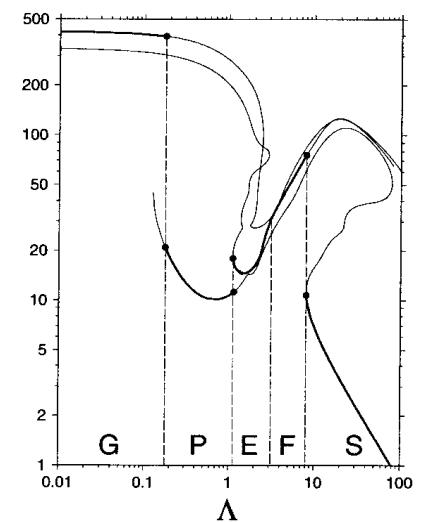


odd Polar mode

(a) RAYLEIGH NUMBER



(b) PHASE VELOCITY

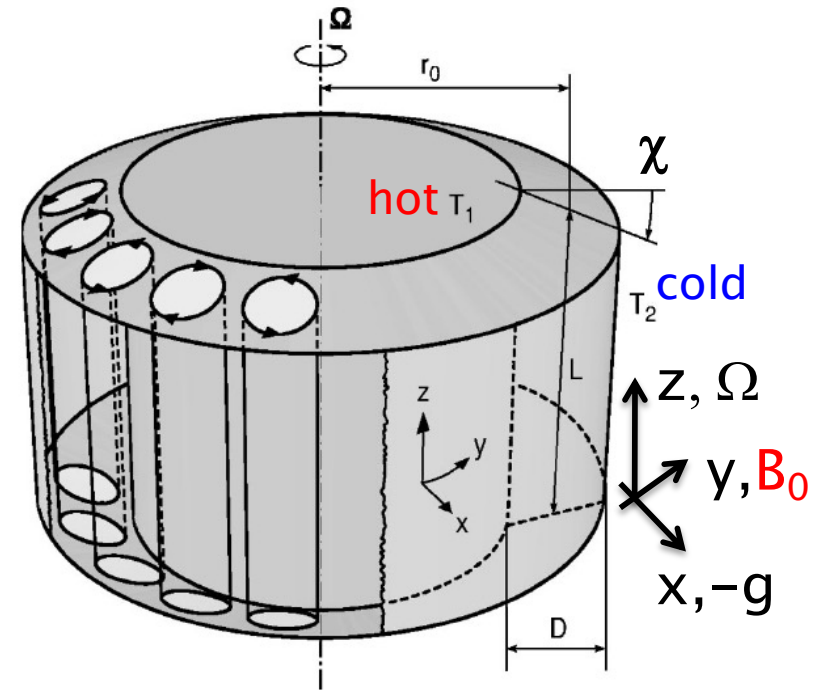


Rotating magnetoconvection
applied by uniform axial field B_z
(Sakuraba 2002)

Busse's annulus model

- Useful to analyse key properties of rotating spherical convection (handy..)
- Settings (Busse 1970; MHD ver. in 1976) :
 - sloping boundaries (with a small angle χ)

$$u_z = \pm \chi u_x \quad \text{at} \quad z = \pm L/2$$
 to give a topographic $\beta = -2\Omega d(\ln H)/dx$
 - almost independent on z ("QG")
 - $\Omega \perp \mathbf{g} \perp \mathbf{B}_0$ (and/or $\mathbf{g} \parallel \mathbf{B}_0$)



- To give a reduced set of linearised equations (dimensionless):

$$\left(\frac{\partial}{\partial t} - \Delta_2 \right) \Delta_2 \psi - \beta^* \frac{\partial \psi}{\partial y} = \frac{Ra}{Pr} \frac{\partial \theta}{\partial y} + \frac{Q}{Pm} \left(\frac{\partial}{\partial y} + \mathcal{P} \frac{\partial}{\partial x} \right) \Delta_2 g$$

$$\left(\frac{\partial}{\partial t} - \frac{1}{Pr} \Delta_2 \right) \theta = \frac{\partial \psi}{\partial y}$$

$$\left(\frac{\partial}{\partial t} - \frac{1}{Pr} \Delta_2 \right) \Delta_2 g = \left(\frac{\partial}{\partial y} + \mathcal{P} \frac{\partial}{\partial x} \right) \Delta_2 \psi$$

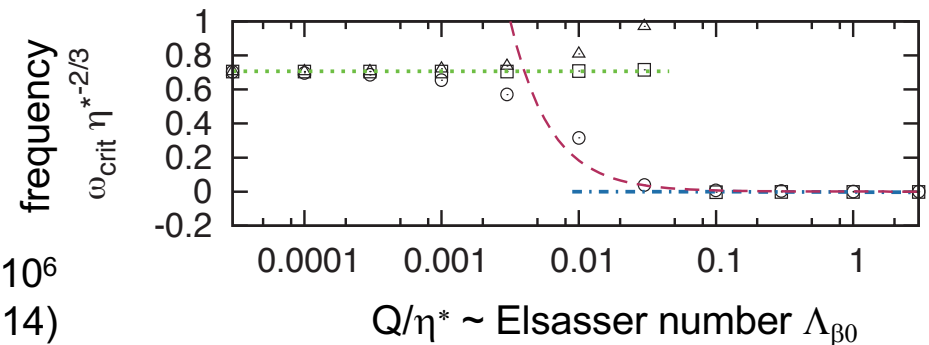
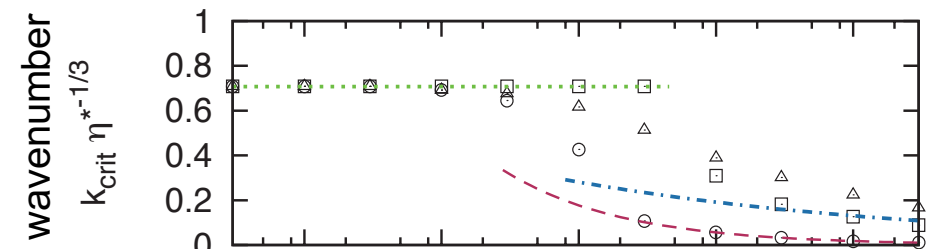
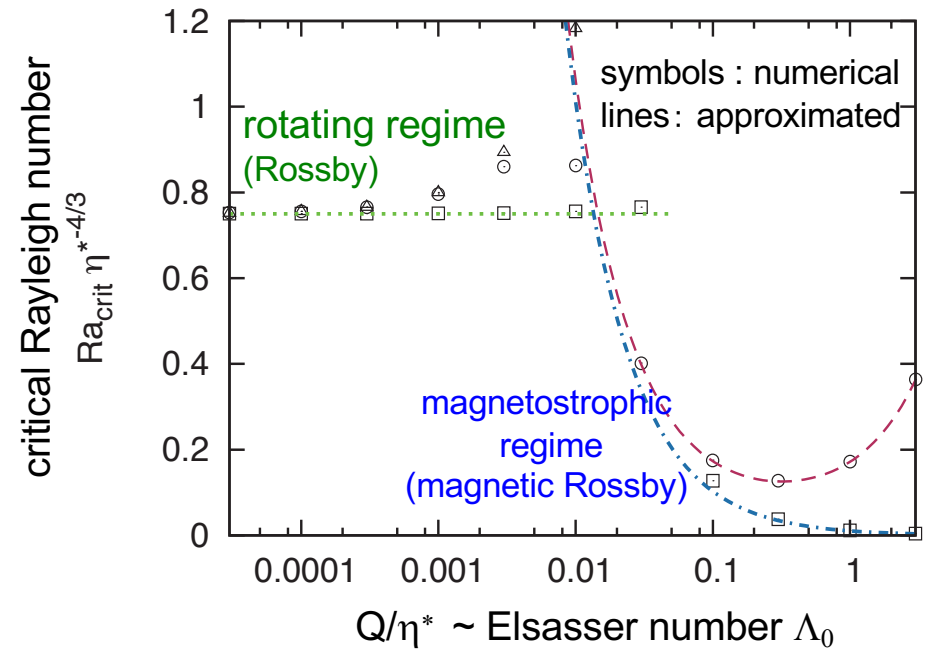
$$Ra = \frac{\alpha g D^3 \Delta T}{\nu \kappa}$$

$$\beta^* = \frac{4\chi \Omega D^3}{\nu L}$$

$$Q = \frac{B_0^2 D^2}{\rho \mu_0 \nu \eta}, \quad \mathcal{P} = \frac{|B_{0s}|}{B_0}$$

Busse's annulus model (cont'd)

- The key properties of spherical convection reproduced by the annulus model
- The marginal curve comprises distinct modes, depending on the regimes
 - thermal Rossby modes (Busse 1970) for small Λ_0
 - for $\Lambda_0 \geq O(E^{1/3})$
slow magnetic Rossby modes ($Pm/Pr \gg 1$)
 or another slow diffusive modes ($Pm/Pr \ll 1$)
- The $\Lambda_0 = O(1)$ regime is well characterised by a balance amongst the Lorentz, buoyancy, (p-grad,) & Coriolis forces
 - with no viscous roles (cf. the rotating conv)
 - the magnetostrophic/MAC balance



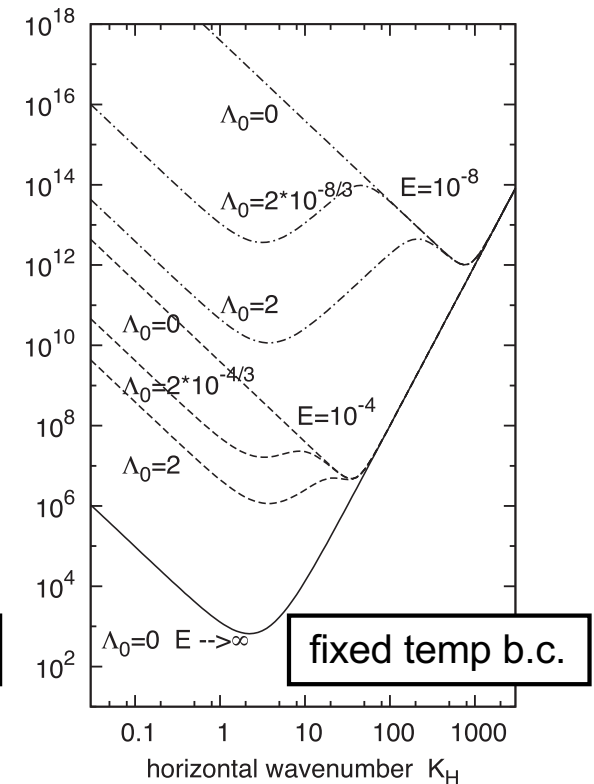
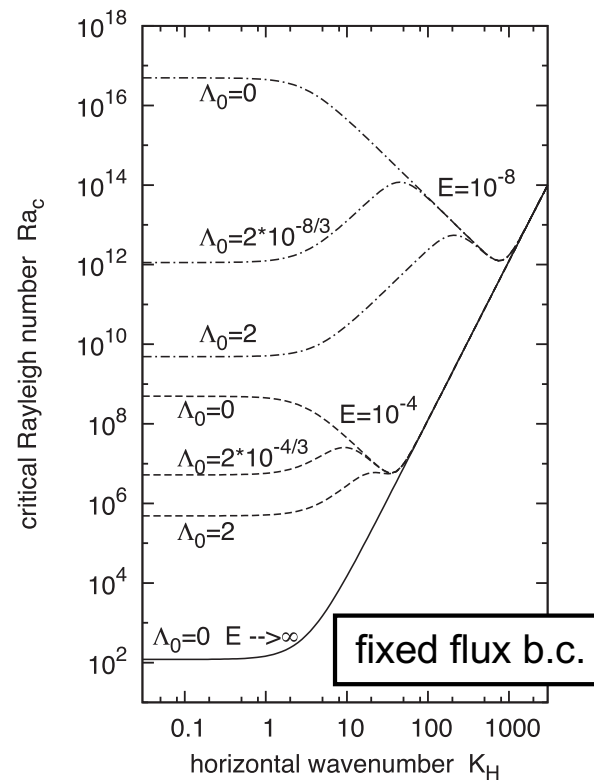
At $\beta^* = 10^6$
(KH, Takehiro & Shimizu, 2014)

Some remarks

- The effects are expected for
 - sufficiently rapid rotation, $E \ll 1$
 - no larger than $E = 10^{-4}$ in linear analyses
 - a proper magnetic field \mathbf{B}_0 (direction & morphology)
 - a proper condition: e.g.
 - when a fixed heat-flux boundary condition rules, the magnetostrophic properties will become more relevant

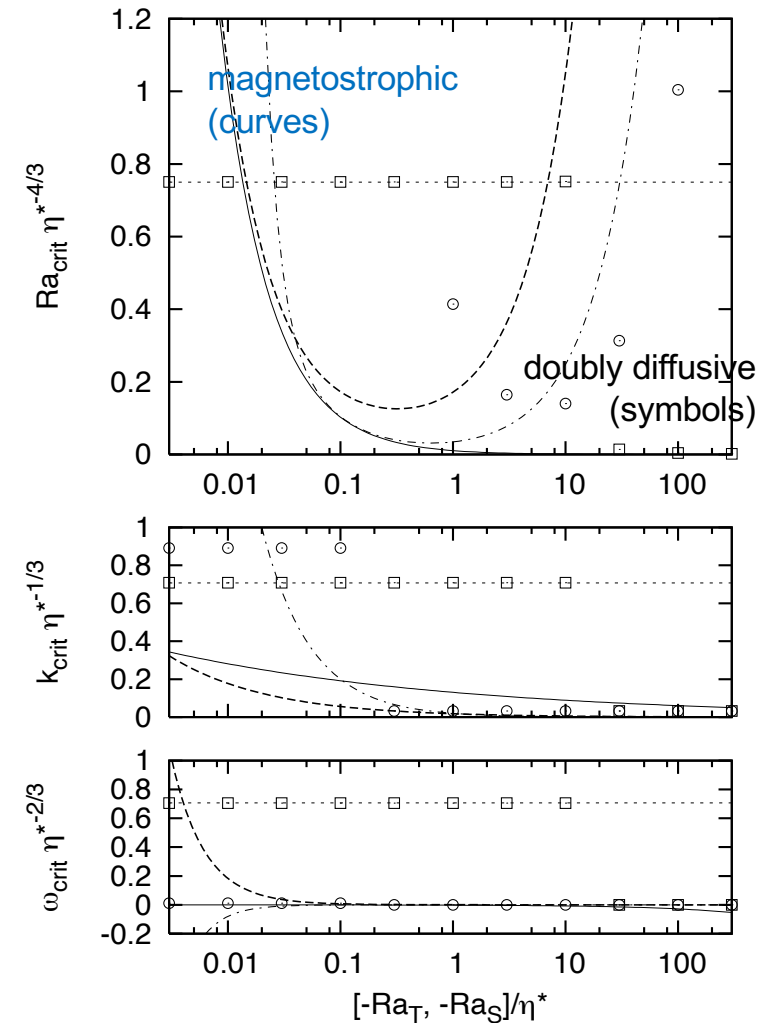
$$Ra_c = \frac{\pi^2}{8} \left[(K_H^2 + \pi^2)^2 + \pi Q + \frac{4\pi^2}{E^2} \frac{K_H^2 + \pi^2}{(K_H^2 + \pi^2)^2 + Q\pi^2} \right]$$

In plane layers where $\Omega \parallel \mathbf{B}_0 \parallel \mathbf{g}$
(KH, Wicht & Christensen, 2012)



Some remarks (cont'd)

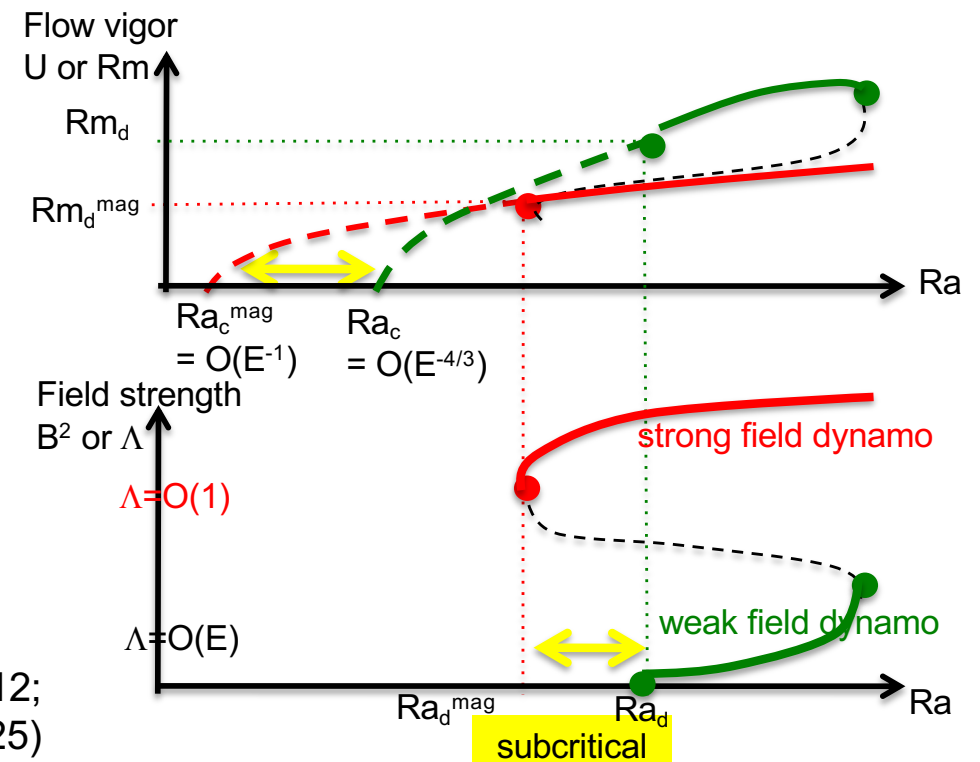
- The problem may be regarded as a doubly diffusive system
- e.g. In the linear Busse-annulus model
 - $\sim Q K_H^2 / Pm$ as $-Ra_S / Pc$
 - e.g. oscillatory regime ($q = Pm / Pr > 1$) as a diffusive regime ($Le = Pc / Pr > 1$; $Ra_T > 0$, $Ra_S < 0$)
 - identical when $\Omega \parallel \mathbf{B}_0 \perp \mathbf{g}$ (after Takehiro-san; in spheres, Sakuraba 2002)
- Rotating double-diffusive convection also yields the Ra-drop if $-Ra_S / \eta^* = O(1)$
 - cf. Elsasser number $\Lambda \sim Q / \eta^*$
 - but not when $-Ra_S / \eta^* = O(E^{1/3})$



Doubly-diffusive vs. magneto- convection at $1/\eta^* = 10^6$ (KH & Simitev, unpublished)

Dynamos

- Rotating magnetoconvection studies have suggested
 - as magnetic field B is strengthened to $\Lambda = O(1)$, the thermal instability Ra_{crit} drops
 - as well as the wavenumber k_{crit} , and wave frequency ω_{crit}
- This led to a speculation of dynamos in the regime:
 - **‘strong-field’ dynamos**
 - or magnetostrophic dynamos, etc.
 - vs. **‘weak-field’ dynamos** in the rotating/viscous regime



(after Roberts 1978; KH & Wicht 2012;
also Dormy 2016, 2025)

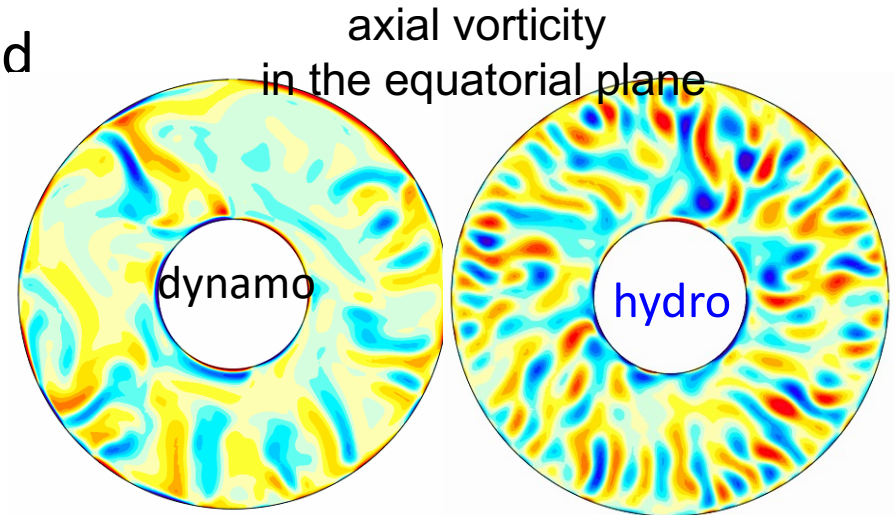
Do magnetostrophic dynamos exist at all?

- Long controversial whether the existence could be proven
 - some indications in plane layer dynamos (e.g. Stellmach & Hansen 2004)
 - what about in spherical dynamos
 - negative? (e.g. Soderlund+ 2012; Roberts & King 2013)
 - positive? (e.g. Sreenivasan & Jones 2011)
- To explore
 - the key signatures as predicted by rotating magneto-convection
 - length scale: spatial structures, scaling laws
 - thermal instability: heat transfer, subcritical/strong-/weak-field dynamos
 - time scale: waves/oscillations
 - the force balances
 - base on the solutions/scaling
 - identifying the regime (e.g. Yadav+ 2016, Dormy 2017), better diagnosing (ongoing)

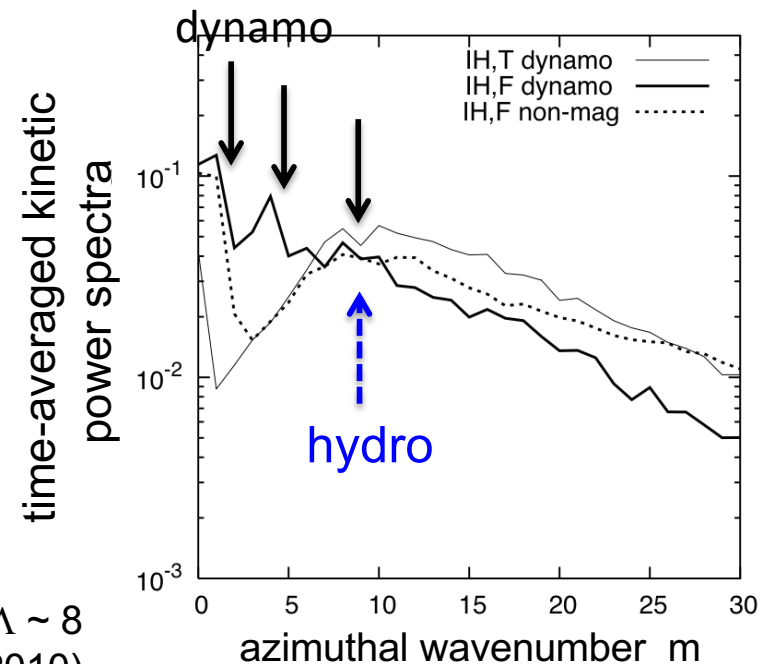
Length scales

- Enlarged convective structures identified

- inside the TC (e.g. Sreenivasan & Jones 2005)
 - cf. in plane layers (e.g. Rotvig & Jones 2002; Stellmach & Hansen 2004)
 - cf. in lab (e.g. King & Aurnou 2015)
- outside the TC (e.g. Sakuraba & Roberts 2009; Hori+ 2010; Takahashi & Shimizu 2012)
 - when generated magnetic fields were dipolar
 - clearer when a fixed heat-flux b.c. ruled?



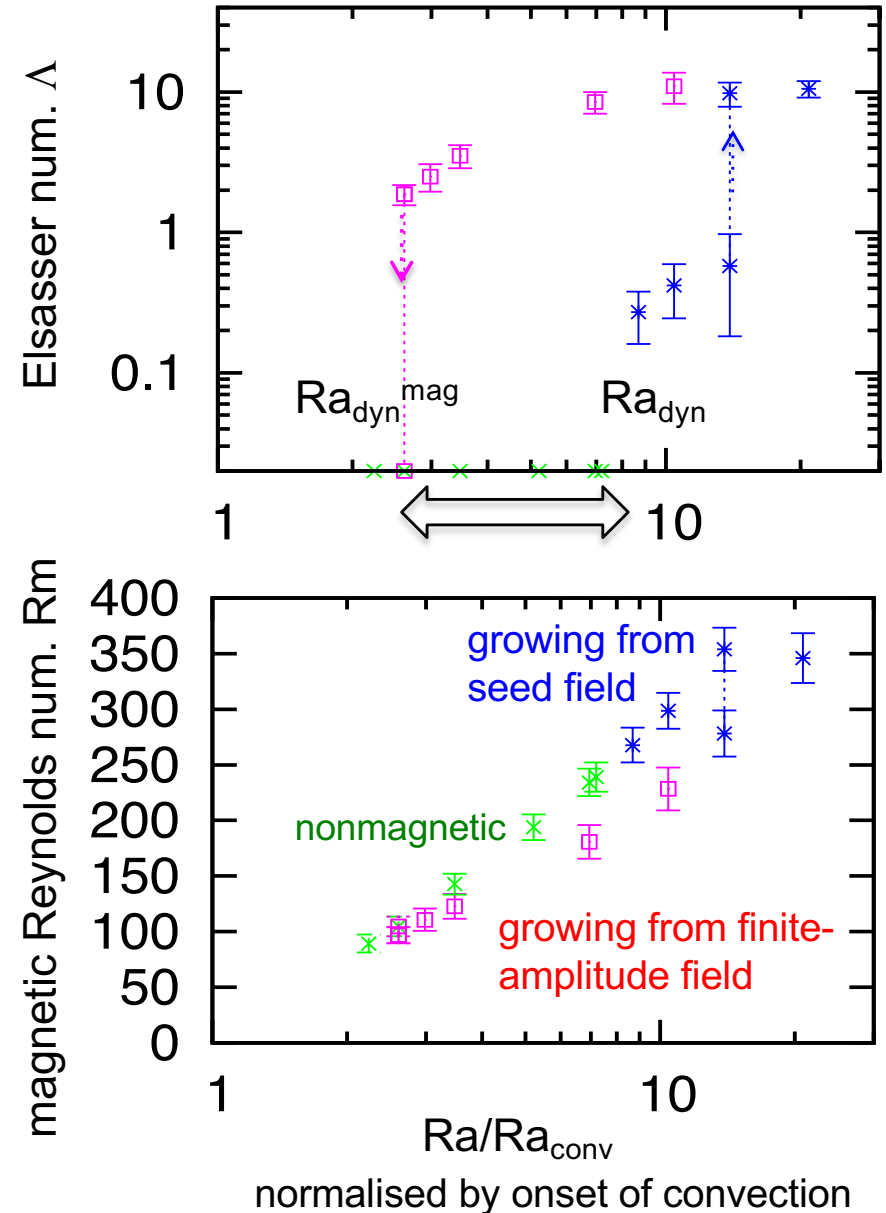
- Characterising length scales feeds into scaling laws



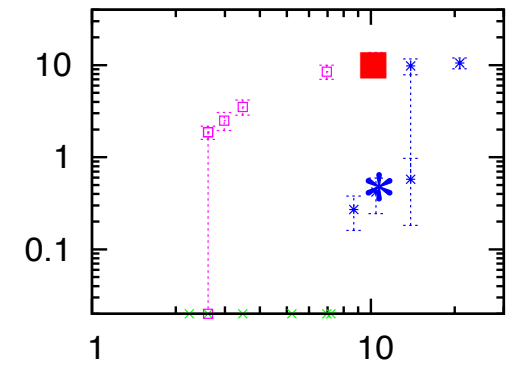
at $E = 10^{-4}$, $Ra/Ra_c = 6.5$, $Pm/Pr = 3$ & $\Lambda \sim 8$
(KH, Wicht & Christensen 2010)

Subcritical, strong- and weak-field dynamos

- Subcritical branches, as well as two branches (bistability), observed
 - quite deep in some cases: $Ra \gtrsim 0.25 Ra_{\text{dyn}}$
 - but none for $Ra < Ra_{\text{conv}}$ (cf. plane layer)
- The subcritical/upper branch:
 - $\Lambda \gtrsim 1$ with dipolar fields only
 - weaker flow vigor ($Rm > 100 \sim Rm_{\text{dyn}}^{\text{mag}}$) & larger convective structures ($1 < m < 4$)
 - ‘strong-field’ dynamos?
- The lower branch:
 - $\Lambda < 1$ with non-dipolar fields only
 - flow vigor ($Rm > 200 \sim Rm_{\text{dyn}}$) & convective structures ($4 < m < 8$) similar to the nonmagnetic convection
 - ‘weak-field’ dynamos?



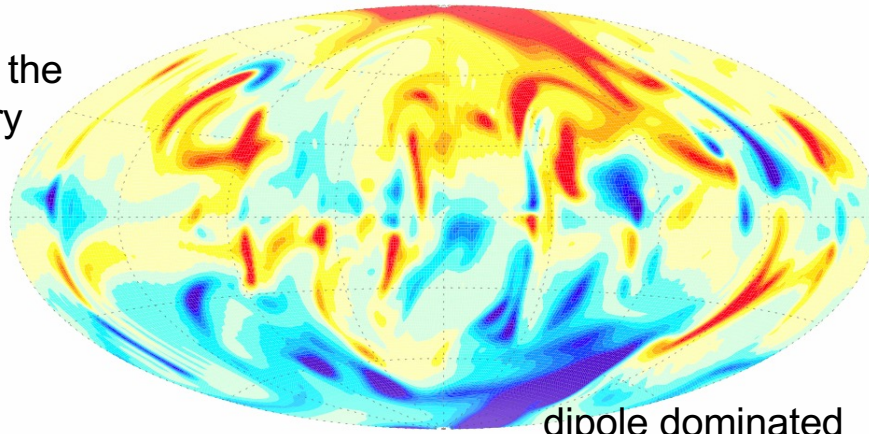
Spatial structures



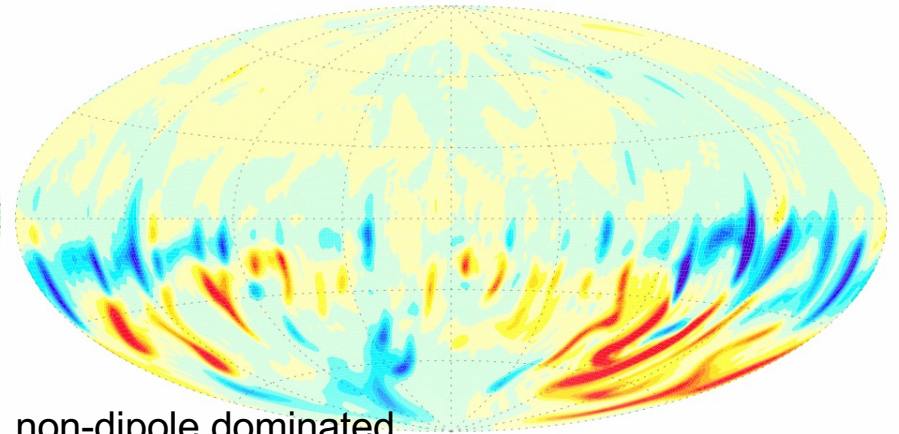
- On the strong-field branch
 - only dipole-dominated fields
 - $\Lambda \gtrsim 1$

- On the weak-field branch
 - only multi-polar fields
 - $\Lambda < 1$

Radial field at the outer boundary

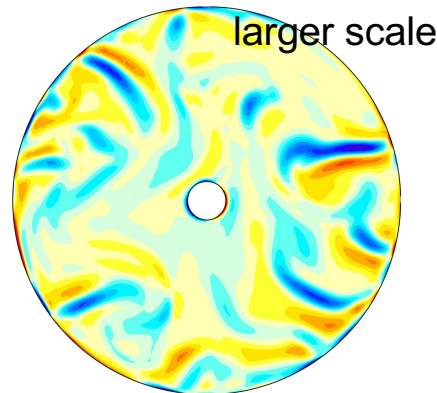


dipole dominated



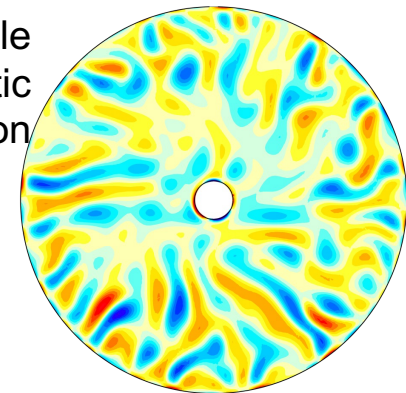
non-dipole dominated

Axial vorticity in the equatorial plane



larger scale

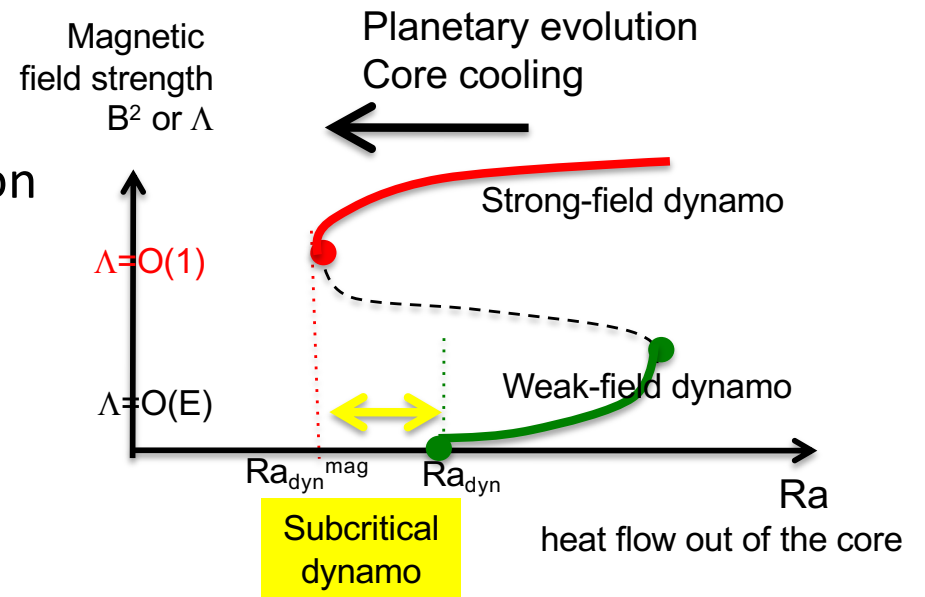
smaller scale
~ nonmagnetic convection



positive: yellow to red
negative: light to dark blue

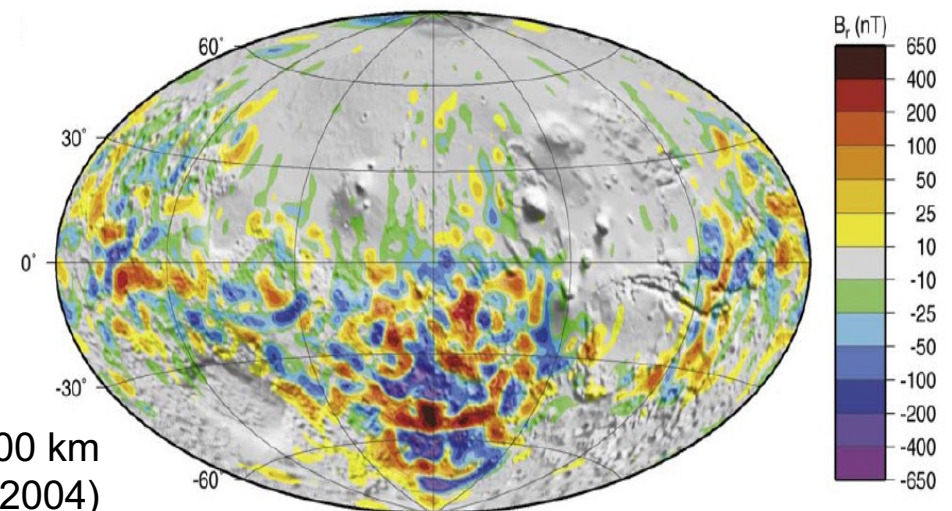
Termination of planetary dynamos

- During a planetary evolution, subcritical dynamo action can
 - maintain a strong field until its termination
 - complete the shut-down
 - Dynamo action cannot simply restart, once buoyancy anomaly and magnetic field become lower than its critical points



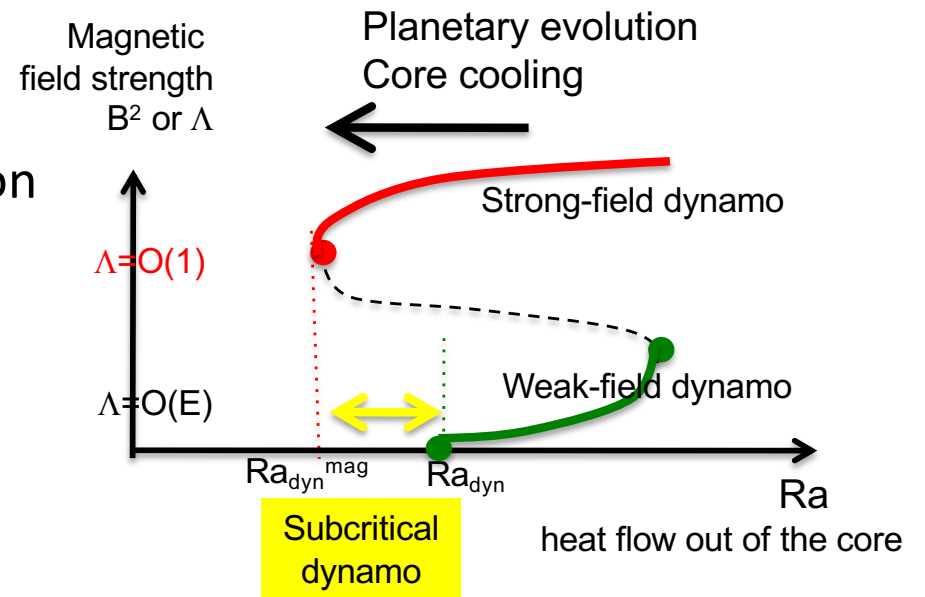
- The scenario worked in early Mars? (e.g. Kuang+ 2008)
 - operated likely between 4.5 – 4 Ga (e.g. Acuna+ 1999; Weiss+ 2002)
 - died quickly, within 20Ma? (Lillis+ 2008)

Br at altitude 200 km
(MGS; Langlais et al. 2004)

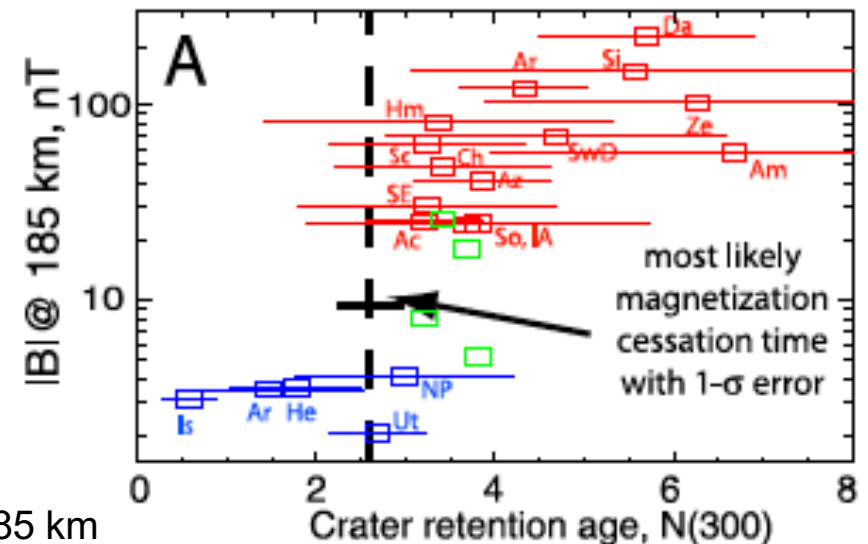


Termination of planetary dynamos

- During a planetary evolution, subcritical dynamo action can
 - maintain a strong field until its termination
 - complete the shut-down
 - Dynamo action cannot simply restart, once buoyancy anomaly and magnetic field become lower than its critical points



- The scenario worked in early Mars? (e.g. Kuang+ 2008)
 - operated likely between 4.5 – 4 Ga (e.g. Acuna+ 1999; Weiss+ 2002)
 - died quickly, within 20Ma? (Lillis+ 2008)



Magnetic field strength at altitude 185 km for 15 large basins (Lillis et al. 2008)

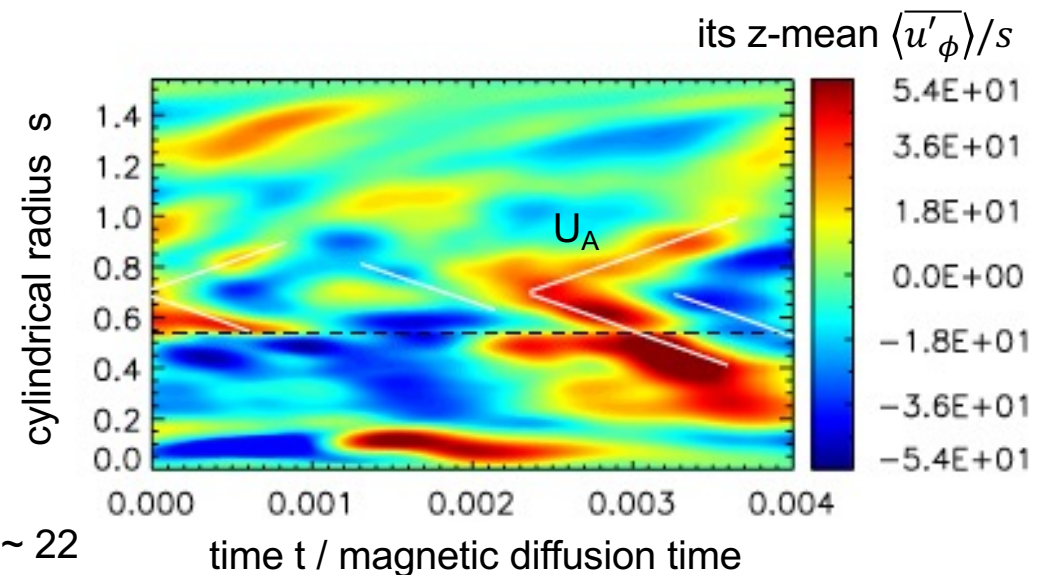
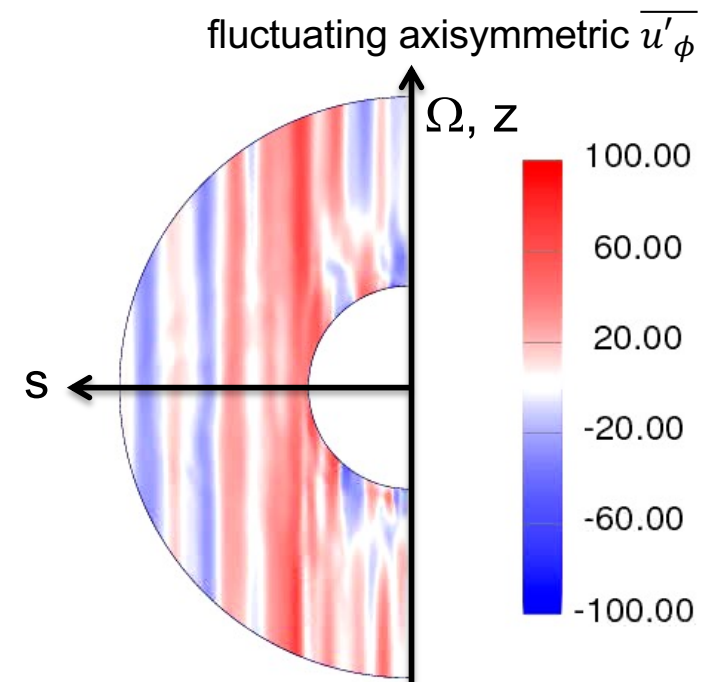
Time scales

- A magnetostrophic balance will lead to
 - nonaxisymmetric modes: e.g. slow magnetic Rossby waves
 - axisymmetric modes: torsional oscillations
- The axisymmetric modes identified (e.g. Wicht & Christensen 2008; Teed et al. 2014):
 - perturbations about the Taylor state
 - wave equation for $\zeta'(s,t) = u'_\phi/s$

$$\frac{\partial^2 \zeta'}{\partial t^2} = \frac{1}{s^3 h} \frac{\partial}{\partial s} \left(s^3 h \frac{\langle \widetilde{B}_s^2 \rangle}{\rho \mu_0} \frac{\partial \zeta'}{\partial s} \right)$$

- propagate along a poloidal field component \widetilde{B}_s
- (details in part 3)

at $E = 10^{-5}$, $Ra/Ra_c = 8$, $Pm/Pr = 5$ & $\Lambda \sim 22$
 (Teed, Jones & Tobias, 2014)



Time scales (cont'd)

- Nonaxisymmetric, slow modes identified:

- retrograde drifts commonly seen in early numerical dynamos
- their speeds accounted for by total phase speeds of wave and mean flow advection, $(\omega_{MR} + \omega_{adv})/m$, where

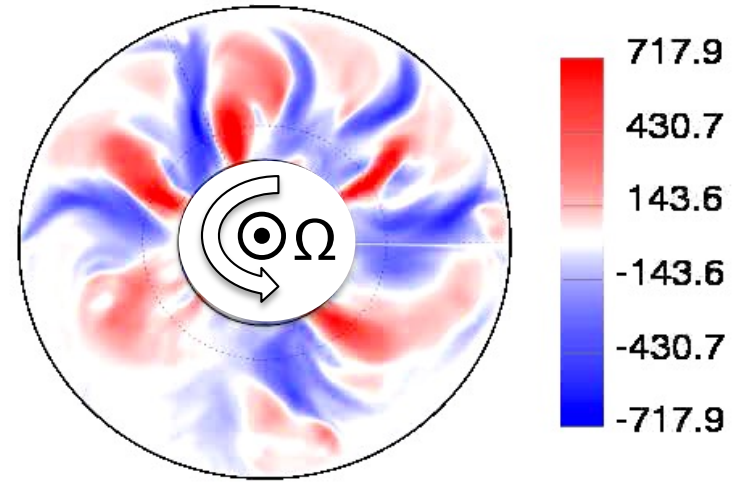
$$\hat{\omega}_{MR} = -\frac{\hat{\omega}_M^2}{\hat{\omega}_R} = -\frac{m^3(r_o^2 - s^2)\langle \widetilde{B_\phi^2} \rangle}{2\rho\mu_0\Omega s^4}$$

- can propagate along a toroidal field component $\widetilde{B_\phi}$

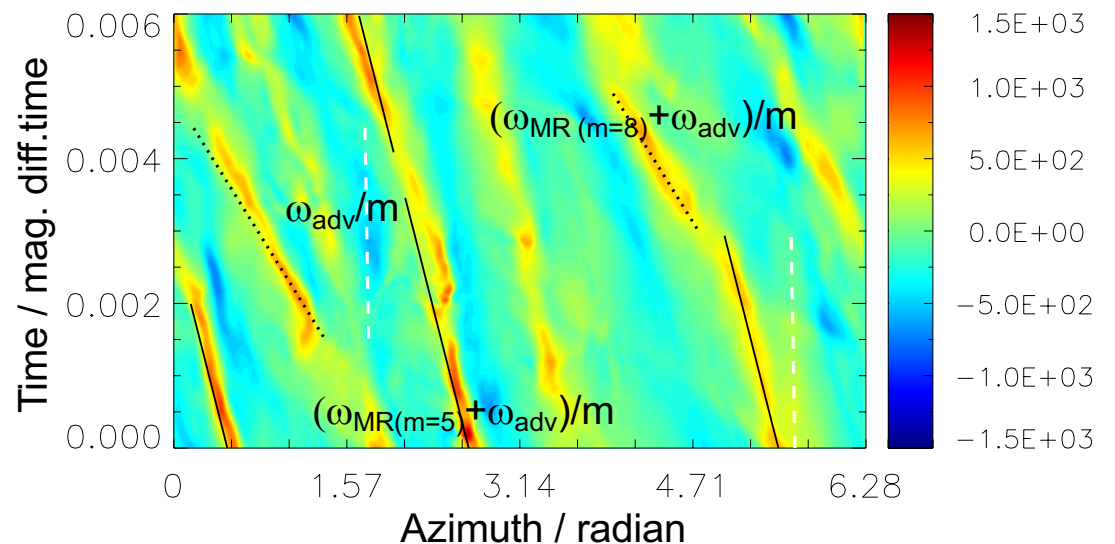
- The waveforms illustrate

- no wave trains
- but **isolated, sharp crests**
- (details in part 2)

z-mean radial velocity $\langle u_s \rangle$
in the equatorial plane



$\langle u_s' \rangle$ at $s=0.5r_o$



at $E = 10^{-5}$, $Pm/Pr = 5$, $Ra/Ra_c = 8$ & $\Lambda \sim 22$
(KH, Jones & Teed, 2015)

Time scales (cont'd)

- Nonaxisymmetric, slow modes identified:

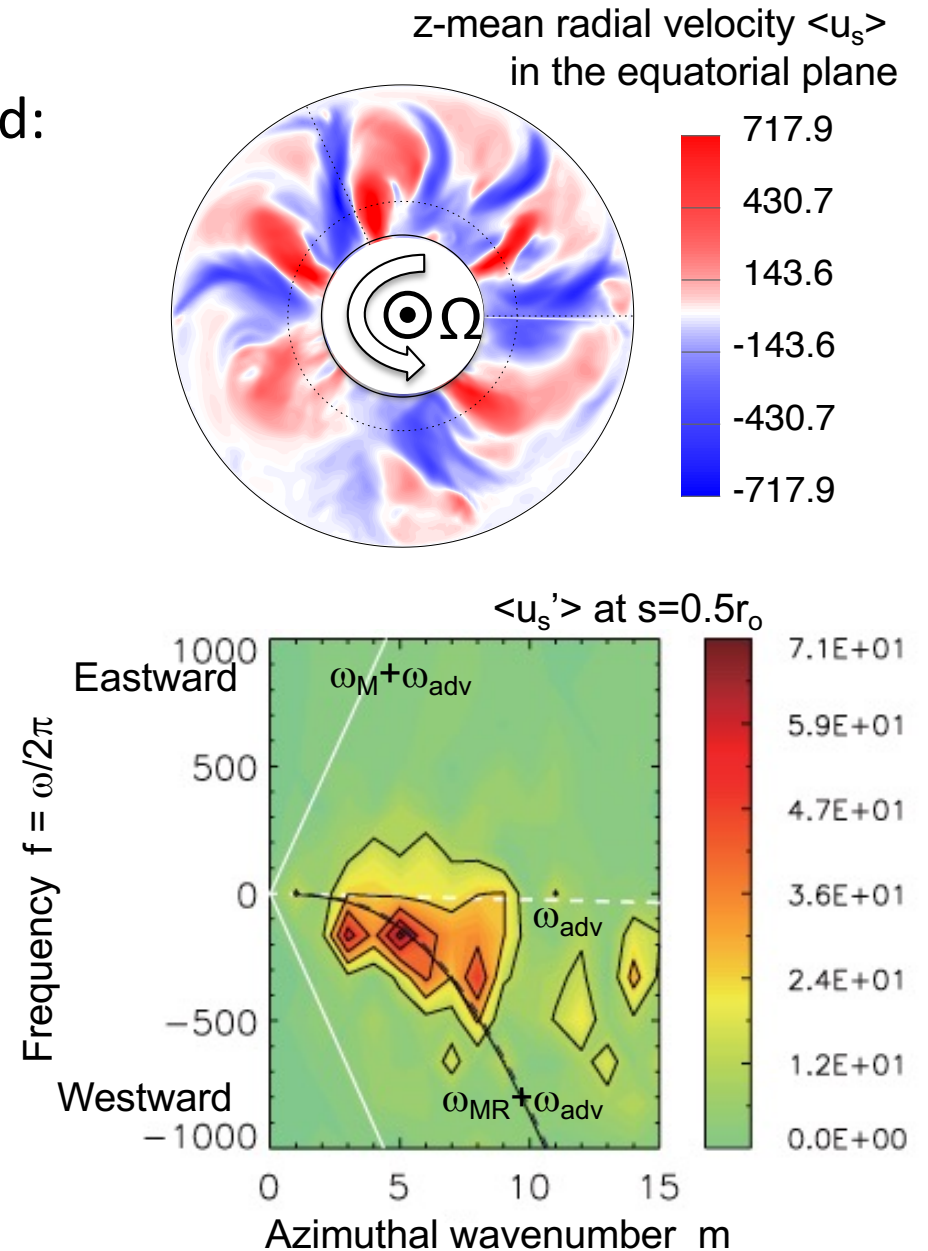
- retrograde drifts commonly seen in early numerical dynamos
- their speeds accounted for by total phase speeds of wave and mean flow advection, $(\omega_{MR} + \omega_{adv})/m$, where

$$\hat{\omega}_{MR} = -\frac{\hat{\omega}_M^2}{\hat{\omega}_R} = -\frac{m^3(r_o^2 - s^2)\langle \widetilde{B}_\phi^2 \rangle}{2\rho\mu_0\Omega s^4}$$

- can propagate along a toroidal field component \widetilde{B}_ϕ

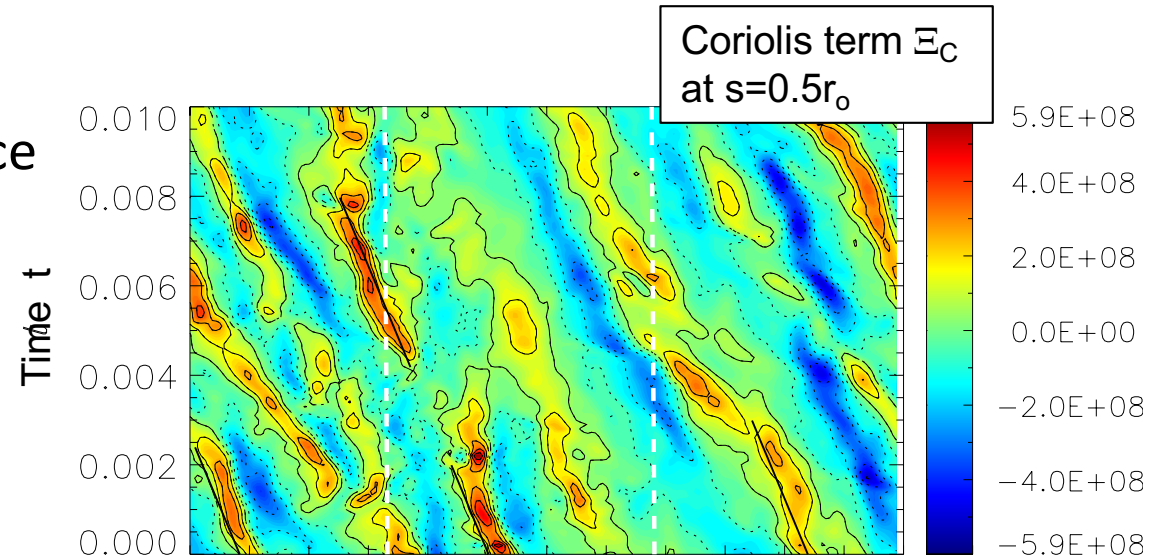
- The waveforms illustrate

- no wave trains
- but **isolated, sharp crests**
- (details in part 2)



Force balances

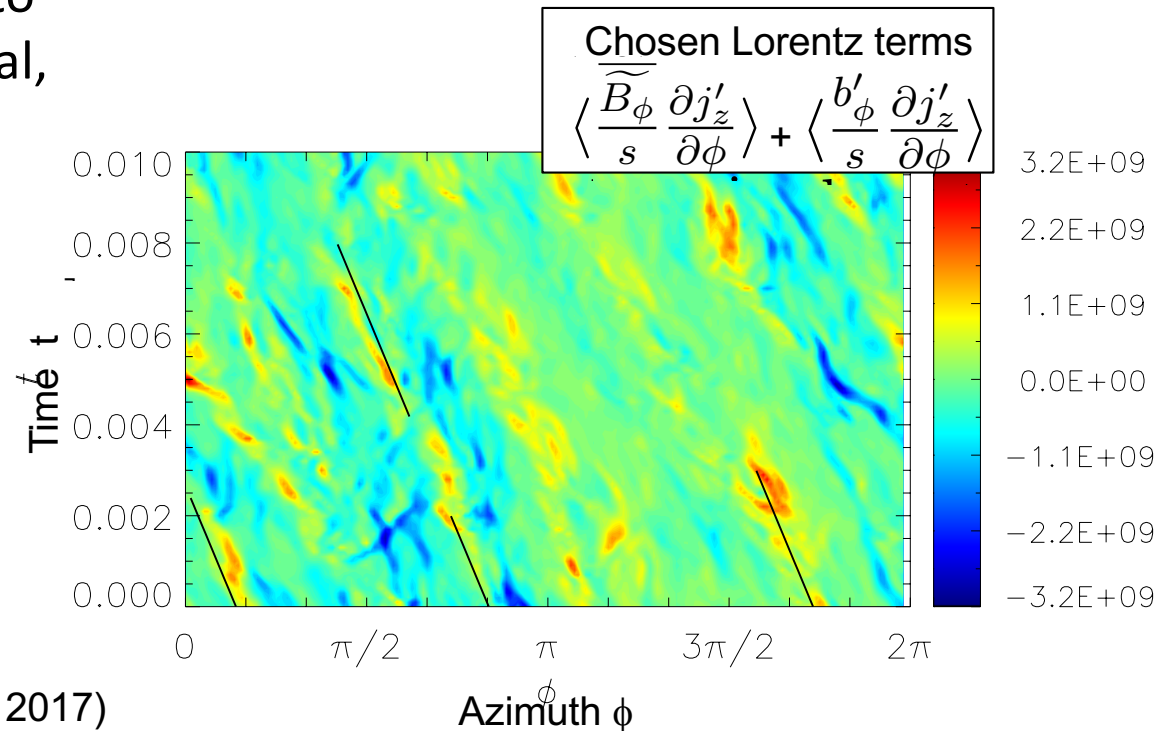
- Exemplifies the dominant balance between Coriolis and Lorentz terms in the axial vorticity eq.
 - Reynolds term remains minor



- The Lorentz term Ξ_L expanded into the restoring force and its residual, e.g.

$$\Xi_L = \frac{Pm}{E} \left[\langle \widetilde{\mathbf{B}} \cdot \nabla j'_z \rangle + \langle \mathbf{b}' \cdot \nabla j'_z \rangle + (\text{other terms}) \right]$$

- the sum of the restoring and leading nonlinear terms tends to reproduce the waveforms



(KH, Teed & Jones 2017)

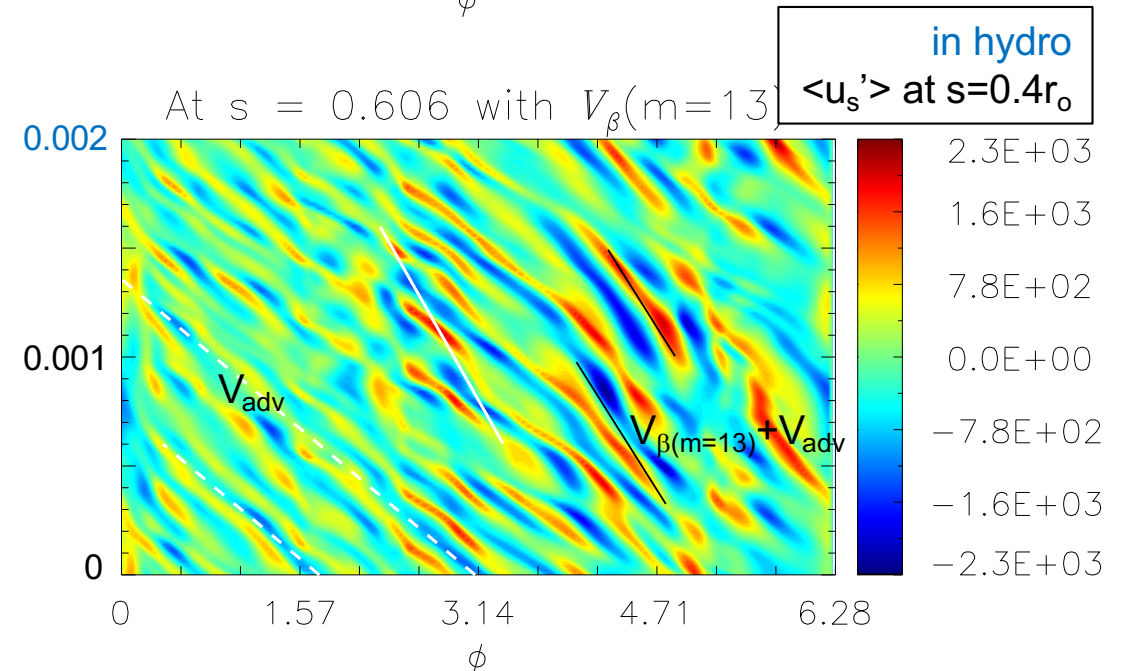
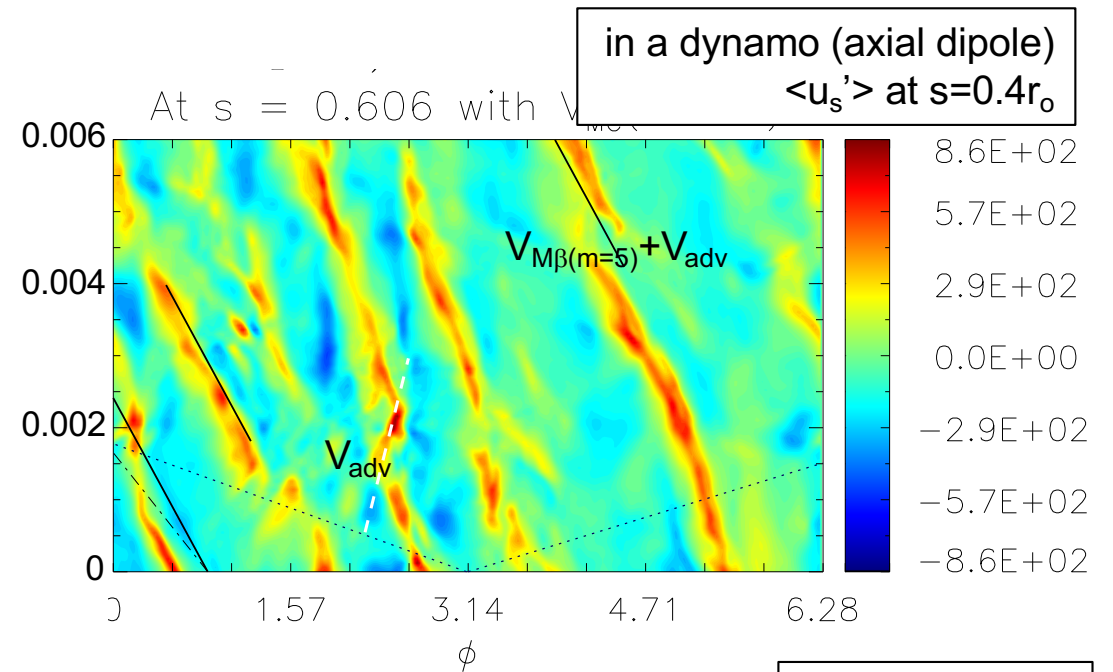
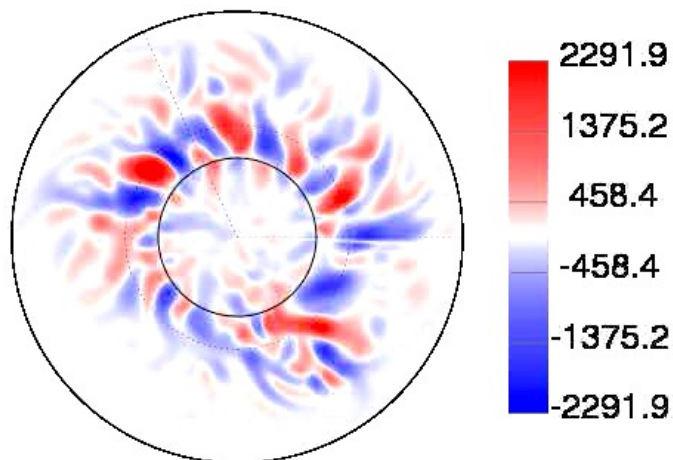
The role of magnetic field

The respective nonmagnetic convection reveals

- much faster variations & smaller-scale spatial structures
- more signals from prograde drifts (with respect to the mean flow)

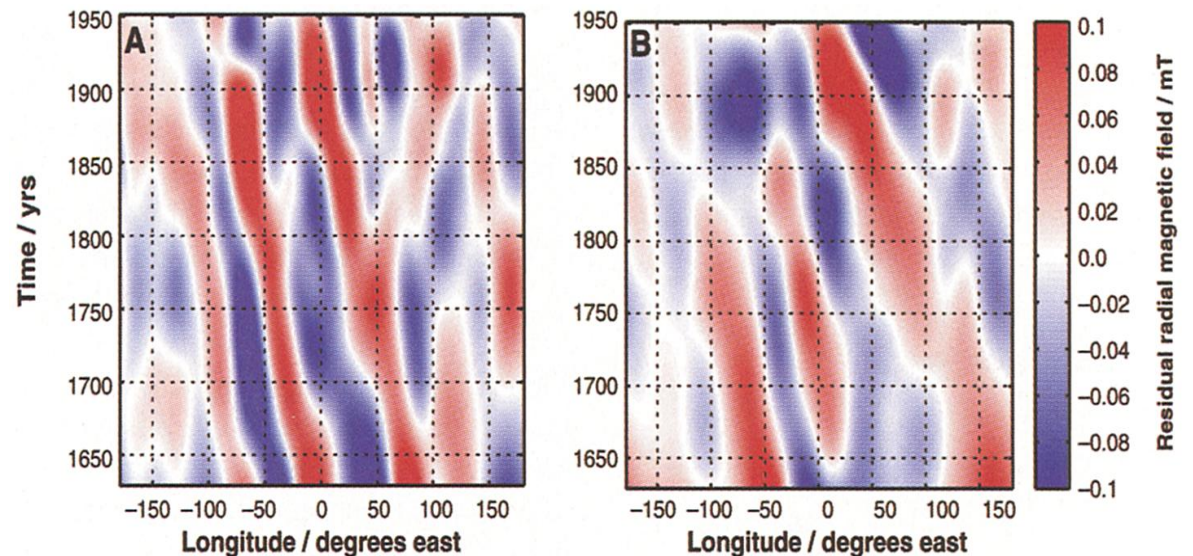
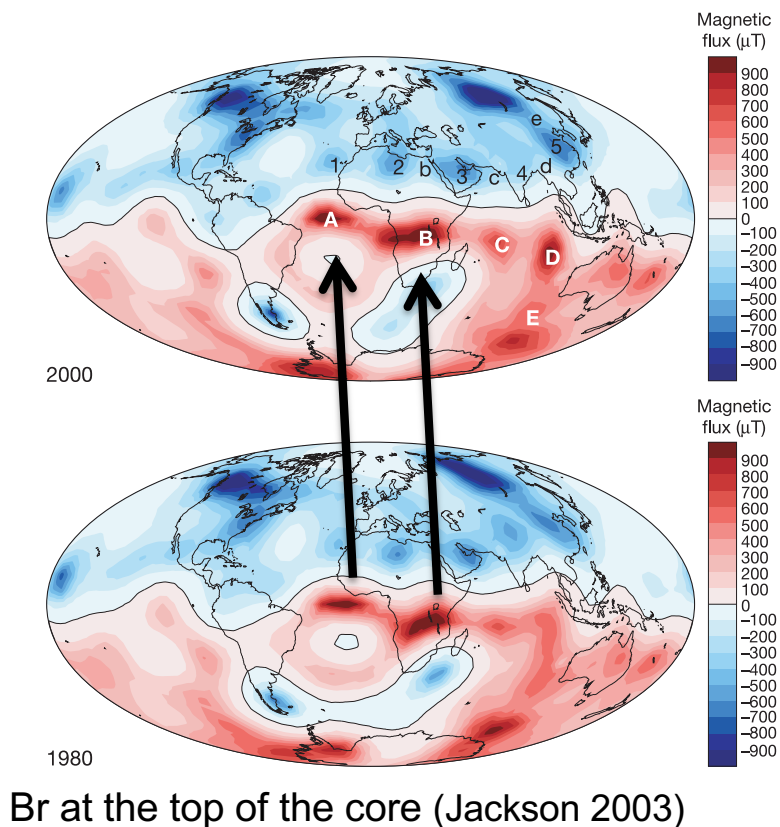
$$\hat{\omega}_\beta = \frac{2\Omega s^2}{(r_o^2 - s^2)m}$$

$\langle u_s \rangle$ in the equatorial plane



Magnetic secular variation

- Possibly linked to the westward drifts or its rapid dynamics
 - the nonaxisymmetric part migrating on timescales of ≥ 300 yrs
 - also for ~ 6 yr westward drift? (Chuliat et al. 2015; Gillet, Gerick, et al. 2022)
 - flow advection? (Bullard et al. 1950) or wave propagation? (Hide 1966)
more likely their mixture



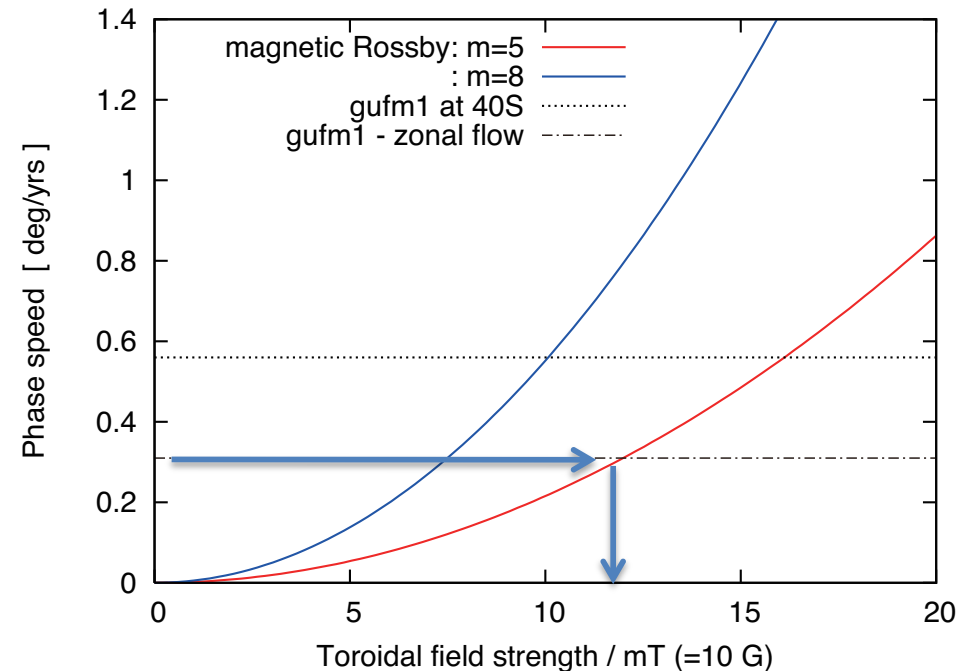
Toroidal field strength within a planetary dynamo

- Assuming the wave enables us to infer the azimuthal field
 - essentially hidden beneath the rocky mantle
 - crucial for dynamo action

- The approximate dispersion relation:

$$\hat{\omega}_{MR} = \omega - \omega_{adv} = -\frac{m^3(r_o^2 - s^2)\langle \widetilde{B_\phi^2} \rangle}{2\rho\mu_0\Omega s^4}$$

- a geomagnetic drift speed of 0.56 °/yr at 40° S (Finlay & Jackson 2003)
- suppose half for a mean flow
- Given m=5, this implies a **toroidal field** $B_\phi \sim 10$ mT at $s \sim 0.8r_o$
 - equivalent to, or stronger than, the poloidal part $B_s \geq 3$ mT (Gillet et al. 2010)

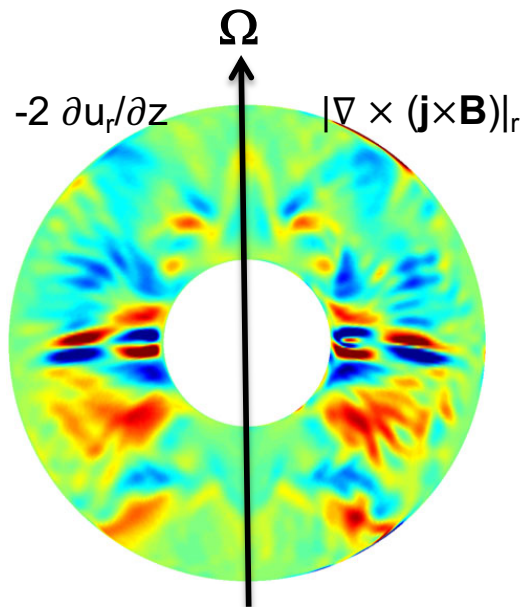


(KH, Jones & Teed, 2015)

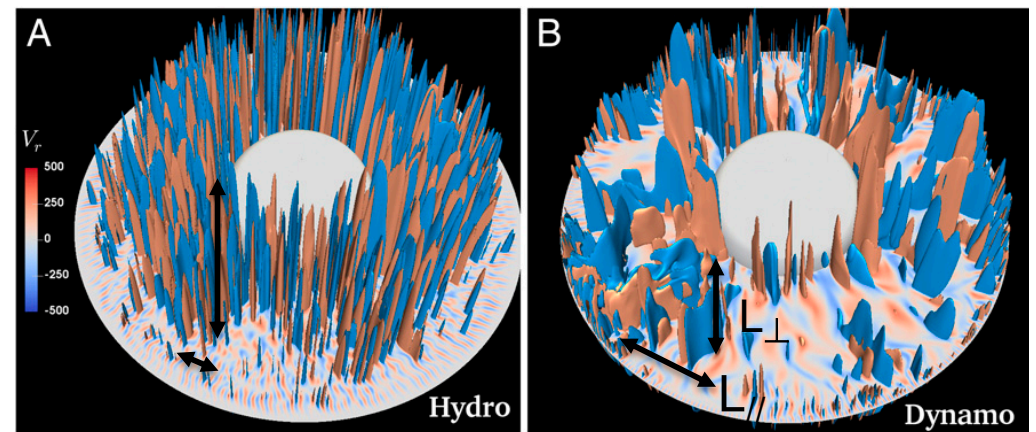
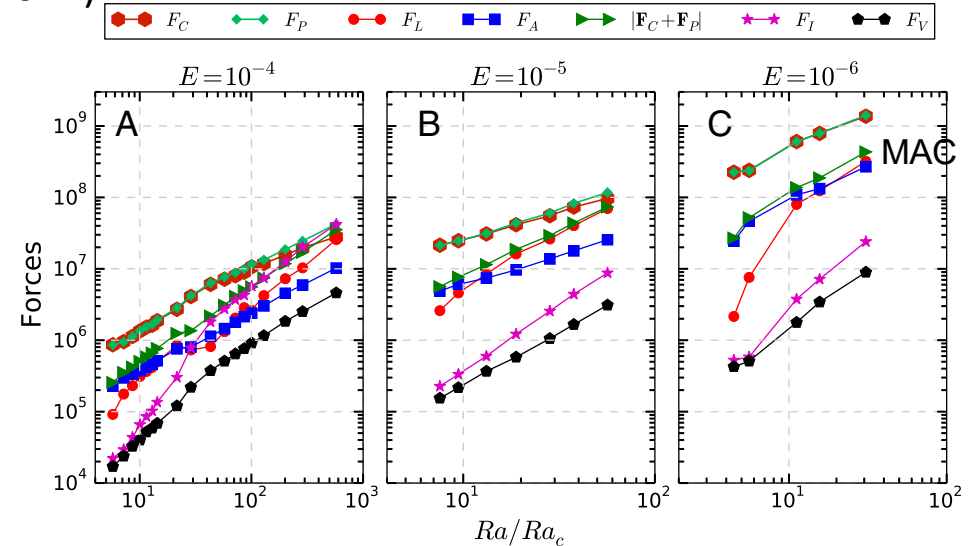
After all: hunt for magnetostrophic dynamos

- Convection-driven spherical dynamos finding (the way to) the Earth/planet-like models (e.g. Yadav et al. 2016; Dormy 2016; Schaeffer et al. 2017)

- in force balances
- in flow properties (length scales, heat transfer, and waves)



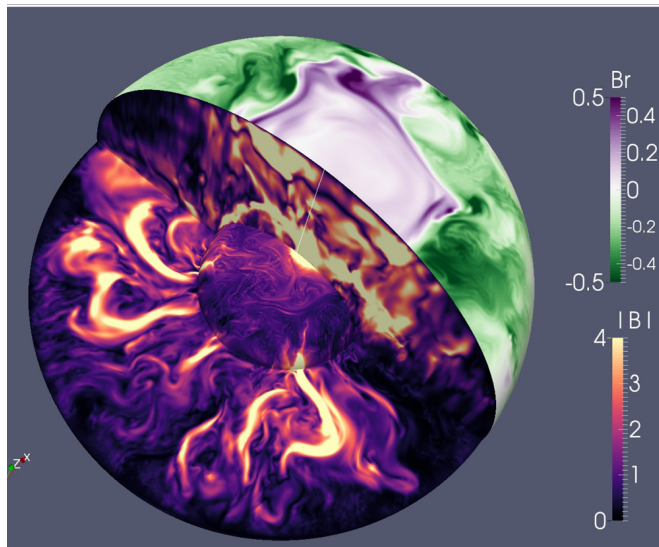
at $Pm/Pr = 18$, $E = 3 \cdot 10^{-4}$, $Ra/Ra_c = 1.7$ on a SF branch $\Lambda \sim 1.1$ (Dormy 2016)



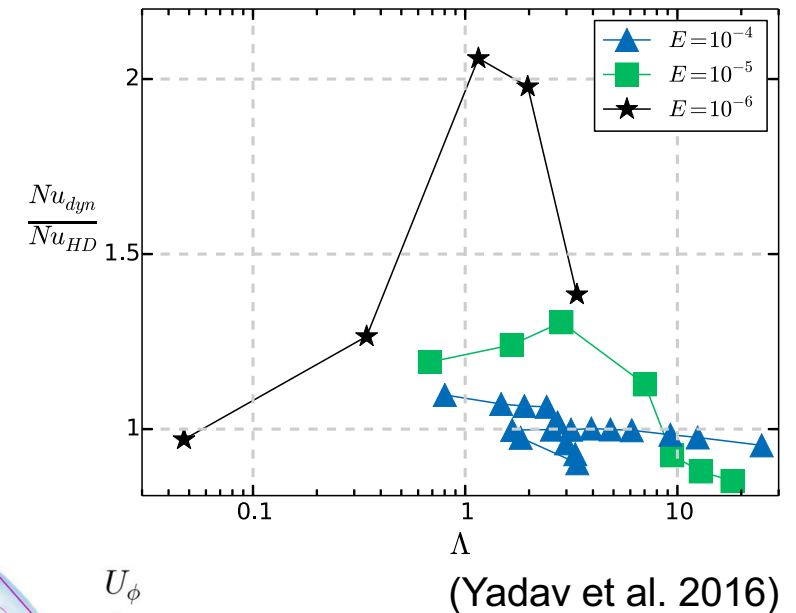
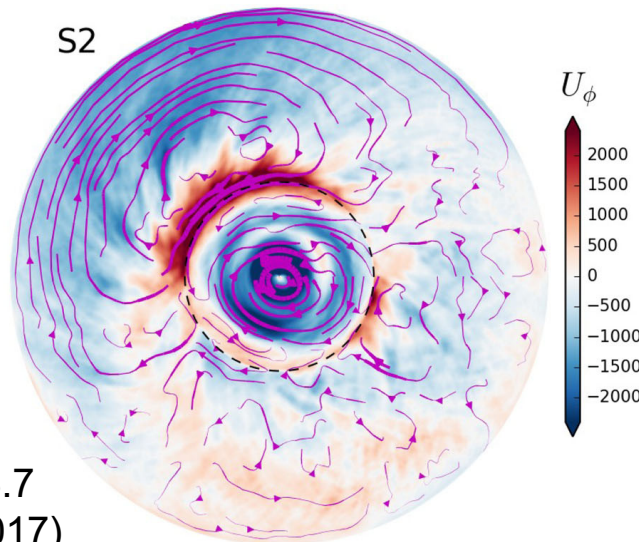
at $E = 10^{-6}$, $Pm/Pr = 0.5$, $\Lambda \lesssim 4$ (Yadav et al. 2016)

After all: hunt for magnetostrophic dynamos

- Convection-driven spherical dynamos
finding (the way to) the Earth/planet-like models
(e.g. Yadav et al. 2016; Dormy 2016; Schaeffer et al. 2017)
 - in force balances
 - in flow properties (length scales, heat transfer, and waves)



at $E = 10^{-7}$, $Pm/Pr = 0.1$, $\Lambda \sim 3.7$
($< 0.05 \tau_{mag}$; Schaeffer et al. 2017)



After all: hunt for magnetostrophic dynamos

- Convection-driven spherical dynamos finding (the way to) the Earth/planet-like models

(e.g. Yadav et al. 2016; Dormy 2016; Schaeffer et al. 2017)

- in force balances
- in flow properties (length scales, heat transfer, and waves)
- in scaling properties (e.g. Aubert et al. 2017)
 - more like the one by Davidson (2013)?
- reversals also possible (Jones & Tsang 2025)

Table 1 Proposed scaling laws (after Christensen 2010)

#	Rule	Author
1	$B_p R_p^3 \propto (\rho \Omega R_p^5)^a$	e.g. Russell (1978)
2	$B^2 \propto \rho \Omega^2 R_c^2$	Busse (1976)
3	$B^2 \propto \rho \Omega \sigma^{-1}$	Stevenson (1979)
4	$B^2 \propto \rho R_c^3 q_c \sigma$	Stevenson (1984)
5	$B^2 \propto \rho \Omega R_c^{5/3} q_c^{1/3}$	Curtis and Ness (1986, modified)
6	$B^2 \propto \rho \Omega^{3/2} R_c \sigma^{-1/2}$	Mizutani et al. (1992)
7	$B^2 \propto \rho \Omega^2 R_c$	Sano (1993)
8	$B^2 \propto \rho \Omega^{1/2} R_c^{3/2} q_c^{1/2}$	Starchenko and Jones (2002)
9	$B^2 \propto \rho R_c^{4/3} q_c^{2/3}$	Christensen and Aubert (2006)

$l_B = \text{Rm}^{-1/2} R_c$
CIA balance?

+ 10 $B^2 \propto \rho^{1/3} R_c^{2/3} q_c^{2/3}$ Davidson (2013)
given $B=B(l, q_c)$
MAC balance

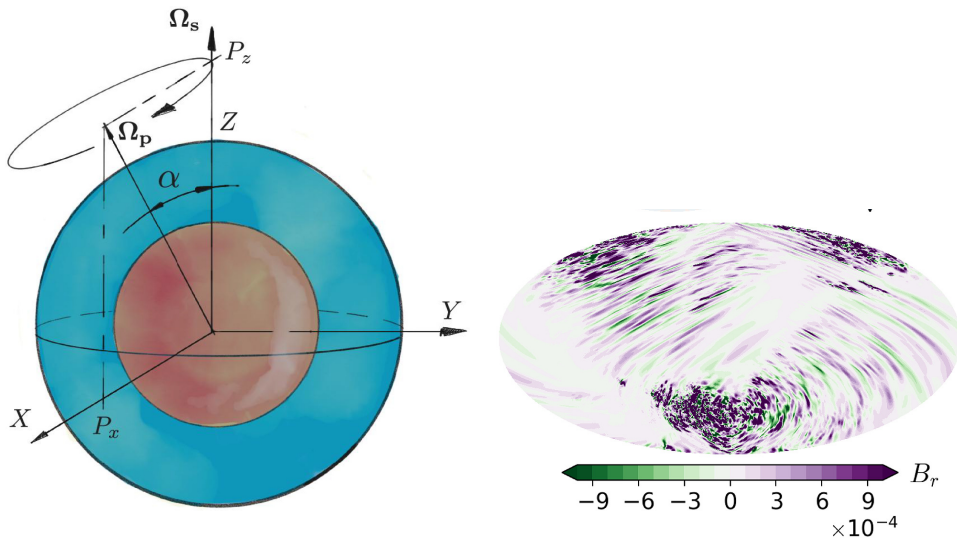
- The proven importance enables us to adopt the approximated approaches too?
 - e.g. taking the limit (Jackson et al.)

Summary

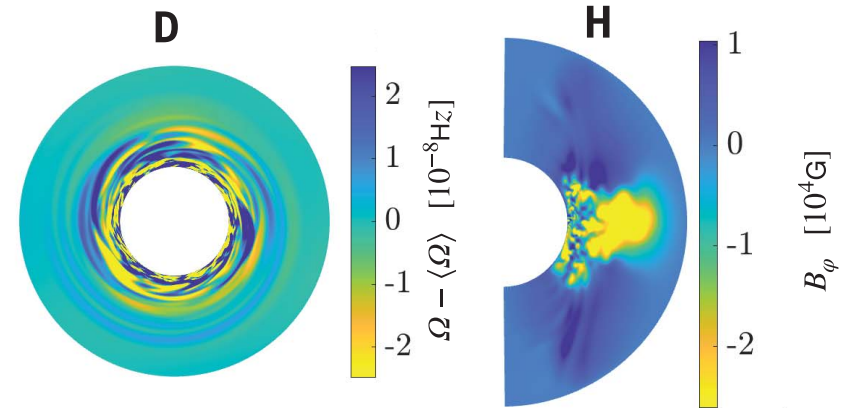
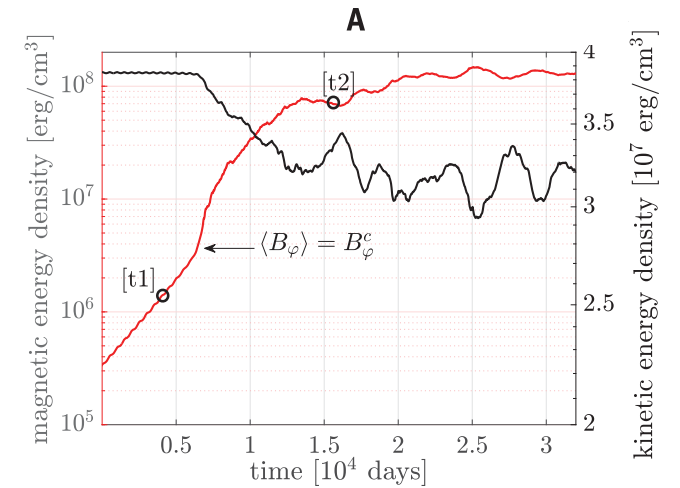
- Magneto-strophic regimes were long speculated for planetary interiors/dynamos
 - where MAC forces will play a predominant role (cf. geo-strophic)
- The regime may be signified by
 - convection & its driven dynamos (subcritical/strong-field)
 - larger length scales (cf. the rotating conv/weak-field)
 - slower waves/oscillations
- Now proving the existence and its branches
 - suggesting Earth/planet-like models dynamically become possible
- Relevant GAFD implications include
 - scaling laws, termination of dynamos, magnetic secular variations

対流/熱以外でもダイナモ

- 他の駆動源による磁場形成
 - 安定成層 (Petitdemange et al. 2023)
 - Taylor-Spruit (Ω 効果 + トロイダル磁場の不安定化)
 - 歳差運動 (Tilgner 2005; Cébron et al. 2019)
 - ほぼ非双極子型 (小スケール) の磁場
 - 波 (Davidson 2014; Davidson & Ranjan 2015)
 - etc.



(Cébron+ 2019)



At $t = t_2$ after the Taylor instability sets in ($N/\Omega = 1.24$; Petitdemange+ 2019)

Solitary magnetic Rossby waves

Kumiko Hori

National Institute for Fusion Science, Japan

Japan Soc. Fluid Mech., 174, Tokyo, September 2019;

J. Fluid Mech. Rapids, 904, R3, 2020



gfd seminars 2
Hokkaido, 15-16 March 2025



Rossby waves

A fundamental class of waves in the rotating dynamics

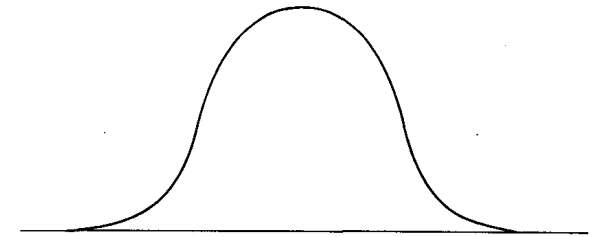
- arising from vortex tube stretching/shrinking
- the simplest dispersion relation: $\omega_R = \frac{\beta k}{k^2 + l^2}$

Nonlinear Rossby waves may reveal coherent structures:

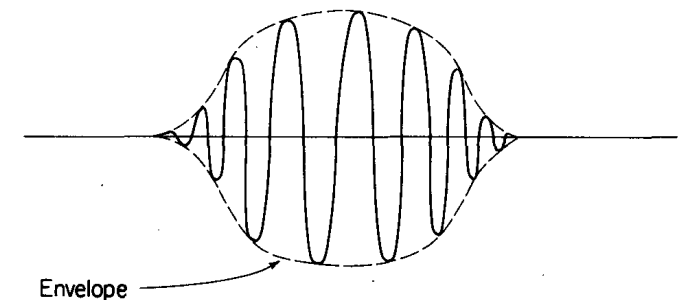
- soliton, cnoidal waves
 - QG PV equation with shear flows and/or topography [Redekopp(1977), Malanotte-Rizzoli(1982)]
 - equatorial shallow-water eq [Boyd(1980)]
- envelope soliton [Yamagata(1980), Boyd(1983)]
- modon, rider [Flierl et al.(1980)]

Theories were applied to Jupiter's GRS, etc.

UNIMONTANE SOLITON
KORTEWEG-DE VRIES EQUATION



ENVELOPE SOLITON
NONLINEAR SCHRÖDINGER EQUATION

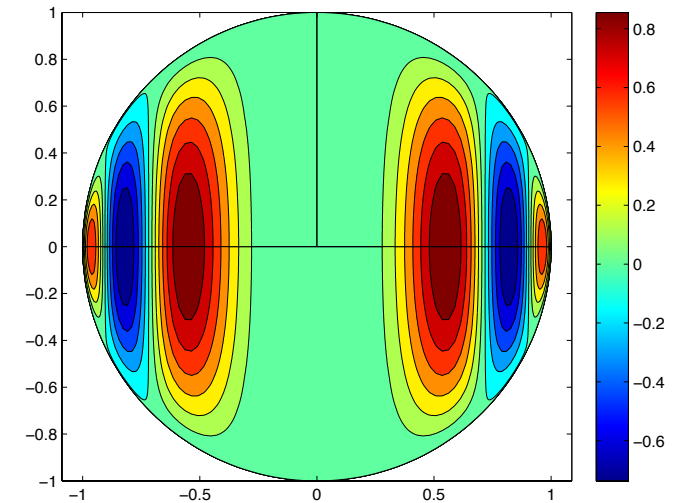


[Boyd(1980)]

Magnetic Rossby waves

The presence of magnetic field may split it into

- fast modes $\sim +\omega_R \left(1 + \frac{\omega_A^2}{\omega_R^2}\right)$
- slow modes $\sim -\frac{\omega_A^2}{\omega_R} = -\frac{(\mathbf{B}_0 \cdot \mathbf{k})^2 |\mathbf{k}|^2}{\rho \mu_0 \beta k}$
 - in a magnetostrophic/MC balance
 - sensitive to the toroidal field
 - preferred for spherical convection at large Pm and moderate Pr



[Malkus(1967)]

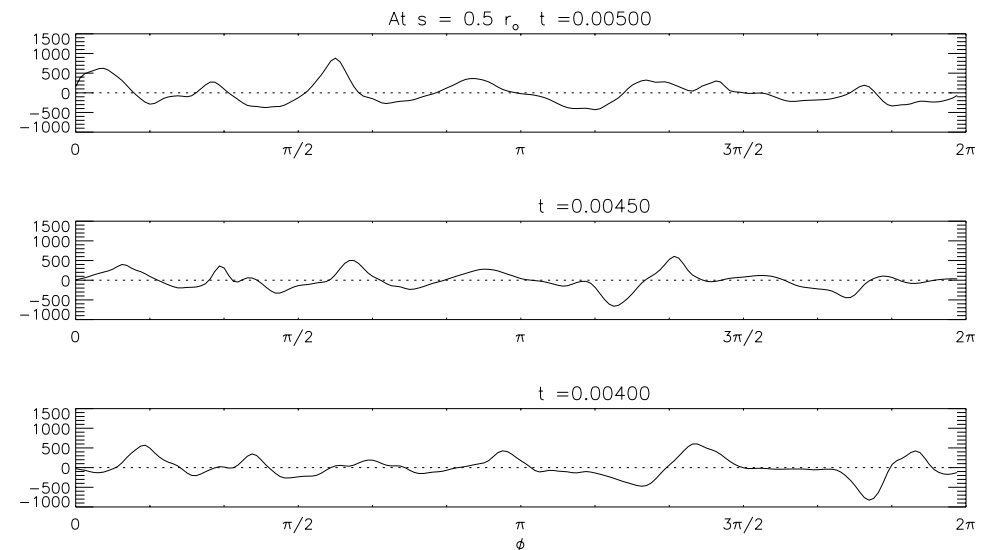
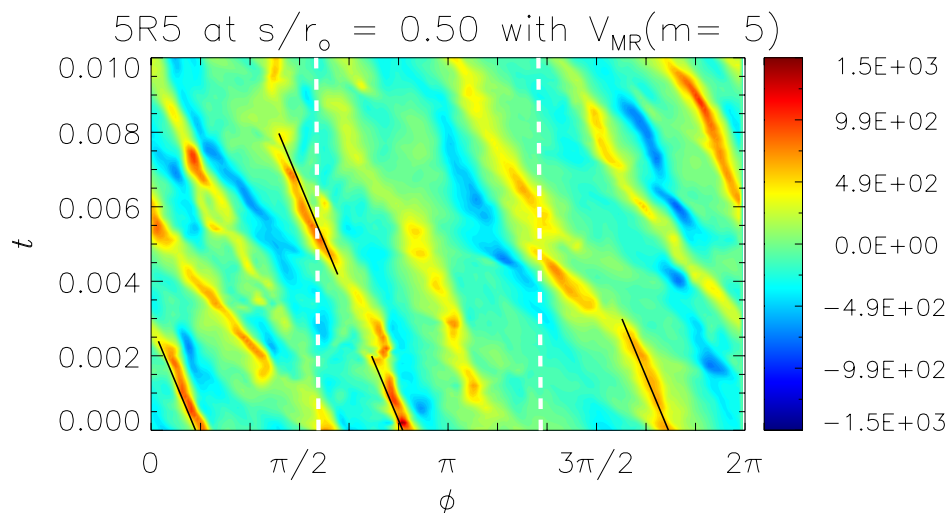
Their potential geo/astro-physical applications to

- slow modes in Earth's fluid core: slow [Hide(1966), Hori et al.(2015)]
- fast modes in a thin stratified layer at the top of the core [Braginsky(1967), Chulliat et al.(2015)]
- fast modes in solar tachocline [Zaqarashvili et al.(2010), McIntosh et al.(2017)]

Linear theory is under debate [Márquez-Artavia et al.(2017)].

Can nonlinear MR waves shape coherent structures?

- isolated, sharp crests seen in spherical dynamo simulations
- solitary waves in equatorial, shallow-water MHD [London(2017)]
 - no mean flow \bar{U} , $\beta \sim \tanh y$, a basic field $\bar{B} \sim \tanh y$
 - fast modes for weak field: cf. [Boyd(1980)]
 - 'a slow magnetostrophic' mode for strong field
- slow modes in QG MHD/MC models [Hori et al.(2020)]
 - to test the role of shear flow \bar{U} , topography β , and magnetic field \bar{B}
 - no stable stratification
- modons in shallow-water MHD [Lahaye & Zeitlin(2022)]



Busse's QG annulus model

A cartesian model useful to analyse the rapidly rotating dynamics in a sphere [Busse(1970)].

Here the geometry is represented by sloping top/bottom boundaries with a small angle χ .

With the rotation axis $\Omega \hat{z}$, we suppose

$$|u_x|, |u_y| \gg |u_z|.$$

In the MHD [Busse(1976), Abdulrahman et al.(2000)] we begin with equations for the axial vorticity,

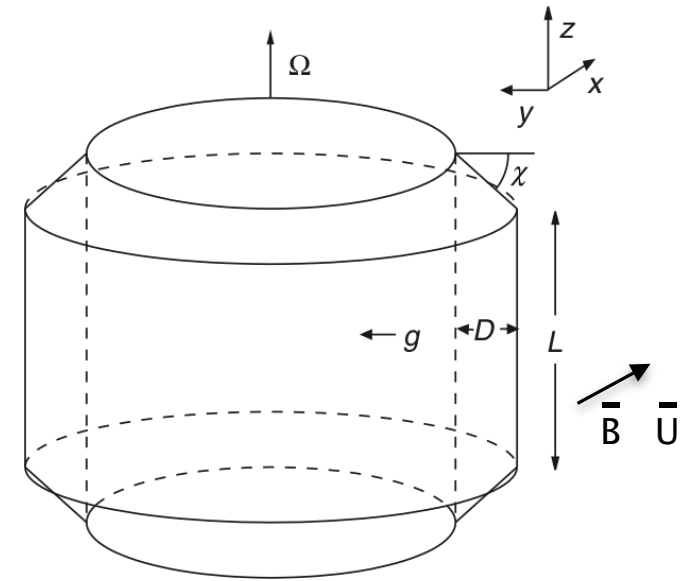
$\xi_z = \hat{z} \cdot (\nabla \times \mathbf{u})$, and the axial electric current,

$$J_z = \hat{z} \cdot \left(\frac{1}{\mu_0} \nabla \times \mathbf{B} \right):$$

$$\frac{\partial \xi_z}{\partial t} + \mathbf{u} \cdot \nabla \xi_z - 2\Omega \frac{\partial u_z}{\partial z} = \frac{1}{\rho} \mathbf{B} \cdot \nabla J_z, \quad (1)$$

$$\frac{\partial \mathbf{B}}{\partial t} = \nabla \times (\mathbf{u} \times \mathbf{B}) \quad (2)$$

with $\nabla \cdot \mathbf{u} = \nabla \cdot \mathbf{B} = 0$. Boundary conditions are $u_z = \pm u_y \chi$ at $z = \pm \frac{L}{2}$ and $u_y = 0$ at $y = 0, D$.



adapted from [Jones(2015)]

Streamfunctions and scaling

Using a streamfunction we can write $\mathbf{u} \sim \nabla \times \psi(x, y)\hat{\mathbf{z}}$. Further, we assume the magnetic field where $|B_x|, |B_y| \gg |B_z|$, and represent $\mathbf{B} \sim \nabla \times g(x, y)\hat{\mathbf{z}}$. The vorticity and the current are given by $\xi_z = -\Delta_2\psi$ and $J_z = -\frac{1}{\mu_0}\Delta_2g$, respectively, with $\Delta_2 = \frac{\partial^2}{\partial x^2} + \frac{\partial^2}{\partial y^2}$.

Now we nondimensionalise variables as

$$\tilde{x} = \frac{x}{\lambda}, \quad \tilde{y} = \frac{y}{D}, \quad \tilde{t} = \frac{t}{\lambda/c_{\text{MR}}}, \quad \tilde{\psi} = \frac{\psi}{c_{\text{MR}}D}, \quad \tilde{g} = \frac{g}{B_0D}, \quad \text{and} \quad \tilde{\chi} = \frac{\chi/L}{\chi_0/L_0}$$

where $c_{\text{MR}} = \frac{c_{\text{A}}^2}{c_{\text{R}}} = \frac{B_0^2/\rho\mu_0}{4\Omega\chi_0\lambda^2/L_0}$. This gives us the dimensionless equations

$$\frac{\partial}{\partial \tilde{t}} \tilde{\Delta}_2 \tilde{\psi} + \frac{\partial(\tilde{\psi}, \tilde{\Delta}_2 \tilde{\psi})}{\partial(\tilde{y}, \tilde{x})} - \frac{c_{\text{R}}}{c_{\text{MR}}} \tilde{\chi} \frac{\partial \tilde{\psi}}{\partial \tilde{x}} = \frac{c_{\text{R}}}{c_{\text{MR}}} \frac{\partial(\tilde{g}, \tilde{\Delta}_2 \tilde{g})}{\partial(\tilde{y}, \tilde{x})} \quad (3)$$

$$\frac{\partial}{\partial \tilde{t}} \tilde{g} = \frac{\partial(\tilde{g}, \tilde{\psi})}{\partial(\tilde{y}, \tilde{x})} \quad (4)$$

with $\delta = \frac{\lambda}{D}$ and $\tilde{\Delta}_2 = \frac{\partial^2}{\partial \tilde{x}^2} + \delta^2 \frac{\partial^2}{\partial \tilde{y}^2}$. Hereafter we drop all tildes.

Magnetostrophic regime

Of interest is the regime when $\frac{c_R}{c_{MR}} = \frac{c_R^2}{c_A^2} \gg 1$. Then the vorticity equation (3) becomes

$$-\chi \frac{\partial \psi}{\partial x} = \frac{\partial(g, \Delta_2 g)}{\partial(y, x)} \quad (5)$$

i.e. the magnetostrophic or MC balance. The slow wave motion at this regime arises from the time-derivative term of the current equation.

(The linearised equations for the uniform basic state allow solutions of the form $e^{i(kx - \omega t)} \sin n\pi y$, i.e. $\omega - \bar{U}k = -\frac{\bar{B}^2}{\chi} k(k^2 + n^2\pi^2)$.)

Two nonlinear terms in the governing equations: $\mathbf{B} \cdot \nabla J_z$ and $\mathbf{u} \times \mathbf{B}$. No roles of the advective term $\rho \mathbf{u} \cdot \nabla \xi_z$ in the vorticity equation.

Gardner-Morikawa transformation

To seek its solitary solutions for a long wave, we introduce new variables with a small parameter ϵ ($\ll 1$):

$$\zeta = \epsilon^{1/2}(x - ct), \quad \tau = \epsilon^{3/2}t \quad (6)$$

where c is a constant (to be determined). Also suppose $\delta = \mathcal{O}(1)$.

The vorticity and induction equations are rewritten as

$$-\chi \frac{\partial \psi}{\partial \zeta} = \left(\frac{\partial g}{\partial y} \frac{\partial}{\partial \zeta} - \frac{\partial g}{\partial \zeta} \frac{\partial}{\partial y} \right) \left(\epsilon \frac{\partial^2}{\partial \zeta^2} + \frac{\partial^2}{\partial y^2} \right) g \quad (7)$$

$$\left(-c \frac{\partial}{\partial \zeta} + \epsilon \frac{\partial}{\partial \tau} \right) g = \left(\frac{\partial g}{\partial y} \frac{\partial}{\partial \zeta} - \frac{\partial g}{\partial \zeta} \frac{\partial}{\partial y} \right) \psi \quad (8)$$

with boundary conditions $\frac{\partial \psi}{\partial \zeta} = 0$ at $y=0,1$.

Asymptotics: reductive perturbation method I

We now expand the dependent variables with ϵ as

$$\psi = \psi_0(y) + \epsilon\psi_1(\zeta, y, \tau) + \dots, \quad g = g_0(y) + \epsilon g_1(\zeta, y, \tau) + \dots, \quad (9)$$

provided the basic state:

$$\overline{U} = \frac{d\psi_0}{dy} \hat{e}_\zeta = \overline{U}(y) \hat{e}_\zeta, \quad \overline{B} = \frac{dg_0}{dy} \hat{e}_\zeta = \overline{B}(y) \hat{e}_\zeta. \quad (10)$$

At $\mathcal{O}(1)$ the vorticity and induction equations, (7)-(8), are both trivial. The vorticity equation (7) at $\mathcal{O}(\epsilon)$ gives

$$-\chi \frac{\partial \psi_1}{\partial \zeta} = \left(\overline{B} \frac{\partial^2}{\partial y^2} - \overline{B}'' \right) \frac{\partial g_1}{\partial \zeta} \quad (11)$$

and so does the induction equation (8)

$$(\overline{U} - c) \frac{\partial g_1}{\partial \zeta} = \overline{B} \frac{\partial \psi_1}{\partial \zeta}. \quad (12)$$

Asymptotics: reductive perturbation method II

Combining the two, we obtain a homogeneous PDE about g_1 :

$$\left[(\bar{U} - c) + \frac{\bar{B}}{\chi} \left(\bar{B} \frac{\partial^2}{\partial y^2} - \bar{B}'' \right) \right] \frac{\partial g_1}{\partial \zeta} = 0 \quad (13)$$

where $'$ stands for the ordinary derivative $\frac{d}{dy}$. Boundary conditions are $\frac{\partial g_1}{\partial \zeta} = 0$ at $y=0,1$.

We assume solutions in the form of $g_1 = G(\zeta, \tau)\phi(y)$ where ϕ should be a solution to the second order ODE:

$$\left[\frac{\bar{B}}{\chi} \left(\bar{B} \frac{d^2}{dy^2} - \bar{B}'' \right) + (\bar{U} - c) \right] \phi = 0 \quad (14)$$

with $\phi = 0$ at $y = 0, 1$. An eigenvalue problem about c and ϕ .

It becomes singular wherever \bar{B}^2/χ has zeros. By contrast, the nonmagnetic case leads to a critical layer where $c \rightarrow \bar{U}$ [Redekopp(1977)].

We focus on nonsingular solutions, i.e. discontinuous spectra.

At $\mathcal{O}(\epsilon^2)$

Now proceed to the next order to determine the amplitude function $\phi(y)$.
The vorticity and induction equations (7)-(8) at $\mathcal{O}(\epsilon^2)$ are

$$-\chi \frac{\partial \psi_2}{\partial \zeta} = \left(\bar{B} \frac{\partial^2}{\partial y^2} - \bar{B}'' \right) \frac{\partial g_2}{\partial \zeta} + \bar{B} \frac{\partial^3 g_1}{\partial \zeta^3} + \left(\frac{\partial g_1}{\partial y} \frac{\partial}{\partial \zeta} - \frac{\partial g_1}{\partial \zeta} \frac{\partial}{\partial y} \right) \frac{\partial^2 g_1}{\partial y^2} \quad (15)$$

$$(\bar{U} - c) \frac{\partial g_2}{\partial \zeta} + \frac{\partial g_1}{\partial \tau} = \bar{B} \frac{\partial \psi_2}{\partial \zeta} + \left(\frac{\partial g_1}{\partial y} \frac{\partial}{\partial \zeta} - \frac{\partial g_1}{\partial \zeta} \frac{\partial}{\partial y} \right) \psi_1. \quad (16)$$

After some algebra, they end up an inhomogeneous PDE for g_2 :

$$\begin{aligned} & \left[\frac{\bar{B}}{\chi} \left(\bar{B} \frac{d^2}{dy^2} - \bar{B}'' \right) + (\bar{U} - c) \right] \frac{\partial g_2}{\partial \zeta} \\ &= -\frac{\partial^3 G}{\partial \zeta^3} \left(\frac{\bar{B}^2}{\chi} \phi \right) - \frac{\partial G}{\partial \tau} \phi \\ & \quad - G \frac{\partial G}{\partial \zeta} \left[\frac{2\bar{B}}{\chi} (\phi' \phi'' - \phi \phi''') - \phi \phi'' \left(\frac{\bar{B}}{\chi} \right)' + \phi^2 \left(\frac{\bar{B}''}{\chi} \right)' \right] \end{aligned} \quad (17)$$

with $\frac{\partial^2 g_2}{\partial \zeta} = 0$ at $y = 0, 1$.

Solvability condition at $\mathcal{O}(\epsilon^2)$

When $\phi = 0$ at the boundaries, the LHS/homogeneous part of (17) has the solutions same as at $\mathcal{O}(\epsilon)$. So the solvability condition to suppress secular terms in the RHS/forcing part is given by

$$\begin{aligned} & \frac{\partial^3 G}{\partial \zeta^3} \int_0^1 \phi^\dagger \left(\frac{\bar{B}^2}{\chi} \phi \right) dy + \frac{\partial G}{\partial \tau} \int_0^1 \phi^\dagger \phi'' dy \\ & + G \frac{\partial G}{\partial \zeta} \int_0^1 \phi^\dagger \left[\frac{2\bar{B}}{\chi} (\phi' \phi'' - \phi \phi''') - \phi \phi'' \left(\frac{\bar{B}}{\chi} \right)' + \phi^2 \left(\frac{\bar{B}''}{\chi} \right)' \right] dy = 0. \end{aligned} \quad (18)$$

where ϕ^\dagger denotes the adjoint eigenfunction.

The result (18) shows a Korteweg-de Vries equation,

$$\frac{\partial G}{\partial \tau} + \alpha G \frac{\partial G}{\partial \zeta} + \gamma \frac{\partial^3 G}{\partial \zeta^3} = 0, \quad (19)$$

if α and γ are both nonzero. Well-known solutions are solitary and cnoidal.

Some remarks

- The presence of \bar{U} only impacts the dispersive term explicitly (unlike nonmagnetic cases). Note the profile of \bar{U} may impact the eigenfunction ϕ and thus the nonlinear term.
- If \bar{B} and χ are both independent of y , (18) is reduced to

$$\begin{aligned} & \frac{\partial^3 G}{\partial \zeta^3} \frac{\bar{B}^2}{\chi} \int_0^1 \phi^\dagger \phi \, dy + \frac{\partial G}{\partial \tau} \int_0^1 \phi^\dagger \phi'' \, dy \\ & + G \frac{\partial G}{\partial \zeta} \frac{2\bar{B}}{\chi} \int_0^1 \phi^\dagger (\phi' \phi'' - \phi \phi''') \, dy = 0. \end{aligned} \tag{20}$$

The nonlinear term vanishes for a harmonic function satisfying $\phi'' = C\phi$ with C being constant. This is the case when \bar{U} is also uniform. A variable basic field or topography or flow is crucial here.

cf. Nonmagnetic case

In the absence of magnetic field, the same methodology implies the $\mathcal{O}(\epsilon)$ -structural equation for $\psi_1 = \phi(y)F(\zeta, \tau)$:

$$(\bar{U} - c) \frac{d^2 \phi}{dy^2} - (\chi + \bar{U}'') \phi = 0. \quad (21)$$

A critical level will arise when $c \rightarrow \bar{U}$. Otherwise, wavy solutions available when $(\chi + \bar{U}'')/(c - \bar{U}) > 0$ (turning level). For the uniform basic state, the speed returns $c - \bar{U} = \frac{\chi}{n^2 \pi^2}$, i.e. the long Rossby wave.

The solvability condition at $\mathcal{O}(\epsilon^2)$ is then given by

$$\frac{\partial^3 F}{\partial \zeta^3} \int_0^1 \phi^2 (c - \bar{U}) dy - \frac{\partial F}{\partial \tau} \int_0^1 \phi \phi'' dy - F \frac{\partial F}{\partial \zeta} \int_0^1 \phi (\phi' \phi'' - \phi \phi''') dy = 0. \quad (22)$$

Recall that the nonlinear term vanishes if \bar{U} and χ are both uniform.

Spherical QG MHD model

We adopt a quasi-geostrophic model in cylinder (s, φ, z) , where the spherical geometry is taken into account [Jones(2015), Canet et al.(2014)].

In the magnetostrophic regime where $Le \sim |\omega_M/\omega_C| \ll 1$, we begin with equations for the axial vorticity, $\xi_z = \hat{z} \cdot (\nabla \times \mathbf{u})$, and the magnetic field, \mathbf{B} :

$$-2\Omega \frac{\partial u_z}{\partial z} = \frac{1}{\rho} \mathbf{B} \cdot \nabla j_z \quad (23)$$

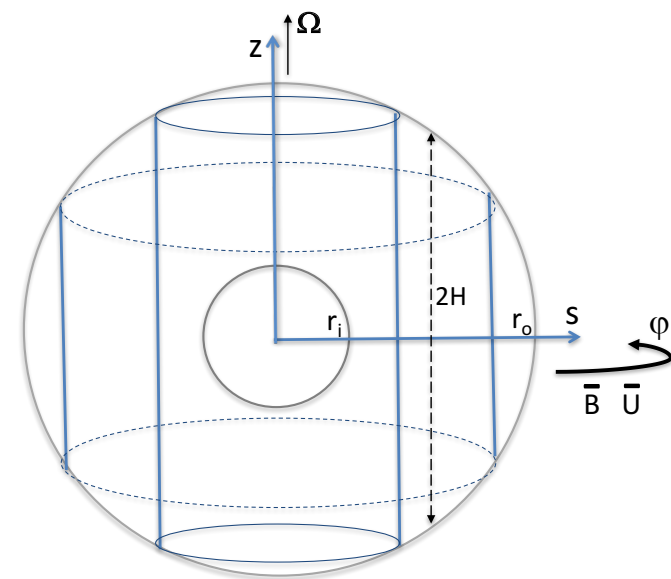
$$\frac{\partial \mathbf{B}}{\partial t} = \nabla \times (\mathbf{u} \times \mathbf{B}) \quad (24)$$

and $\nabla \cdot \mathbf{u} = \nabla \cdot \mathbf{B} = 0$. Boundary conditions are

$$u_z = \mp u_s \frac{s}{H} \quad \text{at} \quad z = \pm H = \pm(r_o^2 - s^2)^{1/2} \quad (25)$$

$$u_s = 0 \quad \text{at} \quad s = r_i, r_o \quad (26)$$

The former gives rise to the topographic beta effect $\beta = -2\Omega \frac{d}{ds} \ln H$. Assume $\mathbf{u} \sim \nabla \times \psi(s, \varphi) \hat{z}$ and $\mathbf{B} \sim \nabla \times g(s, \varphi) \hat{z}$.



Reductive perturbation method

Hereafter all dimensionless: the length and the velocity are scaled by the radius of the outer shell, r_o , and the MC speed, $B_0^2/(2\Omega r_o \rho \mu_0)$, respectively.

To seek its solitary solutions for a long wave, we introduce slow variables with a small parameter ϵ ($\ll 1$):

$$\tau = \epsilon^{3/2} t, \quad \zeta = \epsilon^{1/2} (\varphi - c t) \quad (27)$$

where c is a constant. We now expand the dependent variables with ϵ as

$$\psi = \psi_0(s) + \epsilon \psi_1(\zeta, s, \tau) + \dots, \quad g = g_0(s) + \epsilon g_1(\zeta, s, \tau) + \dots \quad (28)$$

provided the basic flow and magnetic field are purely azimuthal:

$$-D\psi_0 = \bar{U}(s), \quad -Dg_0 = \bar{B}(s) \quad (29)$$

where $D = d/ds$.

At $\mathcal{O}(\epsilon)$: eigenvalue problem

Eqs. (23)-(24) at $\mathcal{O}(\epsilon)$ give a homogeneous PDE about g_1 :

$$\mathcal{L} \frac{\partial g_1}{\partial \zeta} \equiv \left\{ \frac{\bar{B}}{\beta s} \left[\bar{B} \mathcal{D}^2 - D \frac{1}{s} D(s\bar{B}) \right] + \left(\frac{\bar{U}}{s} - c \right) \right\} \frac{\partial g_1}{\partial \zeta} = 0 \quad (30)$$

where the linear operator $\mathcal{L} = \mathcal{L}(s, \partial/\partial s, \bar{B}, \beta, \bar{U}, c)$. Boundary conditions are $\partial g_1/\partial \zeta = 0$ at $s = \eta$ and 1 .

Seek solutions in form of $g_1 = \Phi(s)G(\zeta, \tau)$ to leave the eigenvalue problem

$$\mathcal{L}\Phi = 0 \quad \text{and} \quad \Phi = 0 \quad \text{at} \quad s = \eta, 1. \quad (31)$$

i.e. a second-order ODE. A critical level will arise wherever \bar{B}^2/β has zeros, but not as $c \rightarrow \bar{U}/s$; cf. nonmagnetic cases. Again, seek nonsingular solutions only.

At $\mathcal{O}(\epsilon^2)$: KdV equation?

We proceed to the next order to determine the amplitude function. After some algebra, we obtain an inhomogeneous PDE for g_2 :

$$\begin{aligned} \mathcal{L} \frac{\partial g_2}{\partial \zeta} = & -\frac{\bar{B}^2}{s^3 \beta} \frac{\partial^3 G}{\partial \zeta^3} \Phi - \frac{\partial G}{\partial \tau} \Phi \\ & + G \frac{\partial G}{\partial \zeta} \left\{ \frac{2\bar{B}}{\beta s} [(D\Phi)D^2\Phi - \Phi D D^2\Phi] - \frac{\Phi D^2\Phi}{s} D \frac{\bar{B}}{\beta} + \frac{\Phi^2}{s} D \frac{1}{\beta} D \frac{1}{s} D s \bar{B} \right\} \end{aligned} \quad (32)$$

where $D^2 = (1/s)D_s D$. Boundary conditions are $\partial g_2 / \partial \zeta = 0$ at $s = \eta$ and 1. The solvability condition is given by

$$\begin{aligned} \frac{\partial G}{\partial \tau} \int_{\eta}^1 \Phi^\dagger \Phi s ds + \frac{\partial^3 G}{\partial \zeta^3} \int_{\eta}^1 \Phi^\dagger \frac{\bar{B}^2}{s^2 \beta} \Phi ds \\ + G \frac{\partial G}{\partial \zeta} \int_{\eta}^1 \Phi^\dagger \left\{ \frac{2\bar{B}}{\beta} [\Phi D D^2\Phi - (D\Phi)D^2\Phi] + \Phi (D^2\Phi) D \frac{\bar{B}}{\beta} - \Phi^2 D \frac{1}{\beta} D \frac{1}{s} D s \bar{B} \right\} ds = 0 \end{aligned} \quad (33)$$

with Φ^\dagger being the adjoint eigenfunction. Again, this implies a Korteweg-de Vries equation if the coefficients are both nonzero.

Case study

We investigate the two coefficients for different basic states, provided $\beta = s/(1 - s^2)$ and $\eta = 0.35$.

Solutions to the eigenvalue problem (31) at $\mathcal{O}(\epsilon)$ are found analytically in a couple of cases. For general cases we solve this using the Matlab routine `bvp4c` with a modified boundary condition $\Phi + (1 - s)D\Phi = 0$ at $s = 0.99999$.

In the all cases we obtain nonzero α and γ , i.e. valid KdV equations.

\overline{B}	\overline{U}	n	c	α	γ
s	0	1	-9.7847	-12.854	0.87465
		2	-33.2045	-14.639	1.0480
		3	-70.0655	-26.422	1.1156
$1/s$	0	1	-21.9795	-36.930	1.2464
		2	-78.0389	-31.920	2.1442
		3	-167.788	-70.056	2.8417
$^{\circ}s$	s	1	-8.7847	-12.854	0.87465
$^{\circ}1/s$	s	1	-20.9795	-36.865	1.2464
$^{\circ}s$	$4s(1 - s)$	1	-8.8379	-9.5075	0.90339
$^{\circ}1/s$	$4s(1 - s)$	1	-21.4523	-35.429	1.2659

$^{\circ}$ Cases evaluated with the routine `bvp4c` .

An asymptotic solution: single-soliton

The known solutions to KdV equation are solitary, cnoidal, similarity, and rational [Drazin & Johnson(1989)].

The 1-soliton (solitary wave) solution yields our asymptotic solution, such that

$$\psi(s, \varphi, t) = - \int_{\eta}^s \bar{U} ds - \epsilon \operatorname{sgn}(\alpha\gamma) \left(\frac{\bar{B}}{\beta} D^2 \Phi - \frac{\Phi}{\beta} D \frac{1}{s} D(s\bar{B}) \right) \operatorname{sech}^2 F \quad (34)$$

where

$$F(\varphi, t) = \sqrt{\left| \frac{\alpha}{12\gamma} \right|} \left[\epsilon^{1/2} (\varphi - ct) - \epsilon^{3/2} \operatorname{sgn}(\gamma) \frac{|\alpha|t}{3} \right]. \quad (35)$$

Case 1: for Malkus field

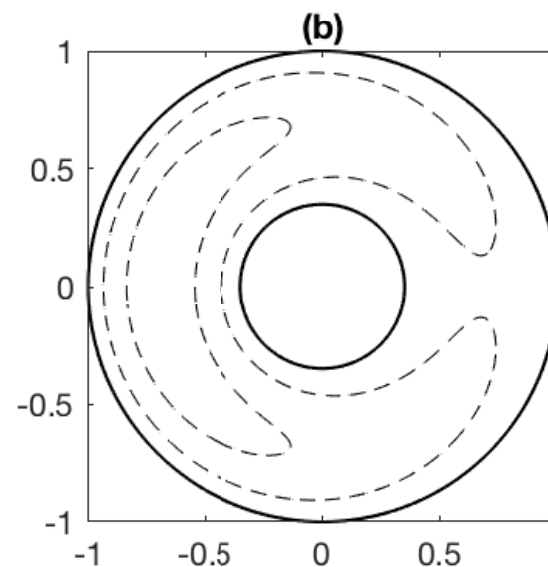
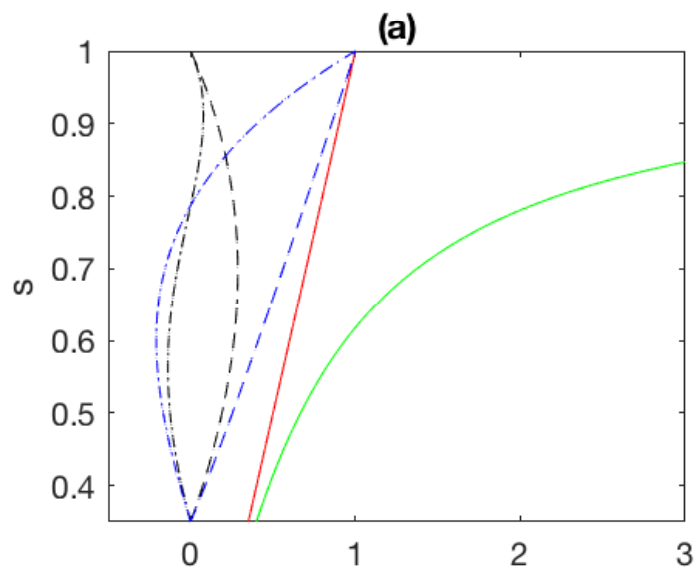
Here is the example for $\bar{B} = s$ (Malkus field; red in figure a). Let $x = 1 - s^2$; the eigenvalue problem (31) at $\mathcal{O}(\epsilon)$ is rewritten as

$$\left[x(1-x) \frac{d^2}{dx^2} - x \frac{d}{dx} + \lambda^2 \right] \Phi = 0 \quad \text{where} \quad \lambda^2 = -\frac{c}{4}. \quad (36)$$

Found to be a hypergeometric equation (A&S Chap. 15). So with the hypergeometric function $F(a, b; c; z) = \sum_{n=0}^{\infty} \frac{(a)_n (b)_n}{(c)_n} \frac{z^n}{n!}$, we find solutions

$$\Phi = (1 - s^2) F(1 + \lambda, 1 - \lambda; 2; 1 - s^2) \quad (37)$$

(black dashed) and $\Phi^\dagger = \frac{\Phi}{1-s^2}$ (black dashed-dotted). This gives $\alpha \approx -12.9$ and $\gamma \approx 0.875$ for $n = 1$, i.e. a clockwise eddy (figure b).



Case 2: for wire field

When $\bar{B} = 1/s$ (electrical-wire field; red in a), the ODE (31) is reduced to

$$\left[x(1-x) \frac{d^2}{dx^2} - x \frac{d}{dx} + \lambda^2(1-x)^2 \right] \Phi = 0, \quad (38)$$

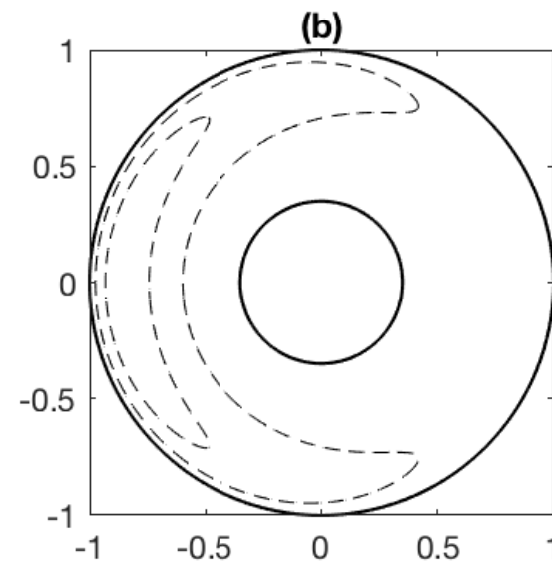
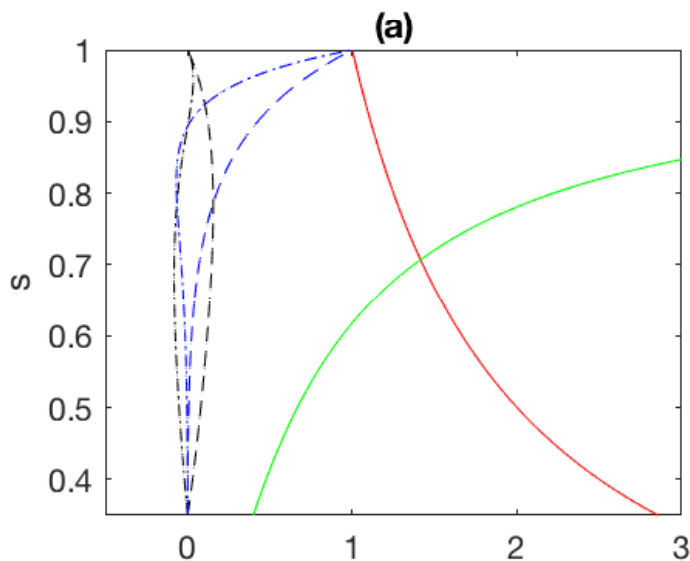
which has a solution

$$\Phi = (1-s^2)e^{\lambda(1-s^2)} H_c(q_c, \alpha_c, \gamma_c, \delta_c, \epsilon_c; 1-s^2) \quad (39)$$

where H_c represents the confluent Heun function (DLMF Chap. 31) with

$q_c = \lambda^2 + 2\lambda - 1$, $\alpha_c = \lambda^2 + 3\lambda$, $\gamma_c = 2$, $\delta_c = 1$ and $\epsilon_c = 2\lambda$ (black in a).

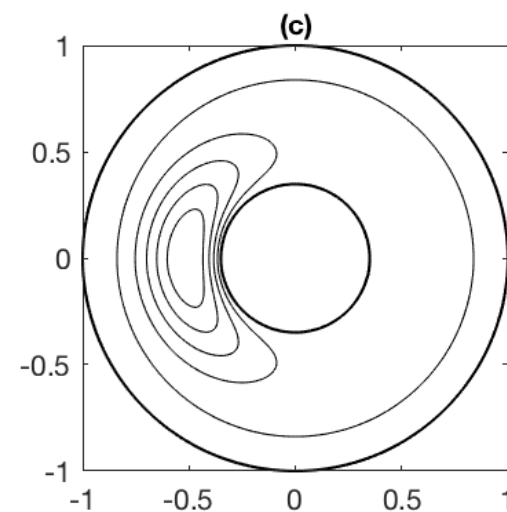
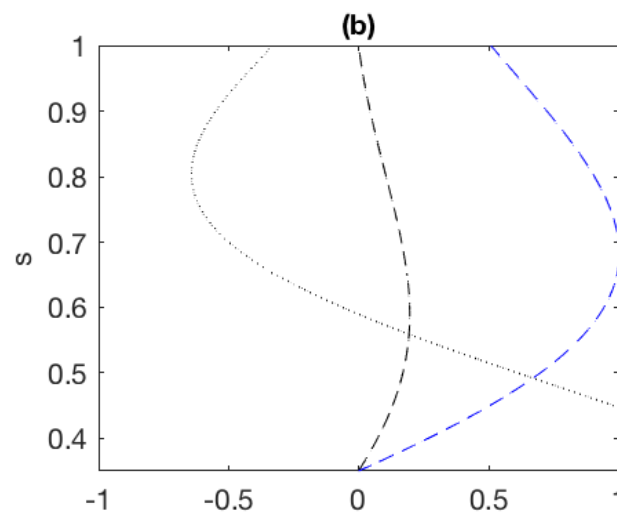
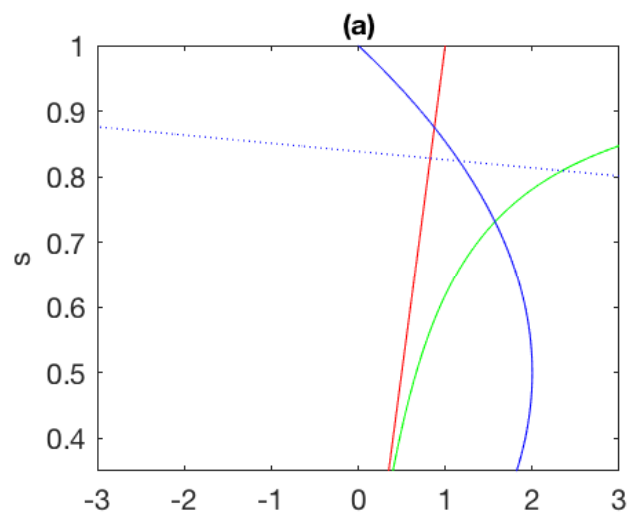
Also $\Phi^\dagger = \frac{s^4}{1-s^2} \Phi$. Now we find $\alpha \approx -36.9$ and $\gamma \approx 1.25$ for $n = 1$. The solitary wave solution is again clockwise but more compact (b).



Case 3: influence of basic zonal flow

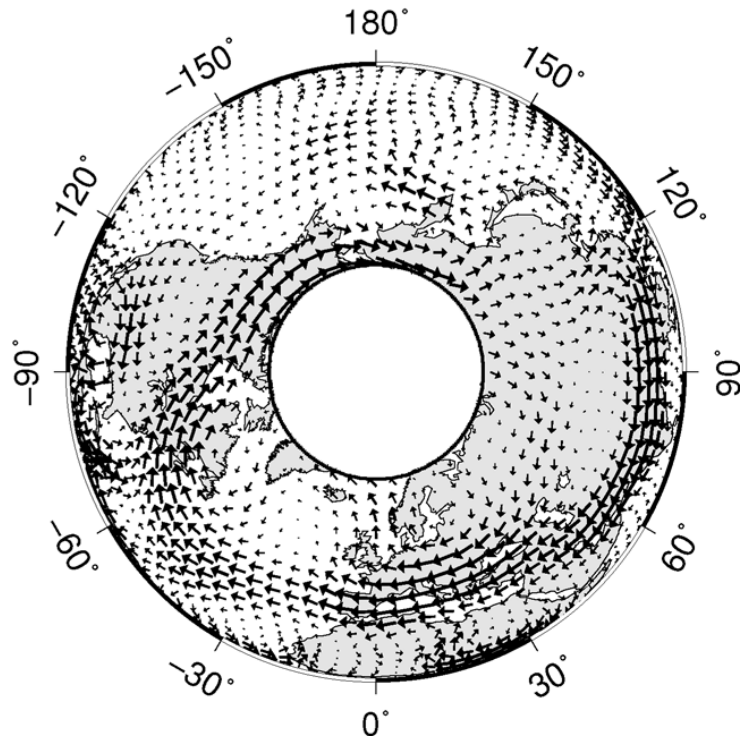
Valid KdV equations are found in the presence of a basic zonal flow. A linear shear, $\bar{U} = s$, simply implies the solid body rotation; a quadratic shear, $\bar{U} = 4s(1 - s)$, weakens the nonlinear effect.

Are the solutions really right even when $c \rightarrow \bar{U}/s$? This is confirmed: we impose an extremely fast flow, $\bar{U} = 80s(1 - s)$, to have such a radius at which $\bar{U}/s - c = 0$ (dotted blue in a), however there are no discontinuities in the vicinity (b and c).



Looks like the anticyclonic gyre in Earth's core?

The solitary wave solutions supports the persistency of an isolated anticyclone, drifting westwardly on timescales of $\mathcal{O}(10^{2-4}\text{yrs})$.

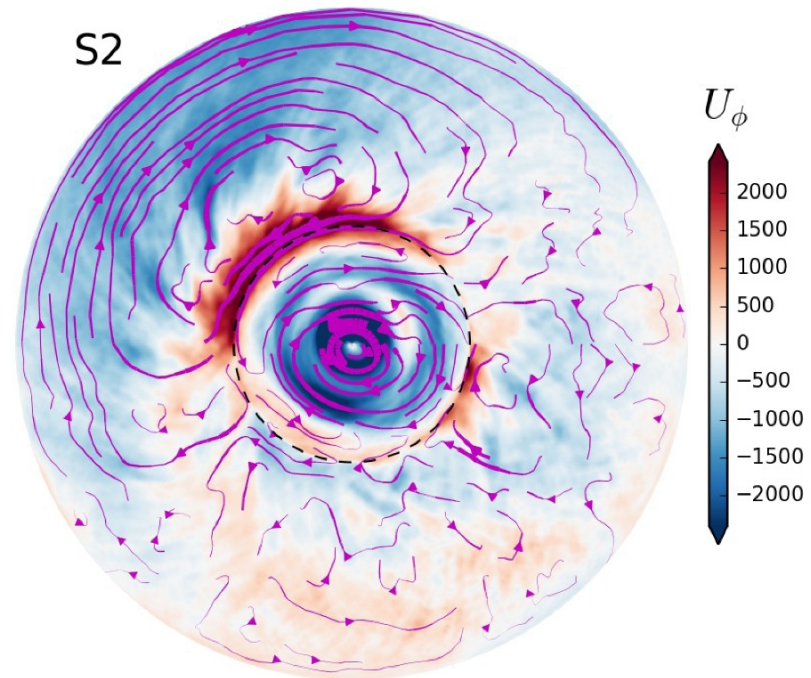


COV-OBS QG core flow model:

average over 1840-1990

[Pais et al.(2015)]

accelerating? [Barrois et al.(2018)]



geodynamo DNS:

average over $0.016\tau_\eta \sim 10^3$ yrs (or less)

low-frequency, columnar

[Schaeffer et al.(2017)]

Summary and some remarks I

The weakly nonlinear analysis in the QG MHD/MC model indicates slow MR waves may shape coherent structures, such as solitons

- the Busse annulus model illustrates this happens when either the basic magnetic field, topography, or mean flow varies in s
- this is exemplified by the spherical analogue
- the single soliton (solitary wave) solution yields an isolated, anticyclonic eddy
- it is nonsingular even when the wave speed approaches the basic angular velocity

Potential geo-/astro-physical implications:

- the eccentric gyre in Earth's core [Pais & Jault(2008)], and then the South Atlantic Anomaly?
- the nest of convection?
- a single vortex in protoplanetary discs?, Jupiter's GBS??

Summary and some remarks II

Note that

- the long waves can be destabilised through any scenarios, e.g.
 - differentially rotating flows [Schmitt et al.(2008), Nornberg et al.(2010)]
 - convection [Sakuraba(2002), Hori et al.(2012)]
 - magnetic diffusivity [Roberts & Loper(1979), Zhang et al.(2003)]
- different basic states (directions/morphologies) will lead to different characteristics

Open questions:

- at strongly nonlinear regimes: envelop soliton, modon, etc.
- DNS/initial value problems
- when there is an internal singularity in \overline{B}^2/β profile
- in 3d spherical systems where the z-dependence is present
- solutions to (cylindrical) KdV equations

References I



Abdulrahman, A., Jones, C.A., Proctor, M.R.E., Julien, K., 2000. Large wavenumber convection in the rotating annulus. *Geophys. Astrophys. Fluid Dyn.*, 93, 227-252.



Acheson, D.J., 1972. The critical levels for hydromagnetic waves in a rotating fluid. *J. Fluid Mech.* 53, 401-415.



Barrois, O., Hammer, M.D., Finlay, C.C., Martin, Y., Gillet, N., 2018. Assimilation of ground and satellite magnetic measurements: inference of core surface magnetic and velocity field changes. *Geophys. J. Int.* 215, 695-712.



Boyd, J.P., 1980. Equatorial solitary waves. Part 1: Rossby solitons. *J. Phys. Oceanogr.* 10, 1699-1717.



Boyd, J.P., 1983. Equatorial solitary waves. Part 2: Envelope solitons. *J. Phys. Oceanogr.* 13, 428-449.



Braginsky, S.I., 1967. Magnetic waves in the Earth's core. *Geomagn. Aeron.* 7, 851-859.



Busse, F.H., 1970. Thermal instabilities in rapidly rotating systems. *J. Fluid Mech.* 44, 441-460.











Busse, F.H., 1976. Generation of planetary magnetism by convection. *Phys. Earth Planet. Int.* 12, 350-358.












Canet, E., Finlay, C.C., Fournier, A., 2014. Hydromagnetic quasi-geostrophic modes in rapidly rotating planetary cores. *Phys. Earth Planet. Int.* 229, 1-15.









References II

-  Chulliat, A., Alken, P., Maus, S., 2015. Fast equatorial waves propagating at the top of the Earth's core. *Geophys. Res. Lett.* 42, 3321-3329.
-  Drazin, P. G. & Johnson R. S., 1989. *Solitons: an Introduction*. Cambridge University Press.
-  Flierl, G.R., et al. 1980. The dynamics of baroclinic and barotropic solitary eddies. *Dyn. Atmos. Oceans* 5, 1-41.
-  Gillet, N., Jones, C.A., 2006. The quasi-geostrophic model for rapidly rotating spherical convection outside the tangent cylinder. *J. Fluid Mech.* 554, 343-369.
-  Gillet, N., Brito, D., Jault, D., Nataf, H.-C., 2007. Experimental and numerical studies of magnetoconvection in a rapidly rotating spherical shell. *J. Fluid Mech.* 580, 123-143.
-  Gilman, P.A., 2000. Magnetohydrodynamics “shallow water” equations for the solar tachocline. *Astrophys. J.* 544, L79-82.
-  Hide, R., 1966. Hydromagnetic oscillations of the Earth's core and the theory of the geomagnetic secular variation. *Phil. Trans. R. Soc. Lond. A* 259, 615-647.
-  Hori, K., Wicht, J., Christensen, U.R., 2012. The influence of thermo-compositional boundary conditions on convection and dynamos in a rotating spherical shell. *Phys. Earth Planet. Int.* 196-197, 32-48.









References III

-  Hori, K., Takehiro, S., Shimizu, H., 2014. Waves and linear stability of magnetoconvection in a rotating cylindrical annulus. *Phys. Earth Planet. Int.*, 236, 16-35.
-  Hori, K., Jones, C.A., Teed, R.J., 2015. Slow magnetic Rossby waves in the Earth's core. *Geophys. Res. Lett.* 42, 6622-6629.
-  Hori, K., Teed, R.J., Jones, C.A., 2018. The dynamics of magnetic Rossby waves in spherical dynamo simulations: A signature of strong-field dynamos? *Phys. Earth Planet. Int.* 276, 68-85.
-  Hori, K., Tobias, S.M., Jones, C.A., 2020. Solitary magnetostrophic Rossby waves in spherical shells. *J. Fluid Mech.*, 904, R3 (14 pp).
-  Jones, C.A., 2015. Thermal and compositional convection in the outer core. In: Schubert, G. (Ed.), *Treatise on Geophysics*, 2nd edition, Vol.8, pp.115-159. Oxford: Elsevier.
-  Lahaye, N., Zeitlin, V., 2022. Coherent magnetic modon solutions in quasi-geostrophic shallow water magnetohydrodynamics. *J. Fluid Mech.*, 941, A15 (22 pp).
-  London, S.D., 2017. Solitary waves in shallow water magnetohydrodynamics. *Geophys. Astrophys. Fluid Dyn.*, 111, 115-130.
-  Malkus, W.V.R., 1967. Hydromagnetic planetary waves. *J. Fluid Mech.* 28, 793-802.
-  Maxworthy, T., Redekopp, L.G., 1980. Possible fluid dynamical interpretation of some reported features in the Jovian atmosphere. *Science* 210, 1350-1351.

References IV

-  MacIntosh, S.W., et al., 2017. The detection of Rossby-like waves on the Sun. *Nat. Astron.* 1, 0086.
-  Malanotte Rizzoli, P., 1982. Planetary solitary waves in geophysical flows. *Advances in Geophysics* 24, 147-224.
-  Márquez-Artavia, X., Jones, C.A., Tobias, S.M., 2017. Rotating magnetic shallow water waves and instabilities in a sphere. *Geophys. Astrophys. Fluid Dyn.* 111, 282-322.
-  Nilsson, A., Suttie, N., Korte, M., Holme, R. & Hill, M., 2020. Persistent westward drift of the geomagnetic field at the core-mantle boundary linked to recurrent high latitude weak/reverse flux patches. *Geophys. J. Int.* doi:10.1093/gji/ggaa249.
-  Nornberg, M. D., Ji, H., Schartman, E., Roach, A., Goodman, J., 2010. Observation of magnetocoriolis waves in a liquid metal Taylor-Couette experiment. *Phys. Rev. Lett.* 104, 074501(1-4).
-  Pais, M.A., Jault, D., 2008. Quasi-geostrophic flows responsible for the secular variation of the Earth's magnetic field. *Geophys. J. Int.* 173, 421-443.
-  Pais, M.A., Morozova, A.L., Schaeffer, N., 2015. Variability modes in core flows inverted from geomagnetic field models. *Geophys. J. Int.* 200, 402-420.
-  Redekopp, L.G., 1977. On the theory of solitary Rossby waves. *J. Fluid Mech.* 82, 725-745.

References V

-  Roberts, P. H., Loper, D. E., 2017. On the diffusive instability of some simple steady magnetohydrodynamic flows. *J. Fluid Mech.* 90, 641-668.
-  Sakuraba, A., 2002. Linear magnetoconvection in rotating fluid spheres permeated by a uniform axial magnetic field. *Geophys. Astrophys. Fluid Dyn.* 96, 291-318.
-  Schmitt, D., Alboussière, T., Brito, D., Cardin, P., Gagnière, N., Jault, D., Nataf, H.-C., 2008. Rotating spherical Couette flow in a dipolar magnetic field: experimental study of magneto-inertial waves. *J. Fluid Mech.* 604, 175-197.
-  Schaeffer, N., Jault, D., Nataf, H.-C., Fournier, A., 2017. Turbulent geodynamo simulations: a leap towards Earth's core. *Geophys. J. Int.* 211, 1-29.
-  Whitham, G.B., 1974. *Linear and nonlinear waves*. New York: Wiley.
-  Yamagata, T., 1980. The stability, modulation and long wave resonance of a planetary wave in a rotating, two-layer fluid on a channel beta-plane. *J. Meteor. Soc. Japan* 58, 160-171.
-  Zaqarashvili, T.V., 2010. Magnetic Rossby waves in the solar tachocline and Rieger-type periodicities. *Astrophys. J.* 709, 749-758.
-  Zhang, K., Liao, X., Schubert, G., 2003. Nonaxisymmetric instabilities of a toroidal magnetic field in a rotating sphere. *Astrophys. J.* 585, 1124-1137.

Torsional oscillations

Kumiko Hori

National Institute for Fusion Science



gfd seminars 3

Hokkaido, 15-16 March 2025



Torsional oscillations/waves

- A special class of Alfvén waves (Braginsky 1970; details in the note) :

- The azimuthal momentum equation integrated over cylindrical surfaces $C = 2\pi s h(s)$ about the rotation axis:

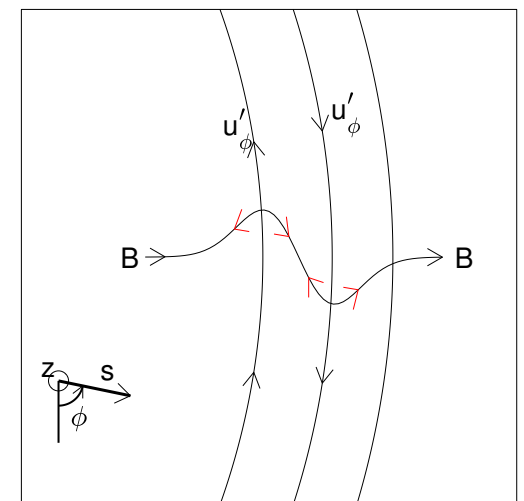
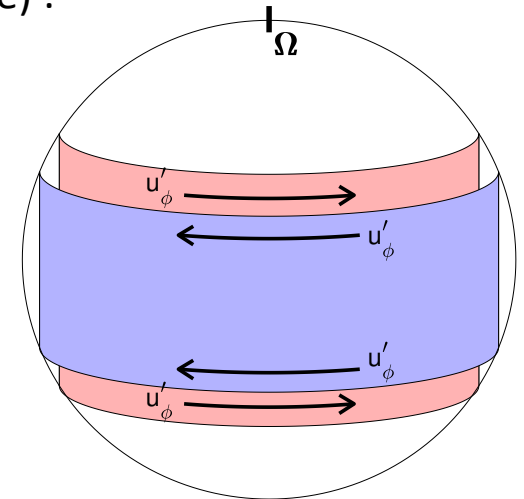
$$\frac{\partial}{\partial t} \int_C \bar{\rho} u_\phi dS + \int_C \hat{e}_\phi \cdot (\nabla \cdot \bar{\rho} \mathbf{u} \mathbf{u}) dS + 2\Omega \int_C \bar{\rho} u_s dS = \int_C \hat{e}_\phi \cdot (\mathbf{J} \times \mathbf{B}) dS$$

- For incompressible fluids, the Coriolis term vanishes
- The magnetostrophic balance yields a steady state (Taylor 1963)
- Cylindrical perturbations on the state, $\langle u'_\phi \rangle = \langle u'_\phi \rangle(s,t)$, can be governed by a homogeneous equation:

$$\frac{\partial^2 \langle u'_\phi \rangle}{\partial t^2} \frac{1}{s} = \frac{1}{s^3 h \langle \bar{\rho} \rangle} \frac{\partial}{\partial s} \left(s^3 h \langle \bar{\rho} \rangle U_A^2 \frac{\partial \langle u'_\phi \rangle}{\partial s} \frac{1}{s} \right)$$

- with Alfvén speed $U_A = (\langle \tilde{B}_s^2 \rangle / \mu_0 \langle \rho \rangle)^{1/2}$
- **outward (+s) and/or inward (-s) propagation,** or **standing waves,** possible

- Can be excited by any mechanisms/instabilities



(after Roberts & Aurnou 2012)

TO as an eigenmode

- Early studies explored the eigenvalue problem of the 1d wave equation
- Normal mode solutions to the governing (full) equations reveal the TO class

Mode classification
(Gerick+ GJI 2020)

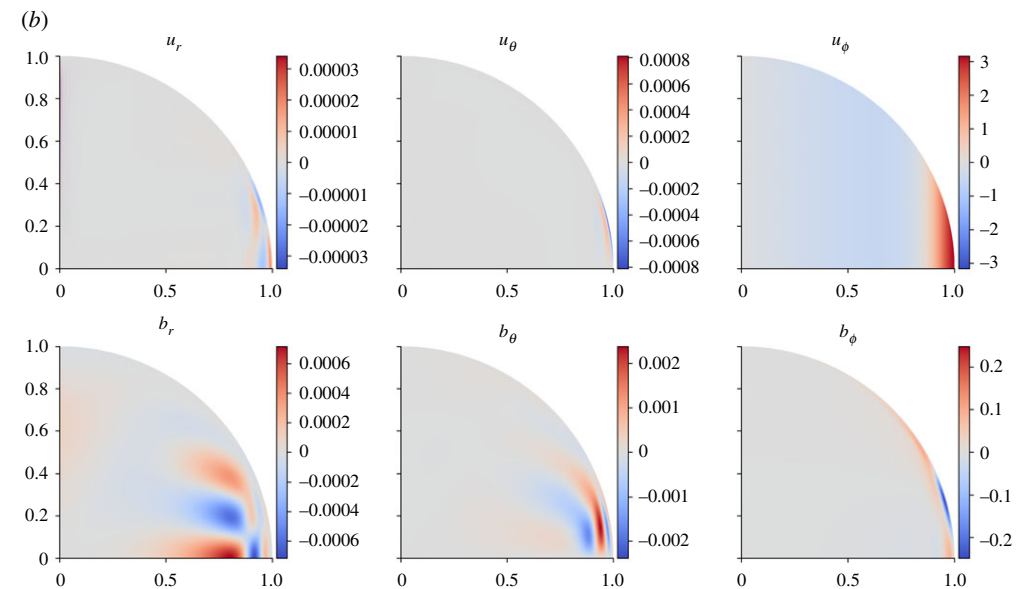
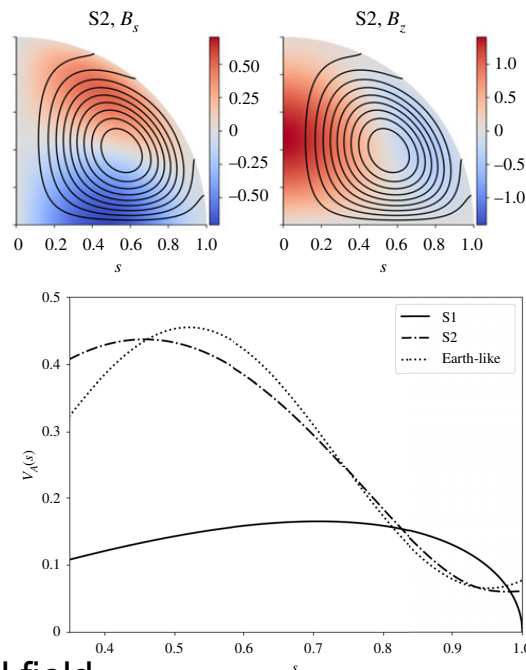
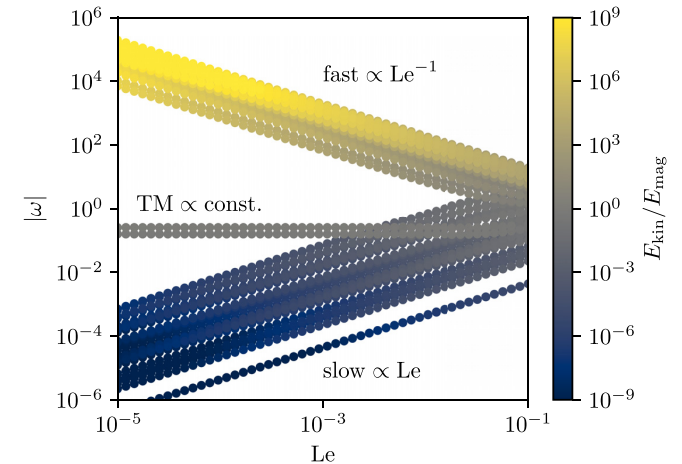


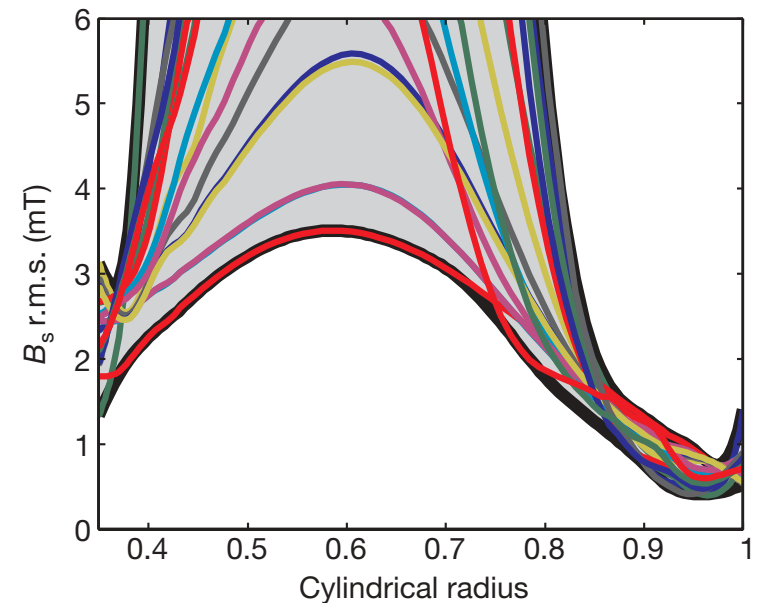
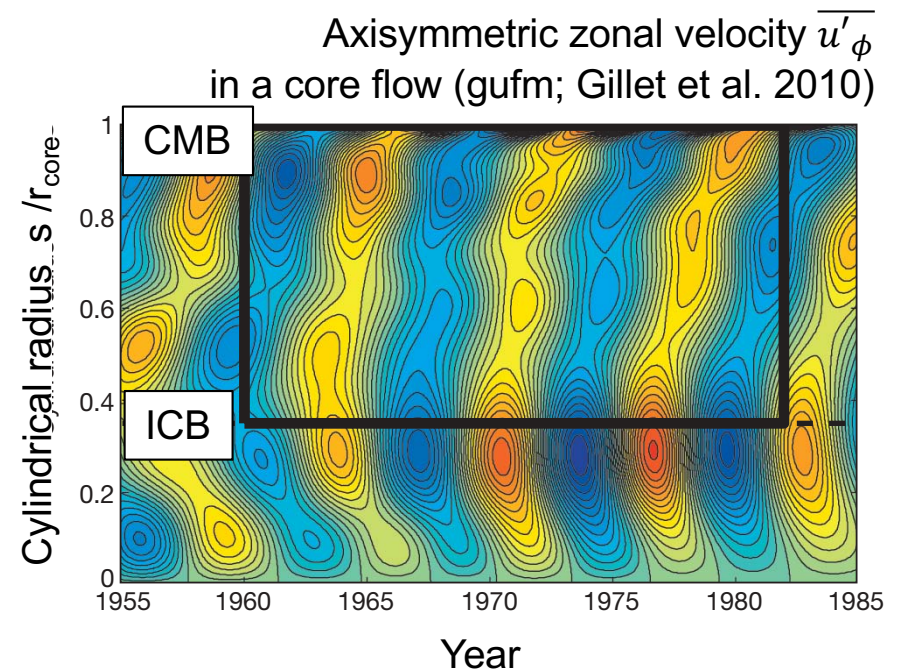
Figure 4. Fundamental torsional normal modes for (a) S1 and (b) S2. They are computed at $Le = 10^{-4}$, $Lu = 2 \times 10^4$ at $N = 175$, $L = 350$. The non-azimuthal flow components are small, as expected, compared to the azimuthal component (see also figure 11). (a) Components of the fundamental torsional mode for S1 with $\sigma = 0.0136$ and $\omega = 0.667$. (b) Components of the fundamental torsional mode for S2 with $\sigma = 0.0066$ and $\omega = 1.034$. (Online version in colour.)

TO for a given poloidal field
(Liu & Jackson, Proc. R. Soc. A 2022)

Torsional waves in Earth's fluid core

Some history..

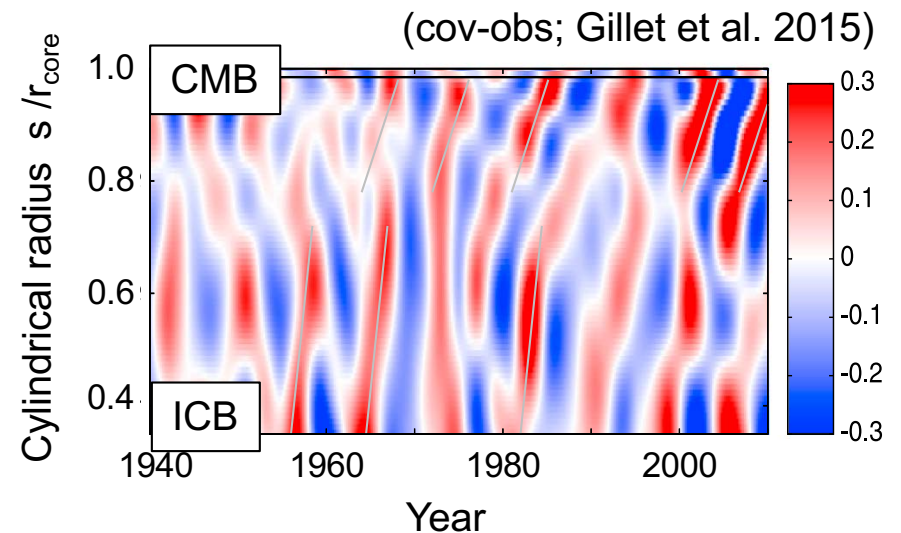
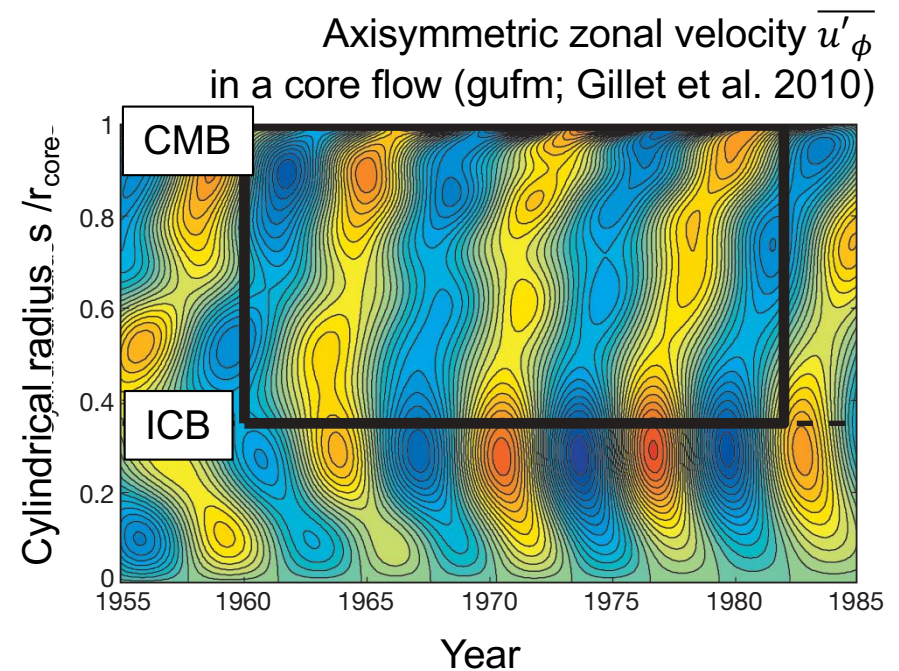
- Proposed to account for ~ 60 yr geomag SV and/or the core flow (e.g. Braginsky 1970; Zatman & Bloxham 1997)
 - in terms of normal mode solutions, i.e. standing form
 - to infer the field strength of $\langle \tilde{B}_s^2 \rangle^{1/2} \geq 0.3$ mT
 - too weak? (e.g. scaling laws; Christensen & Aubert 2006)
- for another signal of 4-9 years (Gillet et al)
 - implying the strength of $\langle \tilde{B}_s^2 \rangle^{1/2} \geq 2$ mT
 - in core flow models inverted from geomag SV
 - compatible with ~ 6 yr variation in the rotation rate (length-of-day) variations too
 - strong filter; unclear geomag signals
 - more likely **travelling** to the equator



Torsional waves in Earth's fluid core

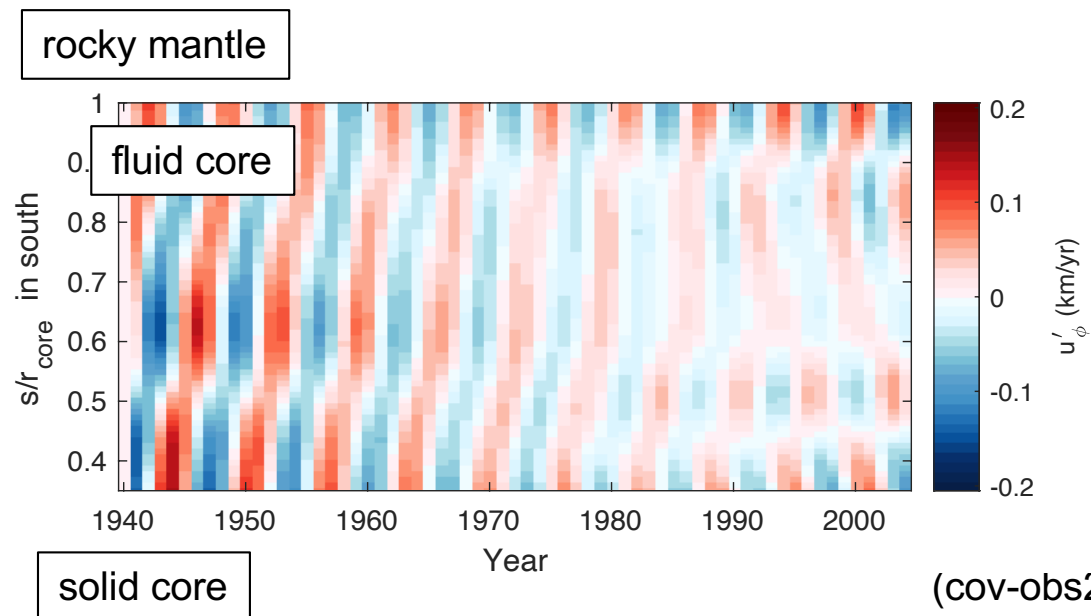
Some history..

- Proposed to account for ~ 60 yr geomag SV and/or the core flow (e.g. Braginsky 1970; Zatman & Bloxham 1997)
 - in terms of normal mode solutions, i.e. standing form
 - to infer the field strength of $\langle \tilde{B}_s^2 \rangle^{1/2} \geq 0.3$ mT
 - too weak? (e.g. scaling laws; Christensen & Aubert 2006)
- for another signal of 4-9 years (Gillet et al)
 - implying the strength of $\langle \tilde{B}_s^2 \rangle^{1/2} \geq 2$ mT
 - in core flow models inverted from geomag SV
 - compatible with ~ 6 yr variation in the rotation rate (length-of-day) variations too
 - strong filter; unclear geomag signals
 - more likely **travelling** to the equator

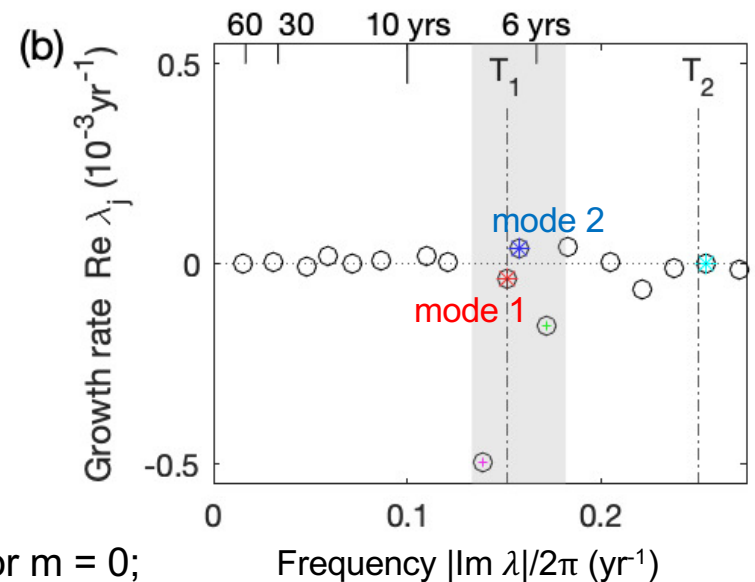
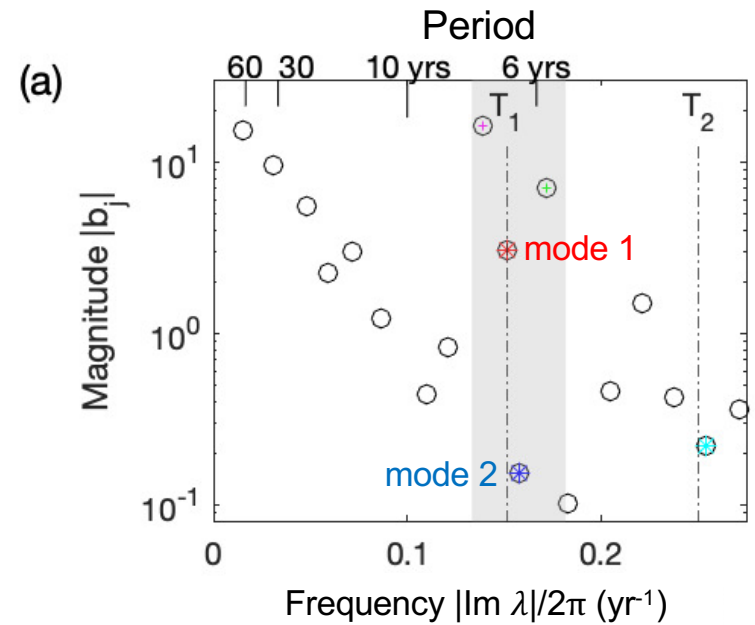


Revisiting geomagnetic data

- DMD over $[\overline{u_\phi'}, \partial \overline{b_s'} / \partial t]$ revealed
 - ~6 yr signals comprising of tiny but wavy (high Q) components
 - fit with CFF field \tilde{B}_s of <3.9 mT
 - their reconstruction reproduces the TO nature reported in u_ϕ , while visualising the magnetic SV of magnitude < 1%

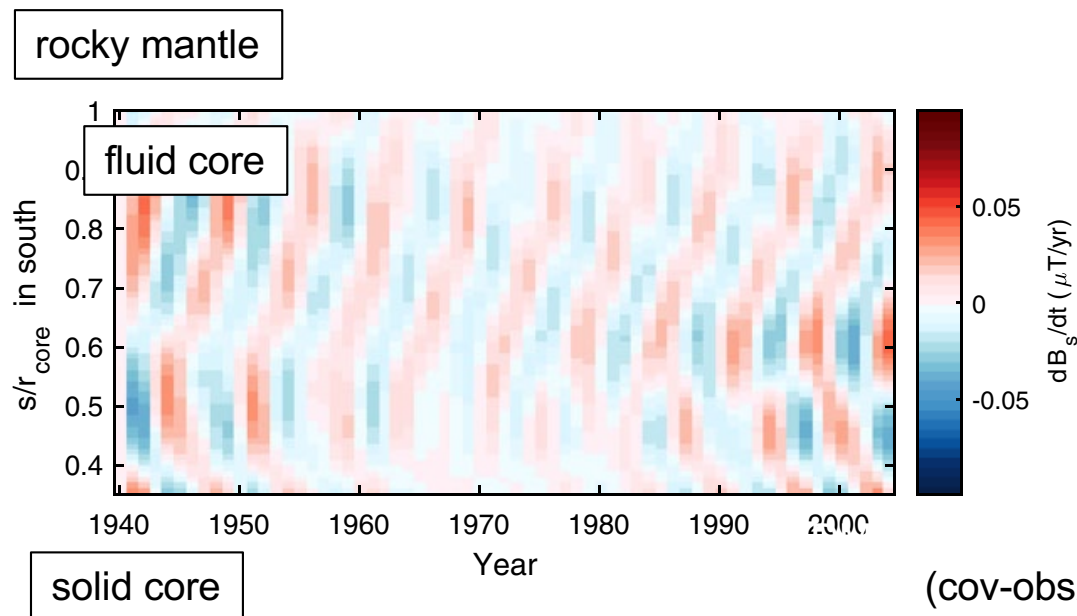


(cov-obs2019 for $m = 0$;
KH, Nilsson & Tobias, RMPP 2023)

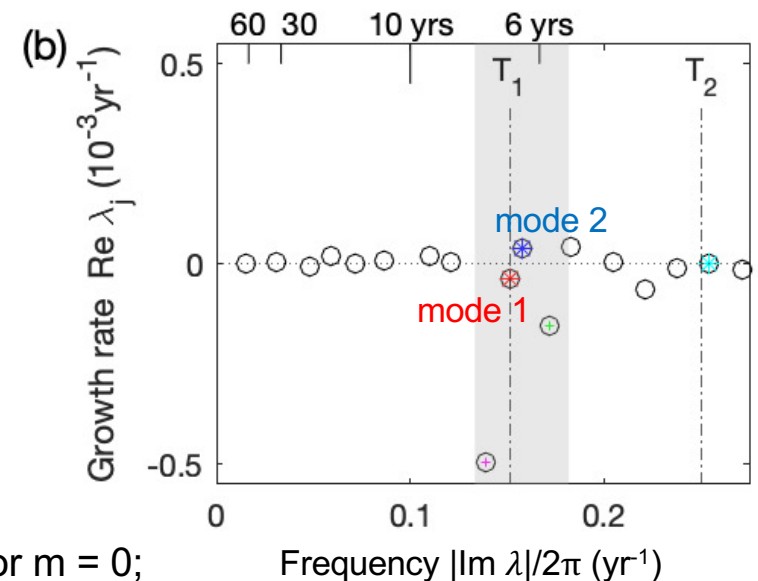
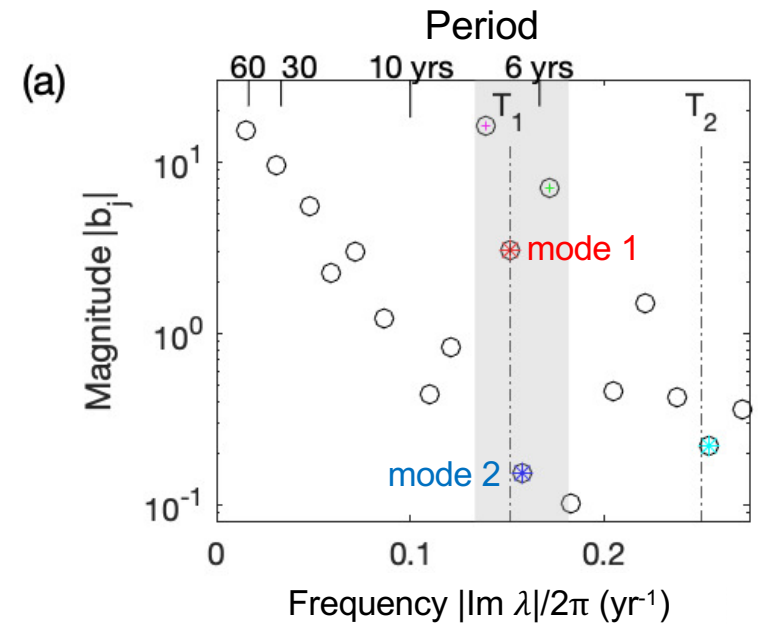


Revisiting geomagnetic data

- DMD over $[\overline{u_\phi'}, \partial \overline{b_s'} / \partial t]$ revealed
 - ~6 yr signals comprising of tiny but wavy (high Q) components
 - fit with CFF field \tilde{B}_s of <3.9 mT
 - their reconstruction reproduces the TO nature reported in u_ϕ , while visualising the magnetic SV of magnitude < 1%



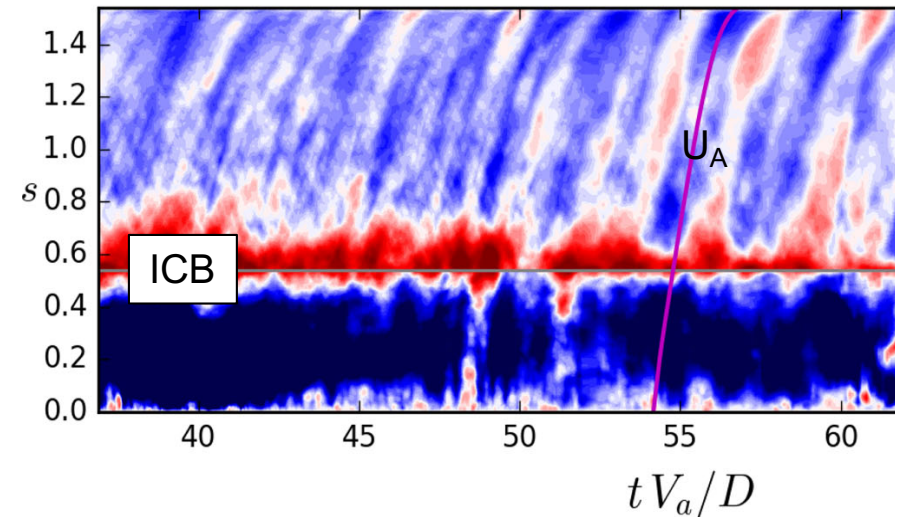
(cov-obs2019 for $m = 0$;
KH, Nilsson & Tobias, RMPP 2023)



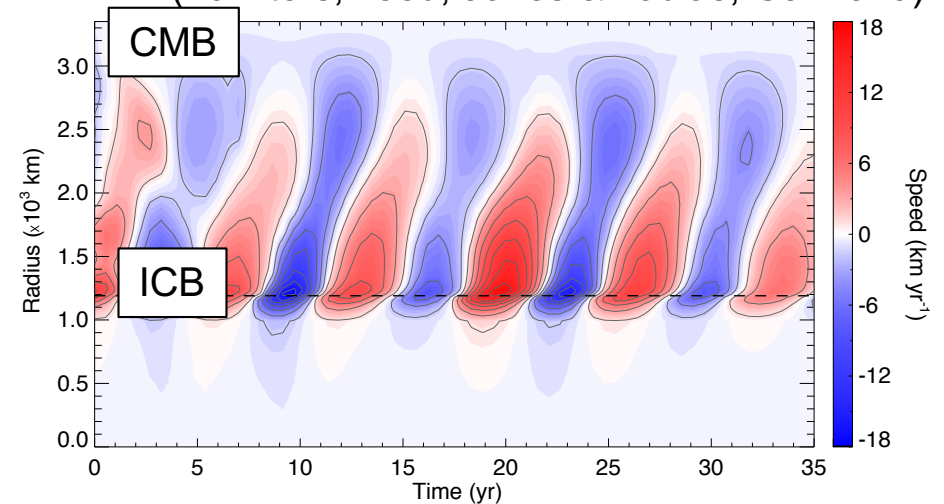
Torsional waves in DNS

- Geodynamo/magnetoconvection simulations support its excitation & travelling nature (e.g. Wicht & Christensen 2010; Teed et al. 2014; Schaeffer et al. 2017)
 - no clear reflection, no standing ‘oscillations’
 - too strong dissipation around CMB?
 - too viscous?
 - dispersive in the spherical cavity?
- Lab experiments also? (Nataf et al.)

in state-of-the-art dynamo simulations
(Schaeffer et al. 2017)



in magnetoconvection simulation
(no filters; Teed, Jones & Tobias, GJI 2019)



Some more discussions

- Excitation mechanisms

- normal modes to be damped at CMB

- in the presence of a conducting material at the bottom of the rocky mantle

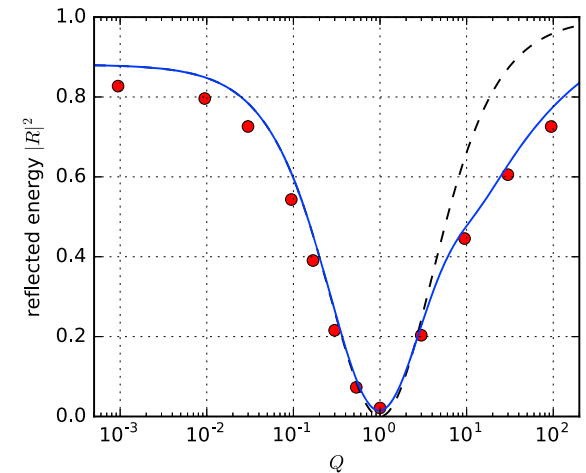
- a reflection rate:
$$R \simeq \frac{1 - Q - \sqrt{Pm}}{1 + Q + \sqrt{Pm}}$$

- with the conductance $G = \int_{-\delta}^0 \sigma_m dx$, conductivity σ_m , and thickness δ

- resonately launched at depth, in the vicinity of ICB

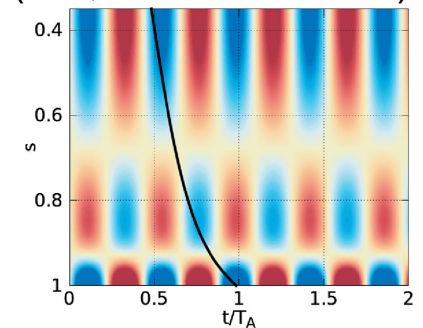
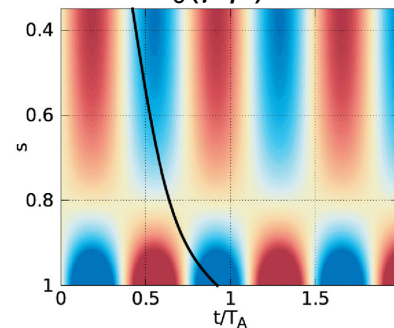
- (forced)

- The conditions

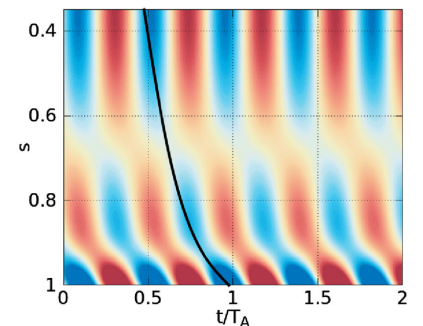
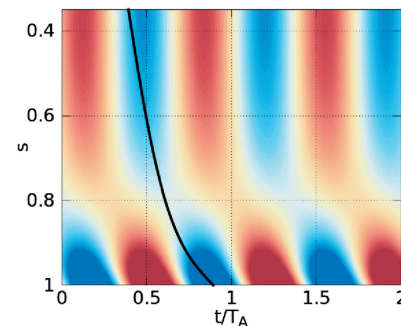


(Schaeffer & Jault 2016)

For $Q = G B_0 (\mu \rho)^{1/2} = 0.02$ (IVP; Gillet et al. 2017)



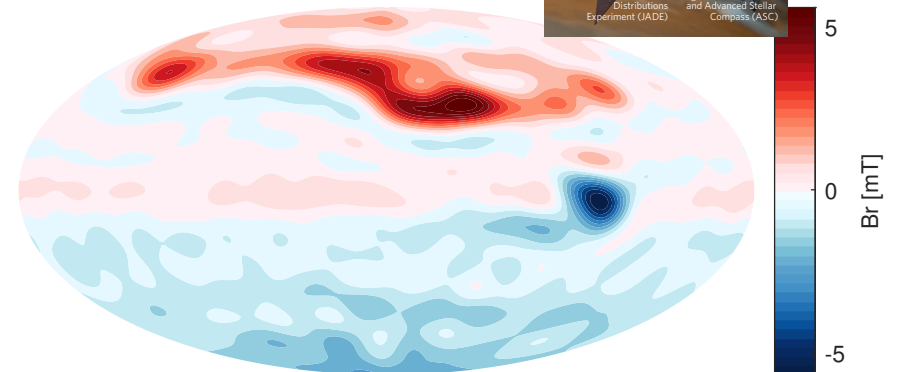
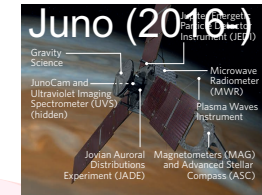
For $Q = 0.5$



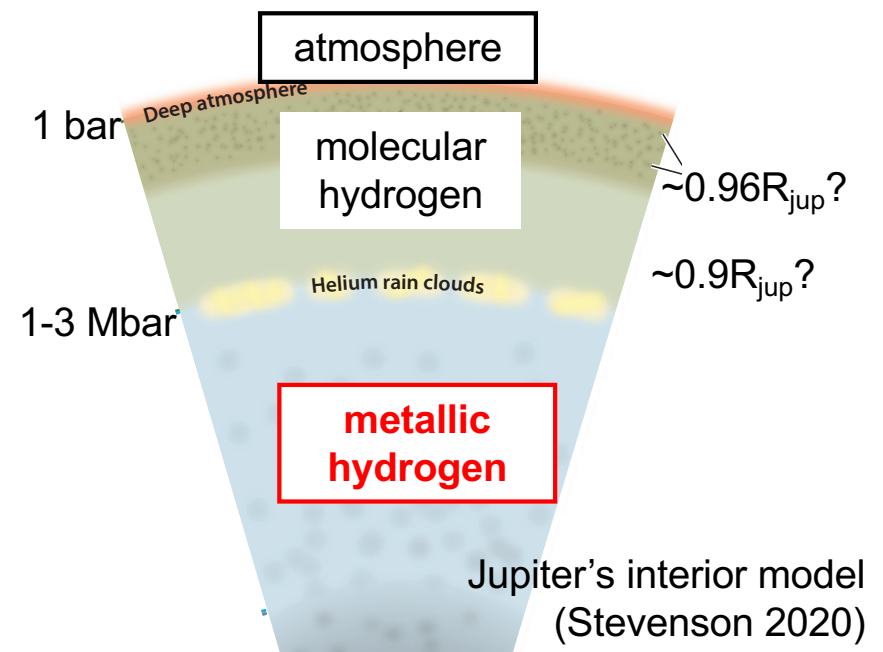
In other planets? e.g. Jupiter

- A prototype of gaseous planets
 - has the strong, global magnetic field
 - generated in the **metallic hydrogen region**
 - the “dynamo” region likely **spans close to the surface**, $< 0.8-0.9 R_{\text{jup}}$
 - cf. in the Earth, $< 0.55 R_{\text{earth}}$

- In the Juno era (2016-now):
 - orbiting at closest levels to a planetary dynamo
 - pre: strong, predominantly axial dipole ($n \lesssim 4$), secular variation?
 - post: localised patches incl. “GBS” ($n \geq 30$), first secular variation in other planets, etc.

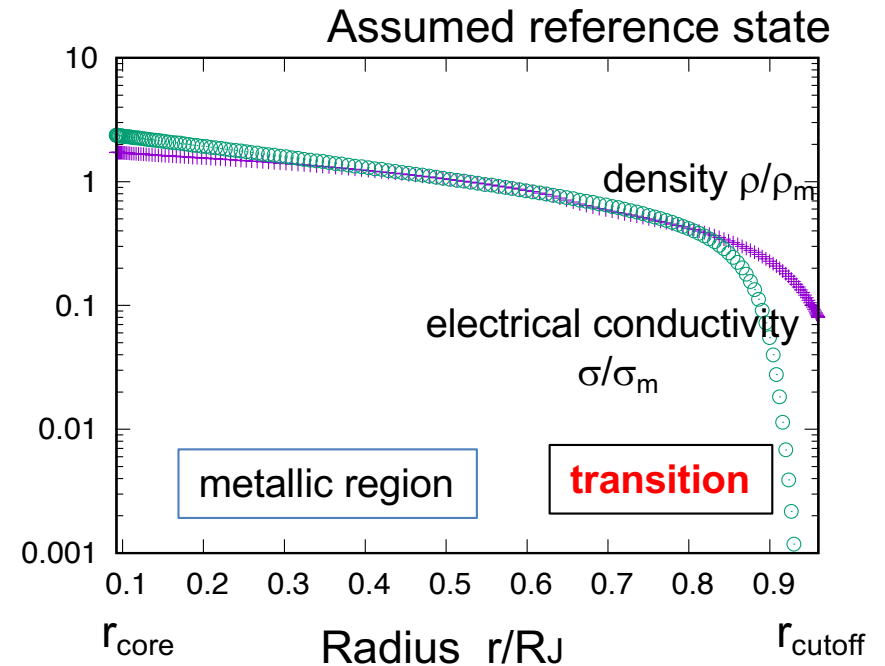


Br near Jupiter's dynamo surface, $\sim 0.85R_{\text{jup}}$
($n \leq 18$; JRM33 in 2016-21)



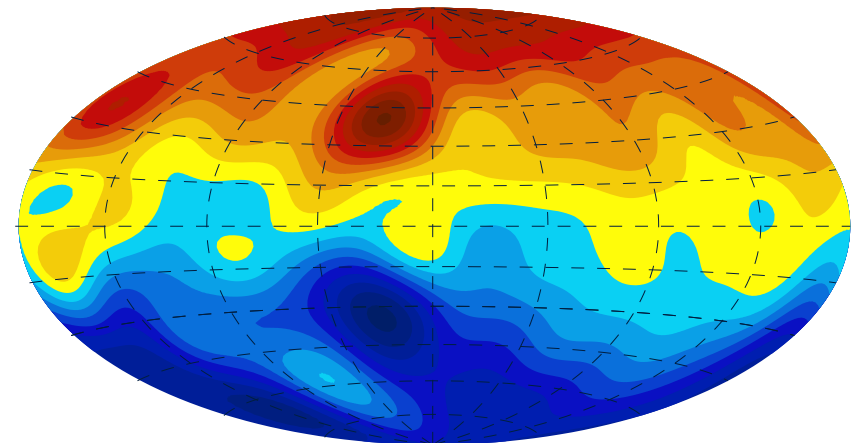
Convection-driven dynamo models for Jupiter

- **Setup** (Jones 2014; also Gastine et al. 2014):
 - model the metallic region & the transition to the molecular region: $0.09R_J \lesssim r \lesssim 0.96R_J$
 - dynamos driven by anelastic, rotating convection (Lantz & Fan 1999; Braginsky & Roberts 1995)
 - a reference state (French et al. 2012):
 - **density contrast**, $\rho(r_{\text{core}})/\rho(r_{\text{cutoff}}) \sim 18$
 - **electrical conductivity** σ begins to drop at $r \sim 0.85\text{-}0.90R_J$



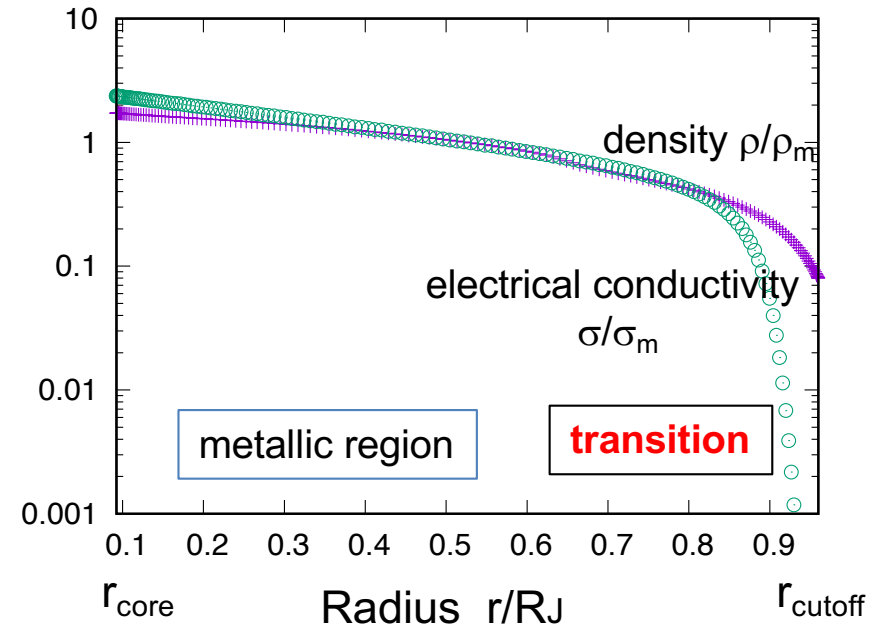
- **Key outcomes:**
 - jupiter-like magnetic fields reproduced

Br at the cutoff radius $r_{\text{cutoff}} \sim 0.96 R_J$
truncated up to $n=10$ (after Jones 2014)

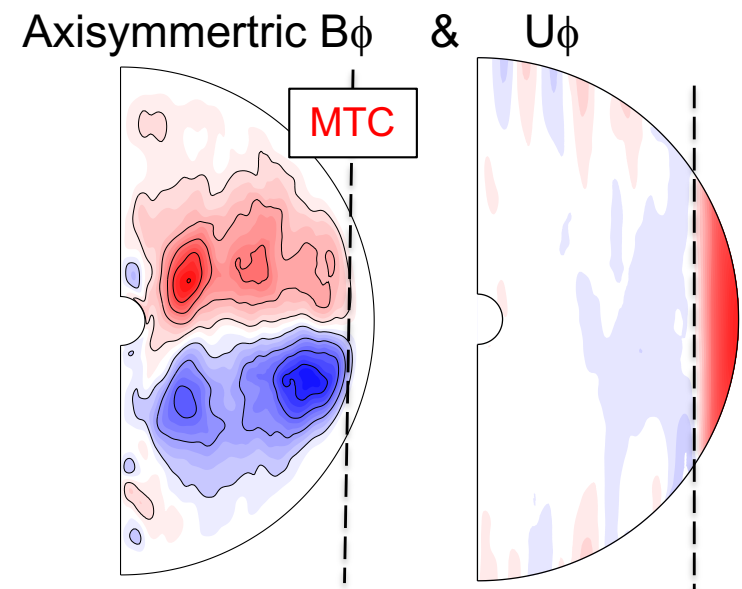


Convection-driven dynamo models for Jupiter

- **Setup** (Jones 2014; also Gastine et al. 2014):
 - model the metallic region & the transition to the molecular region: $0.09R_J \lesssim r \lesssim 0.96R_J$
 - dynamos driven by anelastic, rotating convection (Lantz & Fan 1999; Braginsky & Roberts 1995)
 - a reference state (French et al. 2012):
 - **density contrast**, $\rho(r_{\text{core}})/\rho(r_{\text{cutoff}}) \sim 18$
 - **electrical conductivity** σ begins to drop at $r \sim 0.85\text{-}0.90R_J$



- **Key outcomes:**
 - jupiter-like magnetic fields reproduced
 - a **magnetic tangent cylinder** formed
 - attaching to a “top” of the metallic region at the equator
 - one jet outside the MTC; incoherent inside
 - fluctuating: to be analyzed

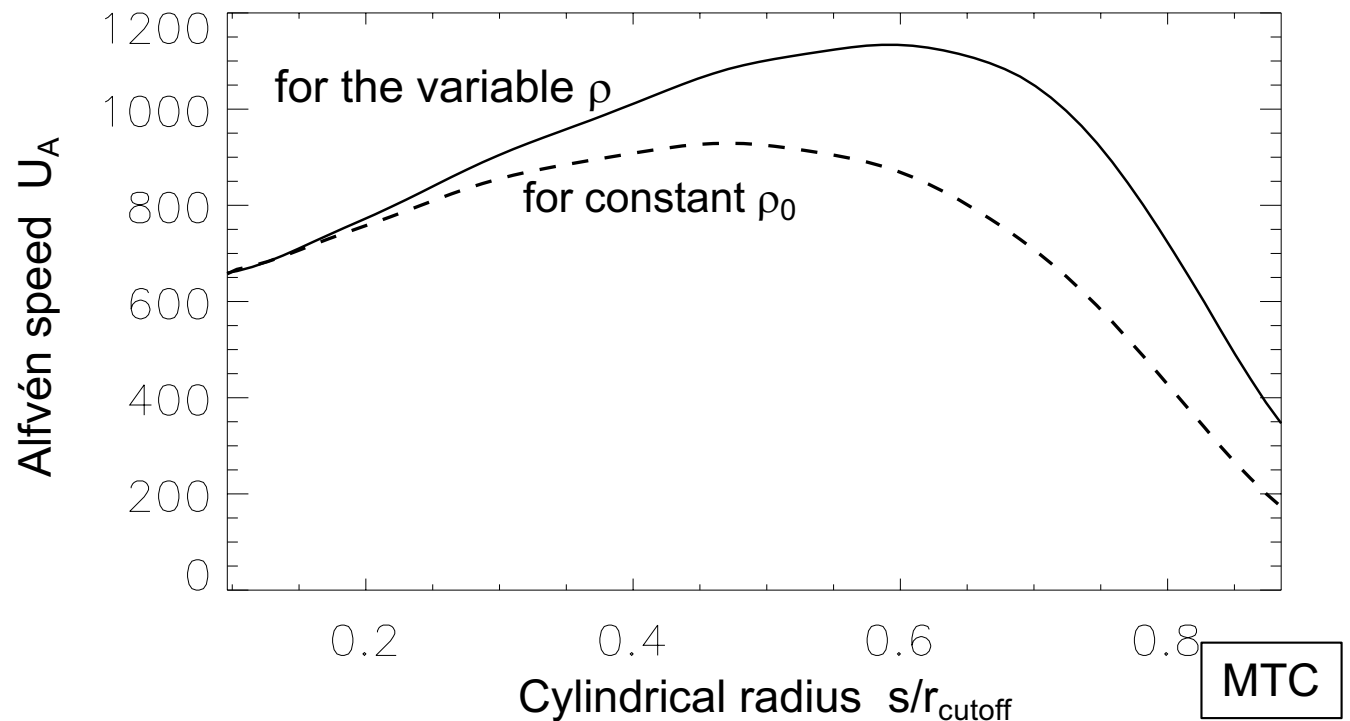


Alfvén speed in the anelastic simulations

- Predicted Alfvén speeds

$$U_A = (\langle \tilde{B}_s^2 \rangle / \mu_0 \langle \rho \rangle)^{1/2} :$$

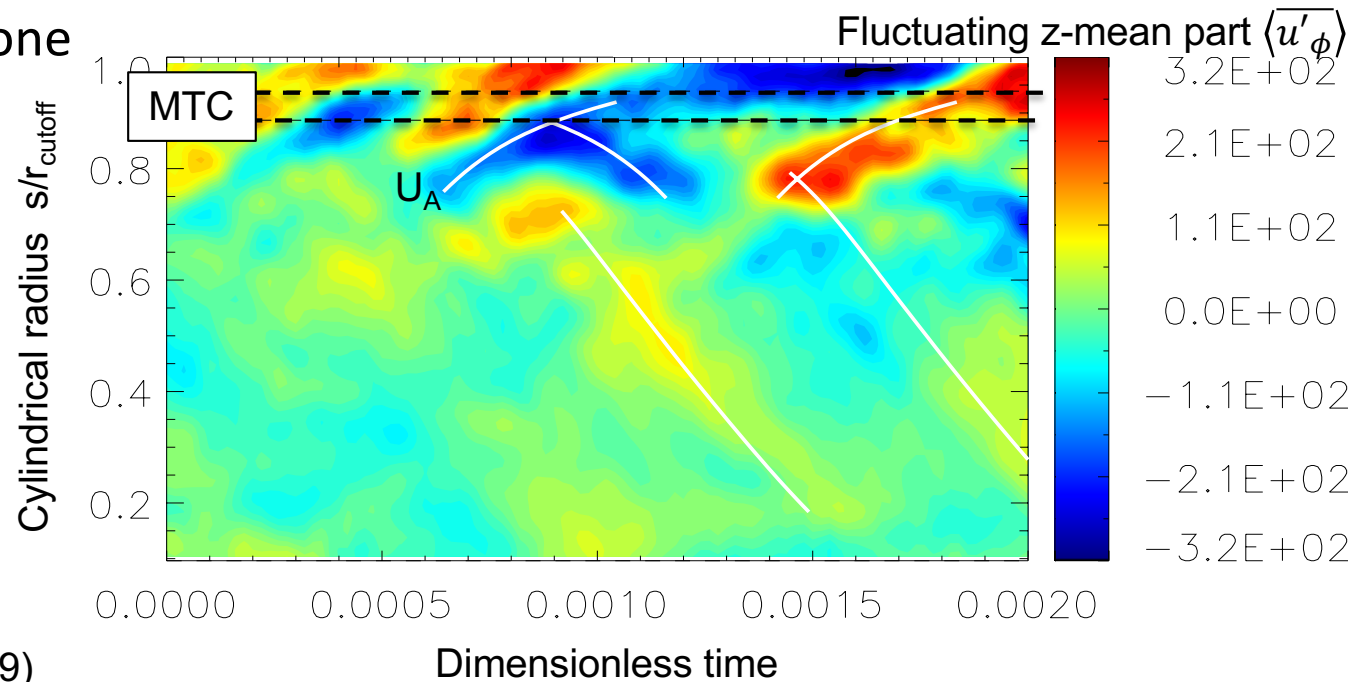
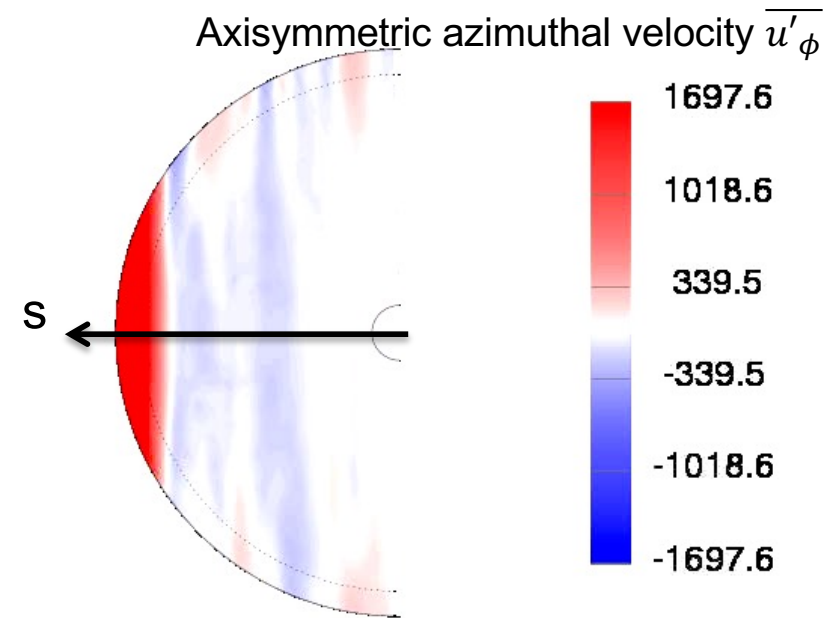
- independent of wavenumbers, i.e. nondispersive
- higher for low ρ , i.e. increasing with s
- drops to the MTC



at $E = 1.5 \cdot 10^{-5}$, $Pm=3$, $Pr = 0.1$, $H=1.4$

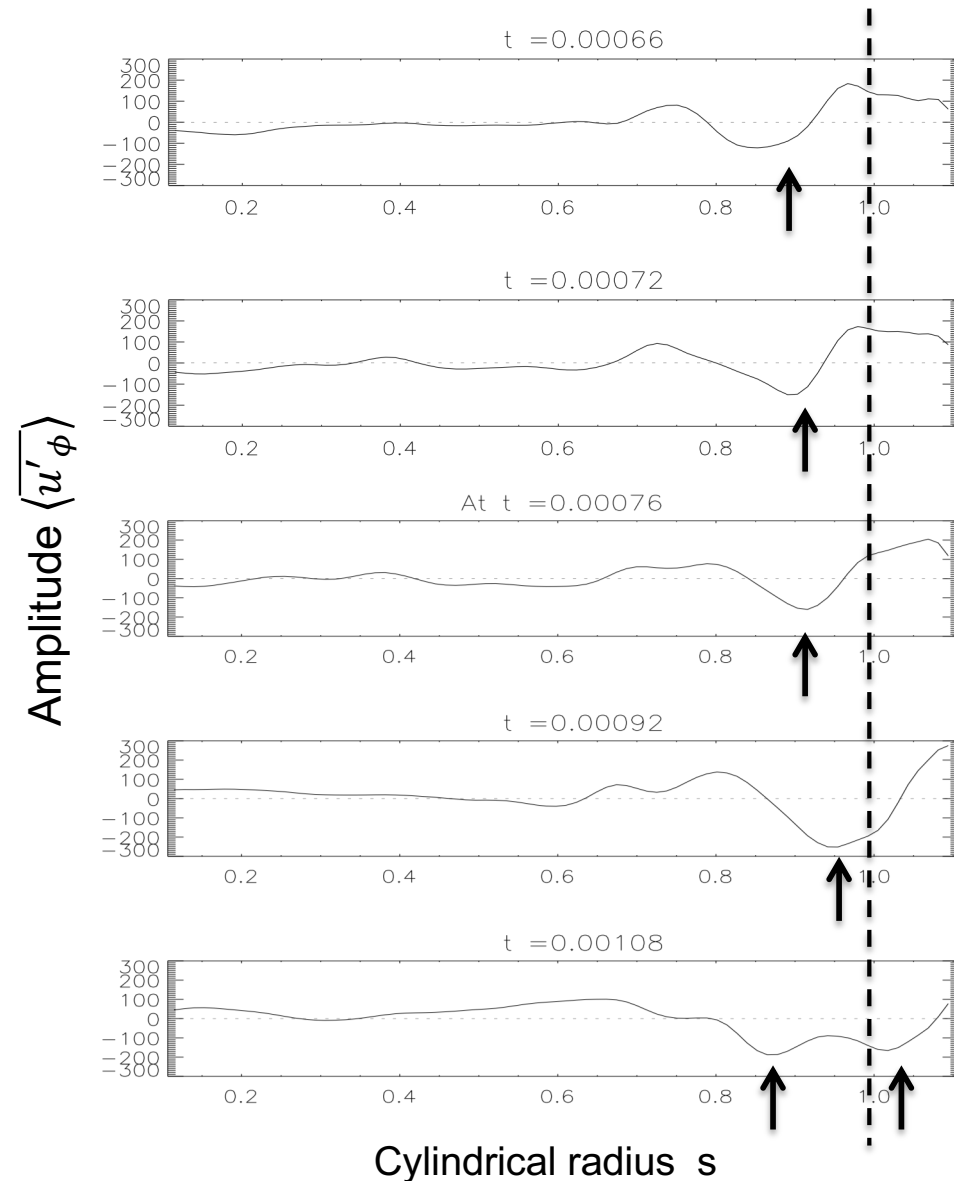
Torsional waves in Jovian simulations

- Identified with the predicted speeds of $U_A = (\langle \tilde{B}_s^2 \rangle / \mu_0 \langle \rho \rangle)^{1/2}$
 - travelling in s , outwardly or inwardly, from an outer radius ($0.6 < s/r_{\text{cutoff}} < 0.8$)
 - faster than convective speed
- **Reflected** at \sim MTC
 - which acts as an interface to the poorly-conducting zone



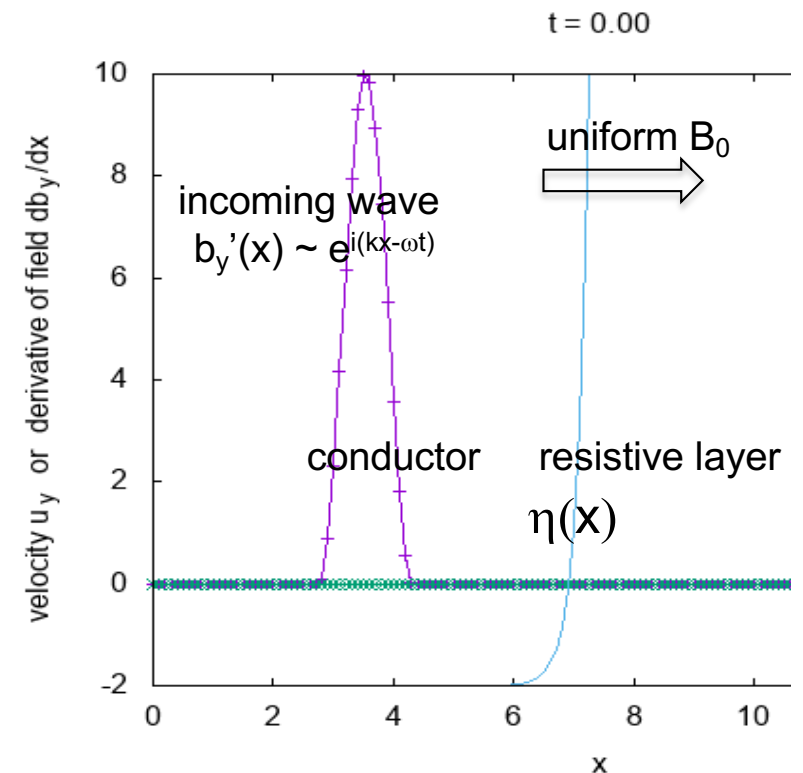
Evolution of torsional waves

- Reflection at \sim the MTC
 - as well as transmission to the outside
 - reflected waves not identical to incident waves
 - due to its spherical geometries, variable background fields, nonlinearities, etc.
- Waveforms can become sharp
 - steepening; weak, unstable
 - typical for inviscid nonlinear waves
 - e.g. water waves, shock waves
 - cf. dispersive, cnoidal/solitary Rossby ones (Hori et al. 2017)



Reflection of Alfvén waves

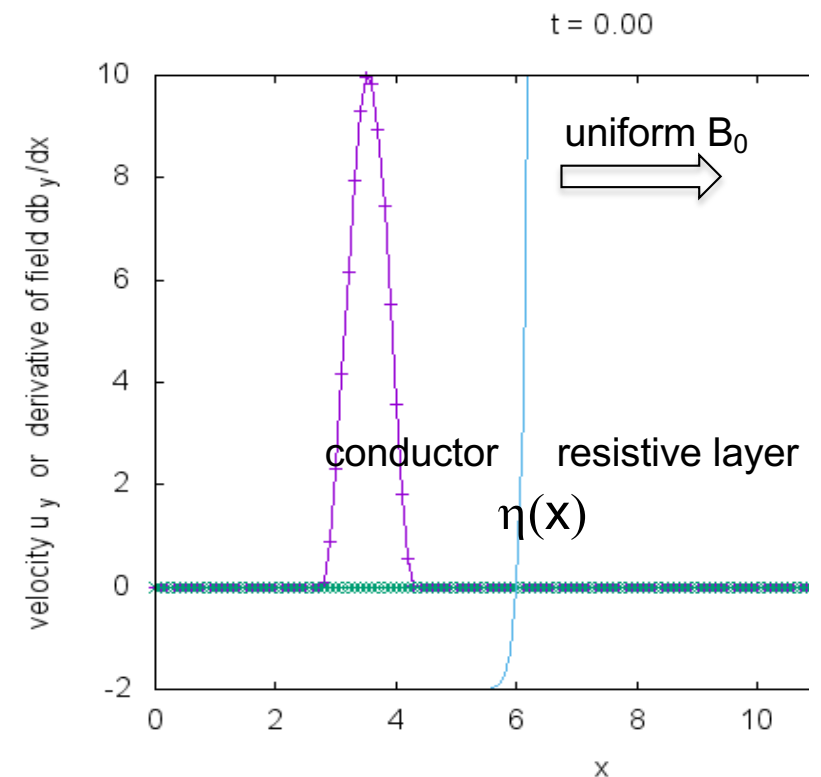
- Possibly due to the change in $U_A = (B_0^2/\rho\mu_0)^{1/2}$ (e.g. Alfvén & Fälthammar 1963)
- More likely due to the drastic change in the electrical conductivity σ , or the magnetic diffusivity $\eta = 1/\mu_0\sigma$
 - Consider a toy model: 1D incompressible models for a wave (k, ω) approaching a resistive layer



(Yamamoto, BEng thesis 2019)

Reflection of Alfvén waves

- Possibly due to the change in $U_A = (B_0^2/\rho\mu_0)^{1/2}$ (e.g. Alfvén & Fälthammar 1963)
- More likely due to the drastic change in the electrical conductivity σ , or the magnetic diffusivity $\eta = 1/\mu_0\sigma$
 - Consider a toy model: 1D incompressible models for a wave (k, ω) approaching a resistive layer

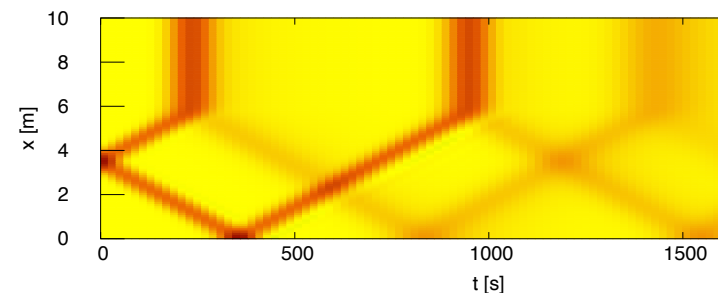
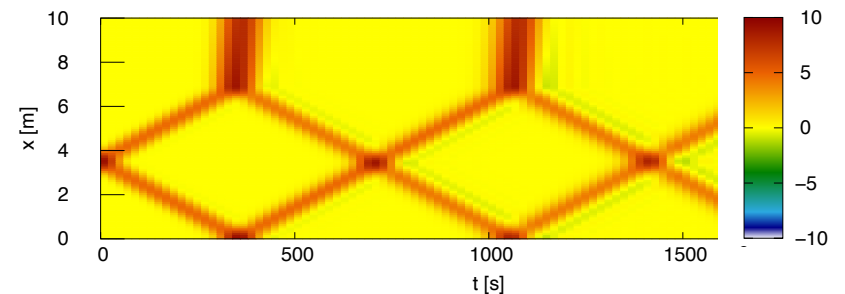
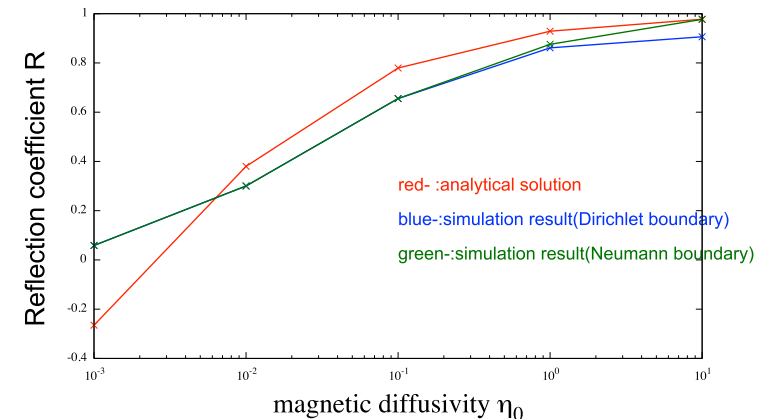


(Yamamoto, BEng thesis 2019)

Reflection of Alfvén waves (cont'd)

- 1D incompressible models for a wave (k, ω) approaching a resistive layer
 - for a jump, $\eta = \eta_0 \Theta(x - x_0)$
 - the reflection coefficient when $\omega \gg V_A^2/\eta_0$:

$$\mathcal{R} = \frac{ik - (1+i)\sqrt{\omega/2\eta_0}}{ik + (1+i)\sqrt{\omega/2\eta_0}}$$
 - the skin depth $(\omega/2\eta_0)^{-1/2}$
 - if $k^2 \ll \omega/\eta_0$, $|R| \sim 1$, i.e. perfect reflection
 - for a smooth change, $\eta(x) = \eta_0 \exp \lambda(x - x_0)$
 - reflections when $k < \lambda$, i.e. the wavelength of the incoming wave is long compared to the transition thickness



u_y for $\eta_0 = 1$
(after Yamamoto, BEng thesis 2019)

Excitation in the dynamo simulations

- Can be evaluated through the forcing terms in the momentum equation:

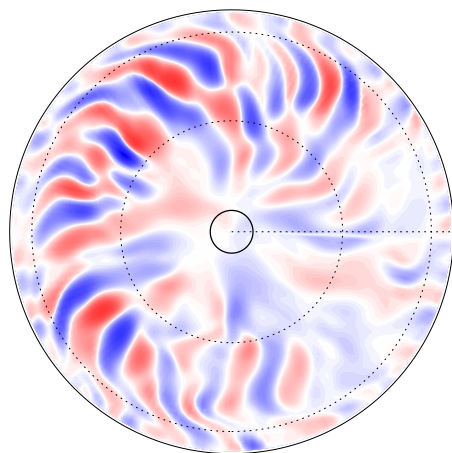
$$F_R = -\frac{1}{s^2 h} \frac{\partial}{\partial s} s^2 h \langle \bar{\rho} \overline{u_s u_\phi} \rangle$$

$$F_{LD} = F_L - F_{LR}$$

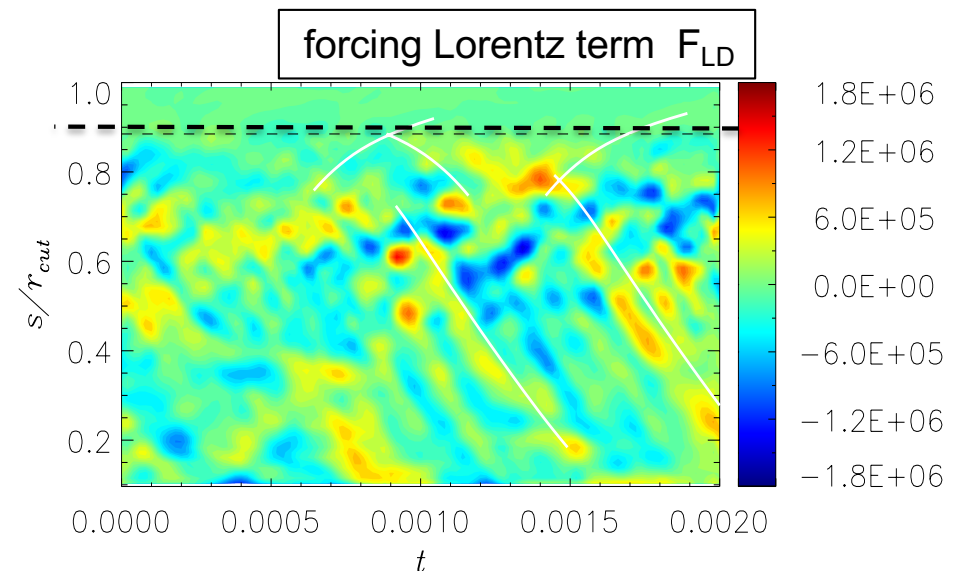
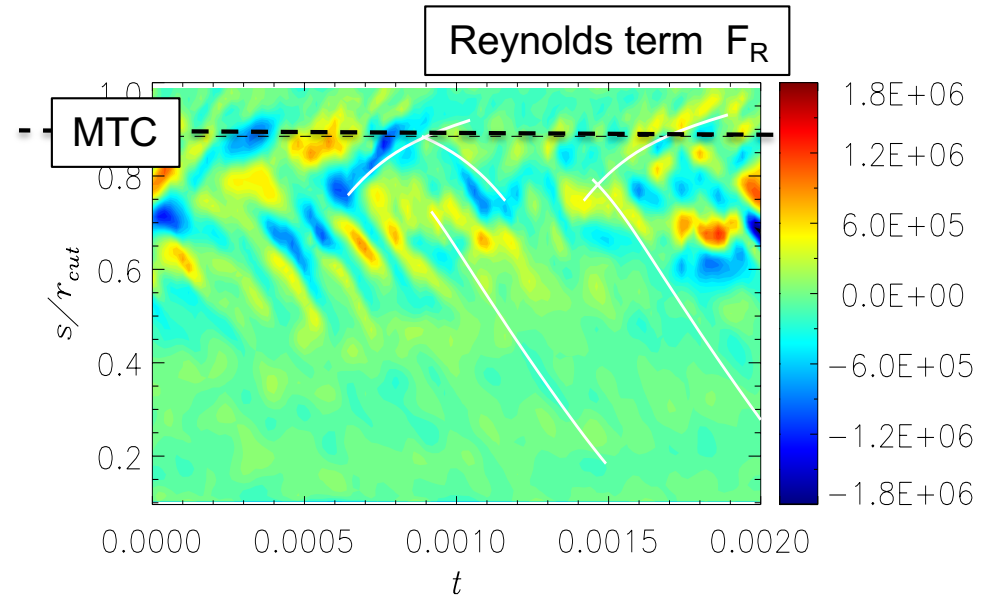
$$= \frac{1}{\mu_0 s^2 h} \frac{\partial}{\partial s} s^2 h \langle \overline{B_s B_\phi} \rangle - \int^\tau \left[\frac{1}{s^2 h} \frac{\partial}{\partial s} \left(s^3 h \langle \bar{\rho} \rangle U_A^2 \frac{\partial \langle \overline{u'_\phi} \rangle}{\partial s} \right) \right] dt$$

- TW initiated by the Reynolds/Lorentz force at an outer radius, $0.6 < s/r_{\text{cutoff}} < 0.8$
- at which it is beaten by convection on timescales of Rossby waves

- Note: distinct from the NatAstro scenario



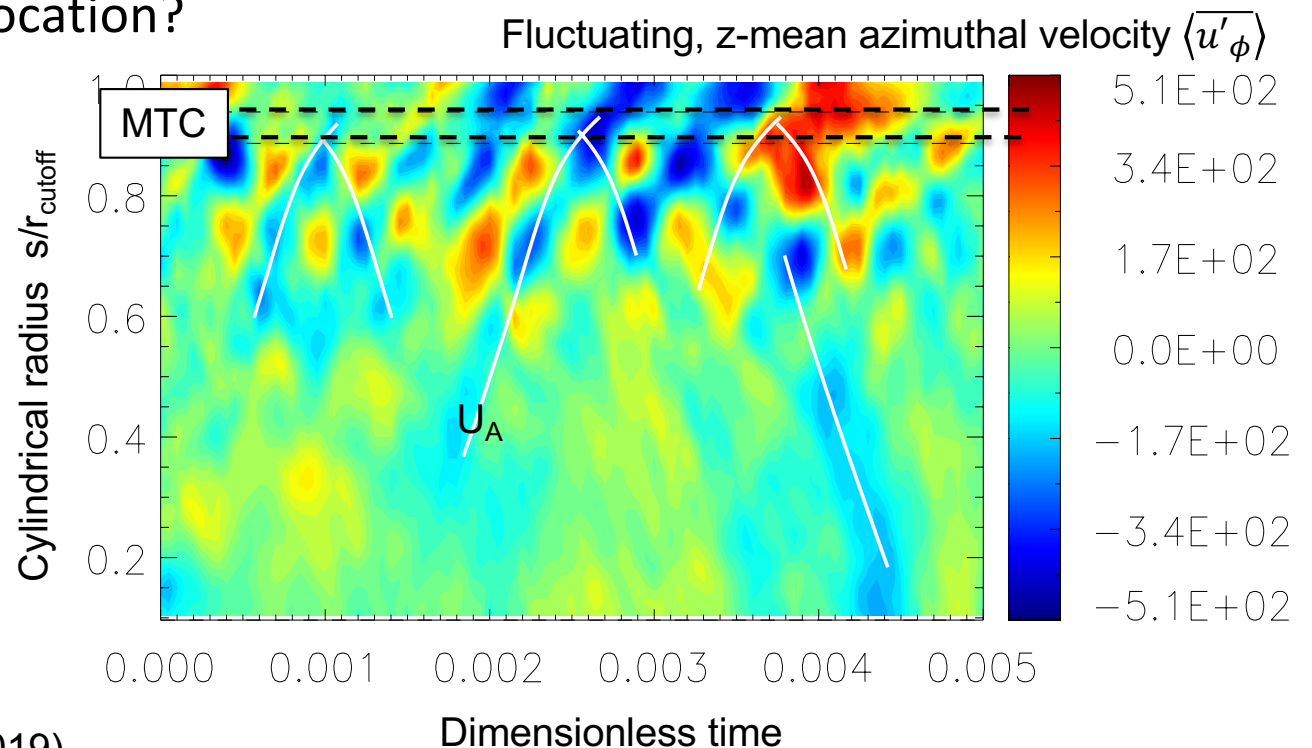
z-mean radial velocity $\langle u_s \rangle$



Torsional ‘oscillations’ possible

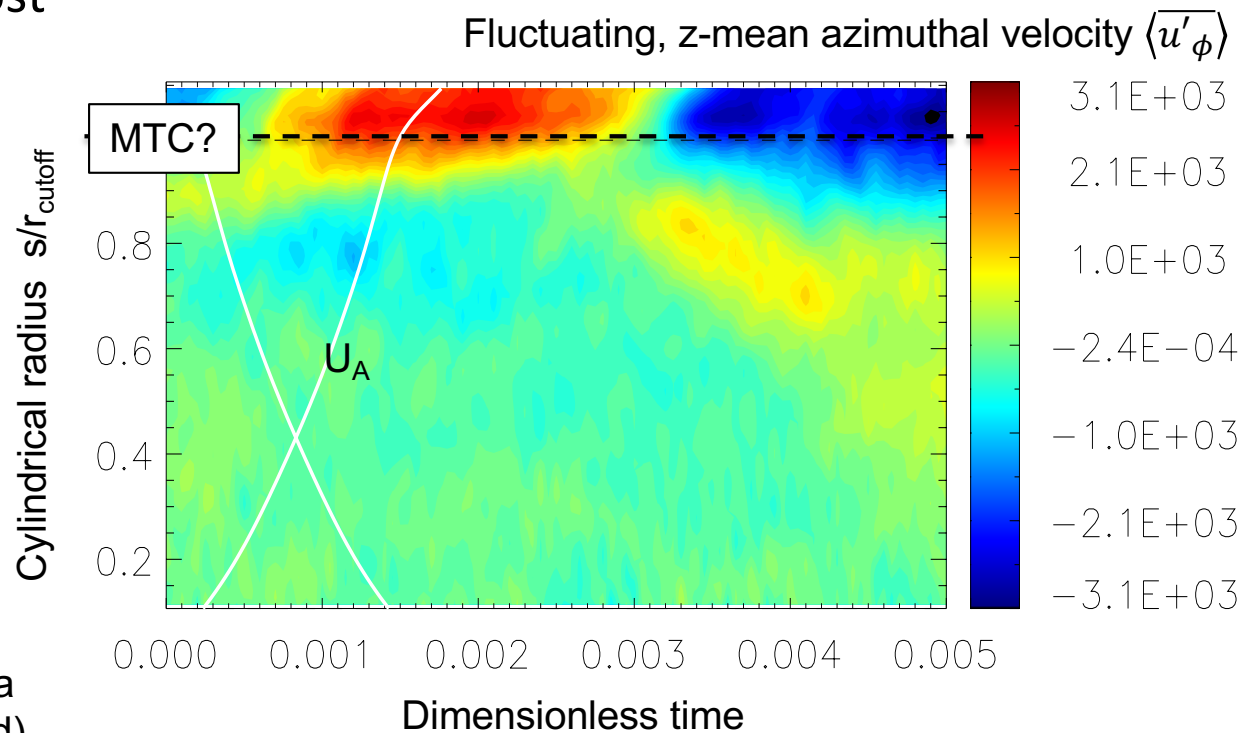
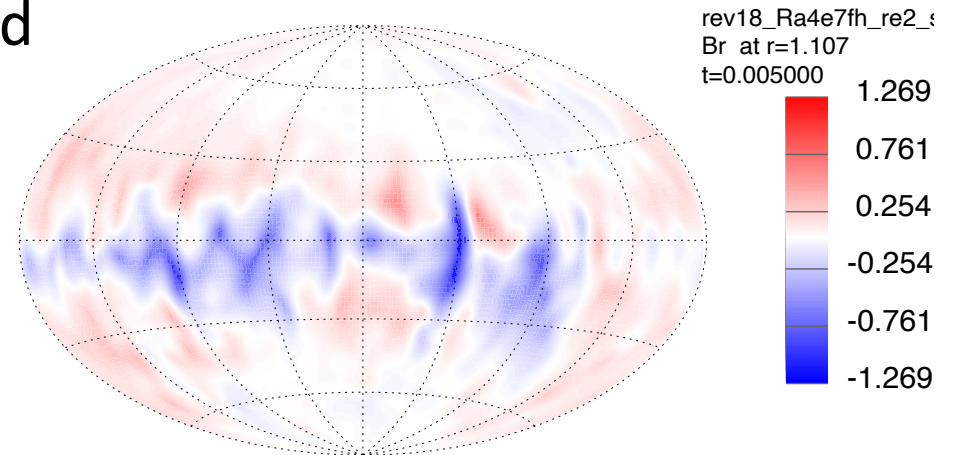
- Zonal flow fluctuations in another case
 - **standing** inside the MTC
 - travelling from an outer radius both inwardly and outwardly
 - superposition with reflected waves enables standing waves
 - only transmitted outside the MTC
 - while being absorbed
- help to determine the location?

- cf. Earth’s CMB
 - the bound between the core fluid and the rocky mantle (Schaeffer & Jault 2016)



Failed cases

- TW were not found if the background magnetic field is less dipolar
 - no longer in magnetostrophic balance
 - MTC becomes smooth and deep
 - cf. even for a dipolar field when the geostrophy is lost (Boussinesq; Teed et al. 2015)



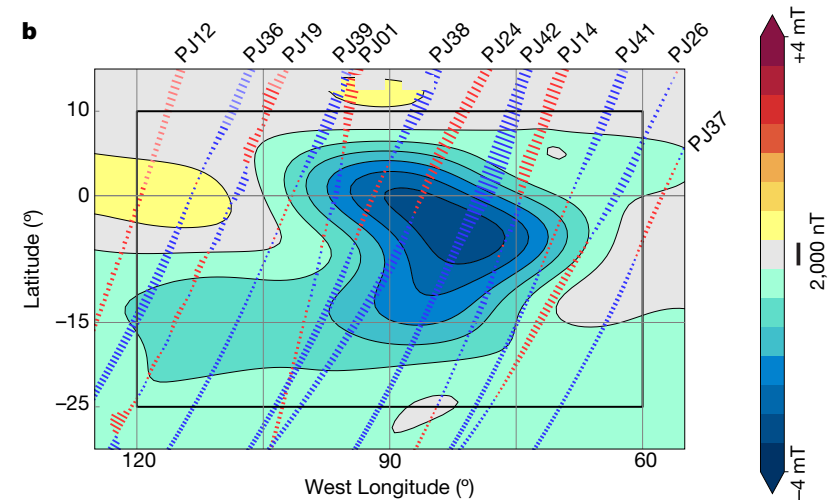
at $E = 1.5 \cdot 10^{-5}$, $Pm=3$, $Pr = 0.1$, higher Ra
(unpublished)

TO in Jupiter?

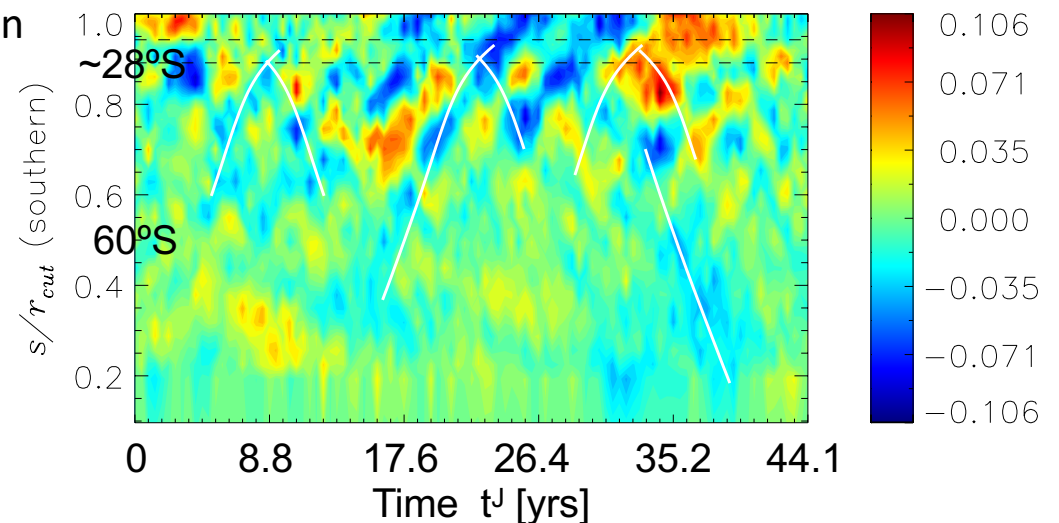
TO may give rise to

- magnetic secular variations
 - thought of magnitude $O(0.1 \text{ mT/yr})$ but unclear signals in simulations/Earth..
 - now some indication by Juno?
 - in the inferred flow of period ~ 4 years & magnitude $\lesssim 0.9 \text{ cm/s}$ (Bloxham et al 2024)
- variations in length-of-day
 - potentially of magnitude $< O(10^{-2} \text{ s})$
 - \sim the accuracy of the System III (1965) rotation rate, relying on radio emission
- **variations in the atmosphere**
 - unlike the rocky Earth!
 - potentially by $\lesssim 10\%$ of mean flows
 - more data of the appearance

Br around GBS & residuals from steady flow (Juno MAG; Bloxham et al. 2024)



$u'_\phi / \max(U_\phi)$ at $\sim 0.96 R_{\text{jup}}$ (after Jones 2014; KH et al. 2019)

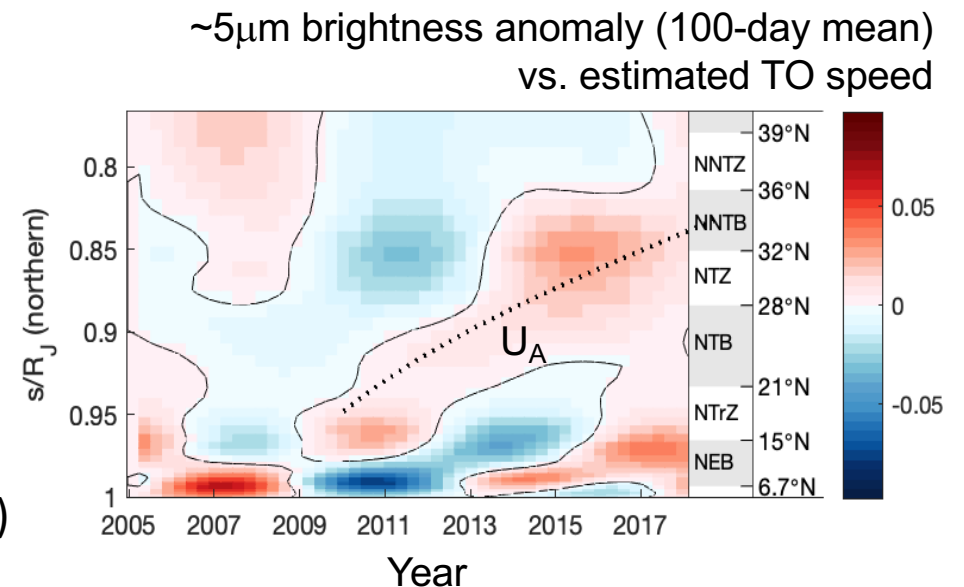
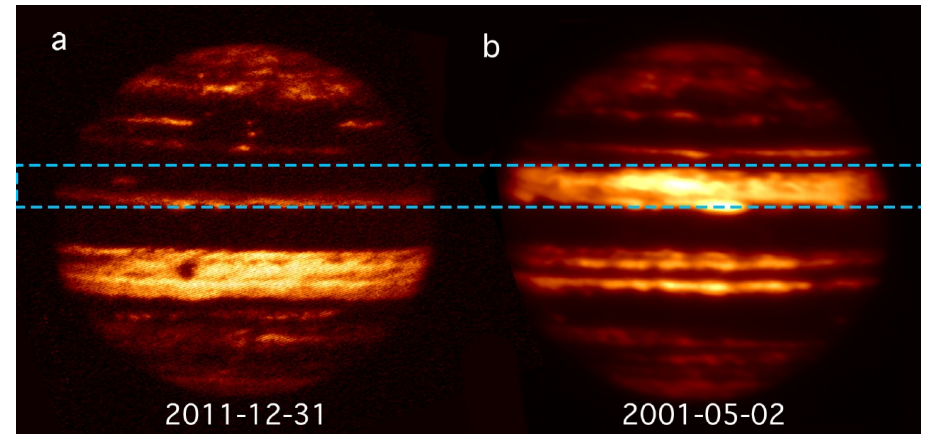


TO in Jupiter?

TO may give rise to

- magnetic secular variations
 - thought of magnitude $O(0.1 \text{ mT/yr})$ but unclear signals in simulations/Earth..
 - now some indication by Juno?
 - in the inferred flow of period ~ 4 years & magnitude $\lesssim 0.9 \text{ cm/s}$ (Bloxham et al 2024)
- variations in length-of-day
 - potentially of magnitude $< O(10^{-2} \text{ s})$
 - \sim the accuracy of the System III (1965) rotation rate, relying on radio emission
- **variations in the atmosphere**
 - unlike the rocky Earth!
 - potentially by $\lesssim 10\%$ of mean flows
 - more data of the appearance (ground-base)
 - **TO signals in infrared/ $\sim 5\mu\text{m}$ images?**

Images at $\sim 5\mu\text{m}$ wavelength
(Antuñano, Fletcher, et al. 2019)



(KH, Jones, Antuñano, Fletcher, Tobias 2023)

Possibly in exoplanets? stars?

With no convective drivings

- Tidally-driven flows (Astoul & Barker, in review/arXiv)
 - magneto-inertial waves play a central role
- MRI-driven?
 - where a basic zonal flow shear acts as a Coriolis effect
 - slow eigenmodes in solar near-surface region? (Vasil et al. 2024)
 - proposed to drive the solar cycle as well as the solar ‘torsional oscillation’ there
 - looks like our TW/O

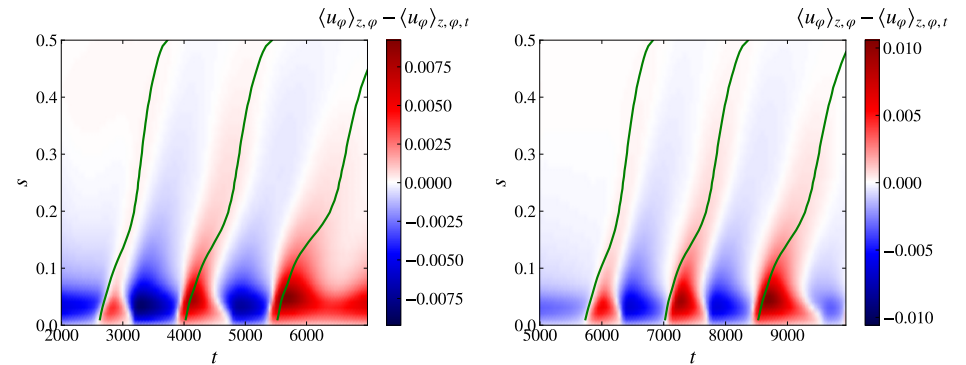


Figure 9. Amplitude of the fluctuating z and φ averaged zonal flow $\langle u_\varphi \rangle_{z,\varphi} - \langle u_\varphi \rangle_{z,\varphi,t}$ versus time t exhibiting propagating torsional Alfvén waves. The time average for the zonal flow $\langle u_\varphi \rangle_{z,\varphi,t}$ is performed where the oscillations are observed. The green curve shows the Alfvén timescale t_A (averaged over an appropriate range). *Left:* $Le = 6 \cdot 10^{-3}$. *Middle:* $Le = 10^{-2}$. *Right:* $Le = 2 \cdot 10^{-2}$.

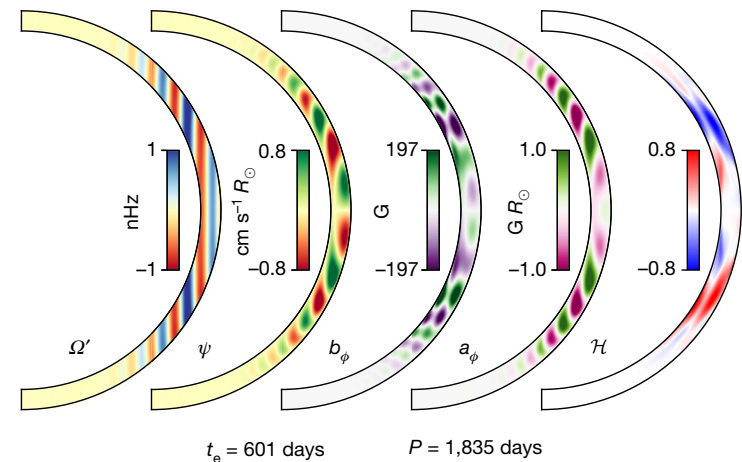


Fig. 2 | Two meridional (r, θ) MRI eigenmode profiles. Longitudinal angular velocity perturbation, $\Omega'(r, \theta) = u_\varphi(r, \theta)/(r \sin(\theta))$; momentum-density streamfunction (φ -directed component; Methods), $\psi(r, \theta)$; longitudinal magnetic field, $b_\varphi(r, \theta)$; magnetic scalar potential, $a_\varphi(r, \theta)$; and current helicity correlation, $\mathcal{H}(r, \theta)$. The timescales t_e and P represent the instability e-folding

Summary

Torsional Alfvén waves may well be excited in Earth and Jupiter

- propagating in cylindrical radius with Alfvén speeds $\sim B_s/\rho^{1/2}$
 - on timescales of $O(10^{0-1}$ yrs)
- demonstrated in geo-/Jovian dynamo simulations
 - when the field is predominantly dipolar
 - preferably propagating in geo- ; possibly standing in jovian
 - by reflections at an interface, MTC, for a sharp transition in conductivity
- giving rise to LoD variations and, in the gas giant, zonal flow changes in the overlying layer
 - unclear signals in magnetic SV
- The detection in the planets: maybe? likely? (on-going)
 - a potential window to infer the interior of the dynamos